Diploma Thesis

M. Sc. eng. Florin MACIUC

May 19, 2004

I dedicate this work to my family, that stood by me as always.

Abstract

I have tried to tackle in this work as many physics subjects as possible. I hope that a broad view was achieved and this not on expense of clarity of each peculiar subject. The framework is: $\mu^+\mu^-$ pair production by athmospheric muons in ALEPH, muon propagation Monte Carlo and candidate selection in data analysis. To separate between trident events and other interaction or coincidences, data analysis tools and a muon transport Monte Carlo were developed. As main conclusion, experimental estimations are consistent with Monte Carlo results. To encrease statistics, the present study must be extended to ALEPH e^+e^- beam data.

Acknowledgements

I am in debt to Professors Claus Grupen and Arif Mailov for useful discussions and suggestions.

Table of Contents

List of Figures

List of Tables

Chapter 1

Introduction

Mistake me not; I would not, if I might,
Change my misfortunes for thy vassalage.

Someone near Erebus

This work is a study of muon interactions with emphasis placed on the so called "trident" interaction:

$$\mu^{+/-} + \text{Static Nucleus} \rightarrow \mu^{+/-} + \text{Quasi-static Nucleus} + \mu^{+} + \mu^{-}$$

Other muon interactions are treated: ionization in elements and compounds (Bragg addition law, Ionization potential, 13% law, etc), positron-electron pair production (average contribution to energy loss and comparison with trident contribution), bremsstrahlung (continuous loss approximation), photonuclear (two alternative parameterizations, contiuous loss approximation).

One of my primary goals, was to find evidence of muon trident events in ALEPH detector data. From a total number of 1397015 events only few candidates were selected. Muon trident hypothesis was probed for each candidate, probabilities being weighted for muon trident as well as for other possible hypotheses.

ALEPH is a particle detector based at CERN. It was placed on LEP ring to get data from e^+e^- collisions. For almost a week (between 21-April-1999 - 29-April-1999) ALEPH was exclusively used to observe cosmic muons coming from Atmospheric Air-Showers (the CosmoALEPH experiment). During this period the e^+e^- beam was not operational.

ALEPH is located underground at a level of 320 meter-water-equivalent. This makes ALEPH an under-ground muon observatory, at shallow depth. The overburden and detector resolution impose a lower limit of surface muon spectrum at 70-75 GeV, and an upper limit of 3 TeV, with the latter being arbitrary chosen to match 100% relative error in ALEPH momentum reconstruction.

Following literature sources, we sould expect a feature (change in chemical composition of primary) related to the knee structure present in primary [1] spectrum. There is hope, that CosmoALEPH may "shed more light" on the subject.

[1] Primary, here, is the cosmic particle that initiates an atmospheric shower with muonic remnants observed underground

1.1 Motivation

Why should be this kind of work undertaken? I believe that I have several answers to this question.

For a start, there is physical understanding of a non-commonly occurring interaction. Trident or $\mu^+\mu^-$ interaction has relatively low probability to occur, with respect to e^+e^- pair production (the latter process being the competing channel).

The process can not be fully treated within the framework of Quantum Electrodynamics. It involves large momentum transfers (larger than double muon mass) and, thus, a Nuclear Form Factor is required, to account for finite nuclear size. The importance of Form Factor when computing reaction rates makes Trident Process an intermediary process between pure leptonic processes and mixed leptonic-hadronic interactions. Needless to say that latter processes are not fully understood, and this would be a reason to study tridents.

In literature, there are still conflicting values for trident theoretical cross-section. Most of professional Monte Carlos developed for muon transport have altogether dropped the very idea of incorporating trident interaction. This is justified if energy loss of primary muon is concerned, but it is a doubtful assumption if muon multiplicity and individual events are as well under study.

An other reason can be that Tridents would appear as background when dealing with some exotic processes. This could happen e.g. in a deep-inelastic processes that would lead to quark jets being formed (see [Vis00]).

Next, there is also the problem of muon multiplicity for an individual event. Underground, especially at large depths, there is an enhancement in muon multiplicity due to muon tridents. This would lead to an observable effect, and would affect multiplicity and spectrum estimations if trident interaction is not taken into account when building simulations.

There are, also, personal and didactic motivations. The field is appealing from point of view of physics involved and it is a good training and skill development ground. Never, were tridents investigated within our framework or in similar cases.

The subject is broad, it involves theoretical aspects, data analysis and Monte Carlo simulations.

Chapter 2

Theory: QED, Form Factor

Not everything that can be counted counts, and not everything that counts can be counted.
Albert Einstein

$\mu^+\mu^-$ pair production by incident muons is approximately a Quantum Electrodynamics process. It is approximately, because the incident muon interacts with the nucleus, a quark close-packed system. To a certain degree, the hadronic part of the interaction can be neglected, and the nucleus can be treated either as Coulomb scattering center, or, more consistently, as a parton distribution with a Form Factor.

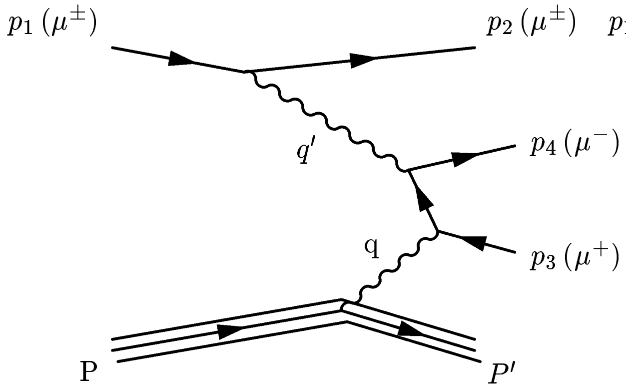

Feynman diagram I

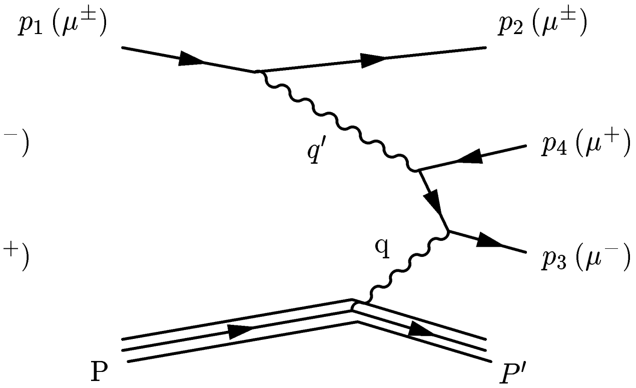

Feynman diagram II
(diagram I with $\mu+$ and μ^- interchanged)

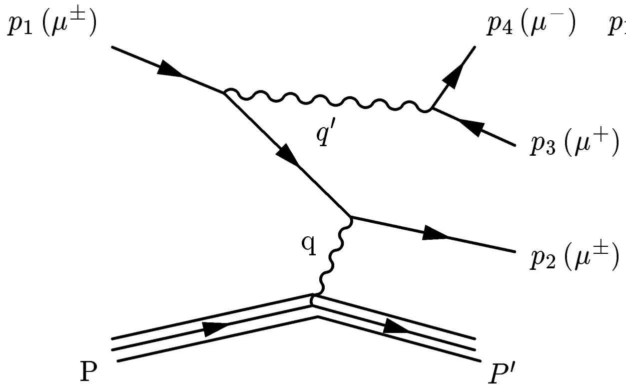

Feynman diagram III
(IV is just III with interchanged secondaries)

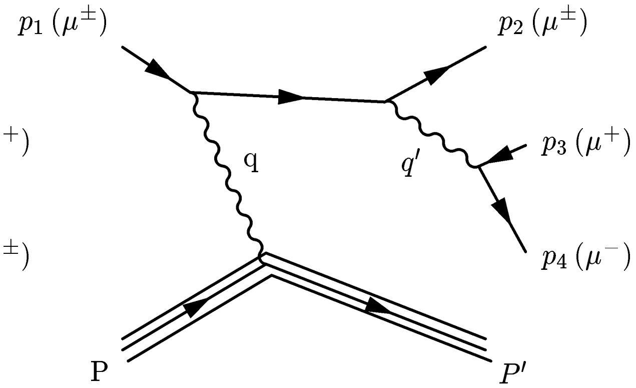

Feynman diagram V
(VI is just V with interchanged secondaries)

The first papers describing $\mu^+\mu^-$ pair production, followed a Coulomb center approximation, e.g. [Kel67]. It was found by recent experiments, that the cited parameterization of $\mu^+\mu^-$ pair production cross-section is overestimating the rate of pair production. This was corrected, recently, by Kelner, Kokoulin and Petrukhin in 1999. They assume a Fermi function Form Factor and an ultra-relativistic approximation for incoming and outgoing particles. The new choice seems in concordance with experimental data.

2.1 Parameterization of trident cross-section

KKP [SRKP99] parameterization of trident cross-section is:

$$\sigma(E,v,\rho)\,dv\,d\rho = \frac{2}{3\pi}\,(Z\alpha r_\mu)^2\,\frac{1-v}{v}\Phi(v,\rho)ln(X)\,dv\,d\rho \tag{2.1}$$

Here $v = \frac{E-E'}{E} = \frac{E_+ + E_-}{E}$ is the fraction of energy transfered to produced pair, $\rho = \frac{E_+ - E_-}{E_+ + E_-}$ the pair asymmetry parameter, r_μ classical muon radius, $\alpha \approx 1/137$ and Z element number. The upper functions are defined:

$$\begin{aligned}\Phi(v,\rho) = \left[\left(2+\rho^2\right)(1+\beta) + \xi\left(3+\rho^2\right)\right] ln\left(1+\frac{1}{\xi}\right) - 1 - 3\rho^2 + \beta\left(1-2\rho^2\right) \\ + \left(\left(1+\rho^2\right)\left(1+\frac{3}{2}\beta\right) - \frac{1}{\xi}(1+2\beta)\left(1-\rho^2\right)\right) ln(1+\xi)\end{aligned} \tag{2.2}$$

with: $\xi = \frac{v^2(1-\rho^2)}{4(1-v)}$, $\beta = \frac{v^2}{2(1-v)}$;

$$X = 1 + U(E,v,\rho) - U(E,v,\rho_{max}) \tag{2.3}$$

with

$$U(E,v,\rho) = \frac{0.65A^{-0.27}BZ^{-1/3}m_\mu/m_e}{1+\frac{2\sqrt{e}m_\mu^2 BZ^{-1/3}(1+\xi)(1+Y)}{m_e E v(1-\rho^2)}}, \tag{2.4}$$

and B=183, e=2.718.. is Neper Number, A atomic weight, $Y = 10\sqrt{\frac{m_\mu}{E}}$, $\rho_{max} = 1 - \frac{2m_\mu}{vE}$, m_μ m_e are muon and electron masses. The cross-section as function of energies is found from:

$$\sigma(E,E_+,E_-) = \frac{2}{E^2 v}\sigma(E,v,\rho) \tag{2.5}$$

Integration limits and kinematic phase-space limits are:

$$\frac{2m_\mu}{E} \le v \le 1 - \frac{m_\mu}{E}, \quad |\rho| \le \rho_{max} \tag{2.6}$$

$$\tag{2.7}$$

Physics underlying the KKP parameterization (see [SRKP99]):

• screening of nuclear charge by atomic electrons is modeled with a Thomas-Fermi model and quantized under an Atomic Form Factor (important only for very low momentum transfers, and, given a limit of $2m_\mu$ negligible overall);

• size of nucleus or parton distribution width is quantized under a Fermi function Form Factor (in contrast

with precedent case this **Nuclear Form Factor has relevance**, preventing overestimation by one order of magnitude of the trident cross-section);
• ultra-relativistic muons in input channel (incident muon) and output channel (two secondaries and the scattered initial muon);
• trident production via atomic electrons is neglected (due to relative difference in amplitude and threshold energy $E_{threshold} = 87.7$ GeV);
• the changes in nucleus state function are neglected (this regards nucleus excitations and hadronization; of course, momentum transfer to nucleus is not neglected);
• "the rest is silence" (in the words of the bard) or, in physics lingua franca, Quantum Electrodynamics at work.

2.2 Integration of the parameterized cross-section formula

Integration of the differential cross-section is done following a Gauss-Legendre integration algorithm ([WPF92], [Tit99] or [CER]) or Romberg method based on trapezoidal rule. The algorithm for one dimensional integration is extended to higher dimensional case, and an adaptive step size implemented. The methods estimate at each step the relative error in integration and adapt the step to increase precision.

The Romberg method appear to generate results with low errors, but long running times. The following plots 2.1 to 2.6 are achieved by both methods: Romberg and Gauss-Legendre. Gauss algorithm of integration is based on function decomposition on Legendre (or other base polynomials) polynomials and the integration step is not constant but has values equal with root values for polynomial equations.

For the following integrations the upper statements remain valid. Other methods were tried, but the time needed, for the adaptive extensions to convergence, was too long. Romberg and Gauss-Legendre algorithms give results that match to 4 digits.

In the next numerical result, from this chapter or the subsequent chapters, the highest precision achievable was requested (achievable in terms of tools used). Due to long integration times the Romberg method was not implemented for e^+e^- pair production and the precision was reduced. However the result is exact within 3 digits, and only small bumps and dips are distorting the cross-section plot.

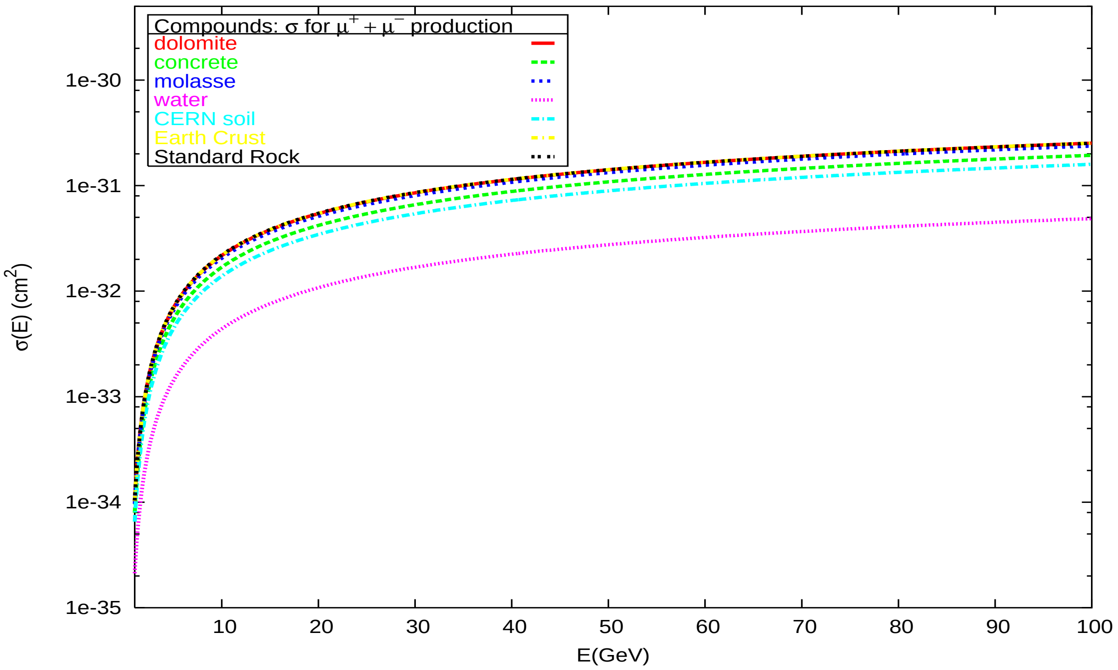

Figure 2.1: Muon trident cross-section per target nucleus in 7 compound materials

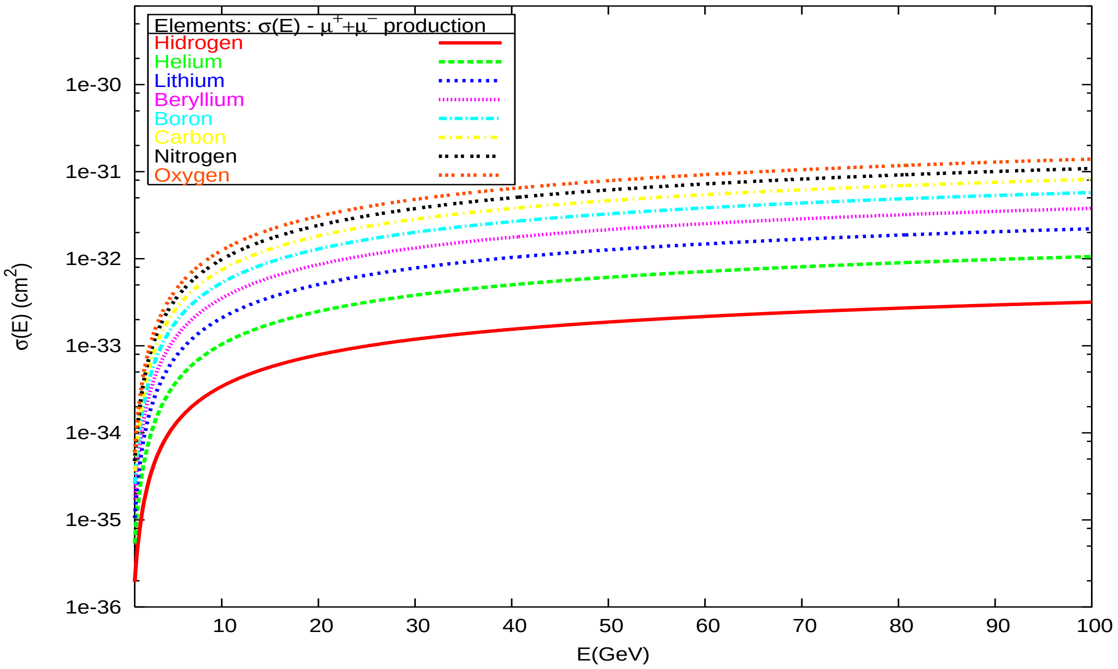

Figure 2.2: Muon trident cross-section per target nucleus, elements I.

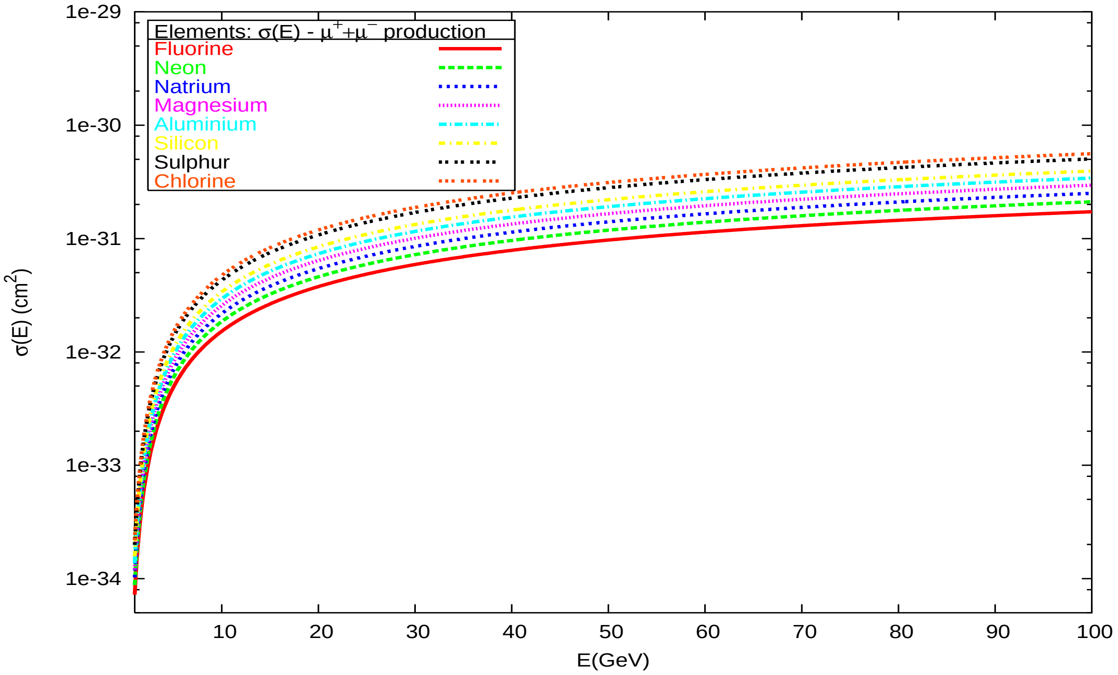

Figure 2.3: Muon trident cross-section per target nucleus, elements II.

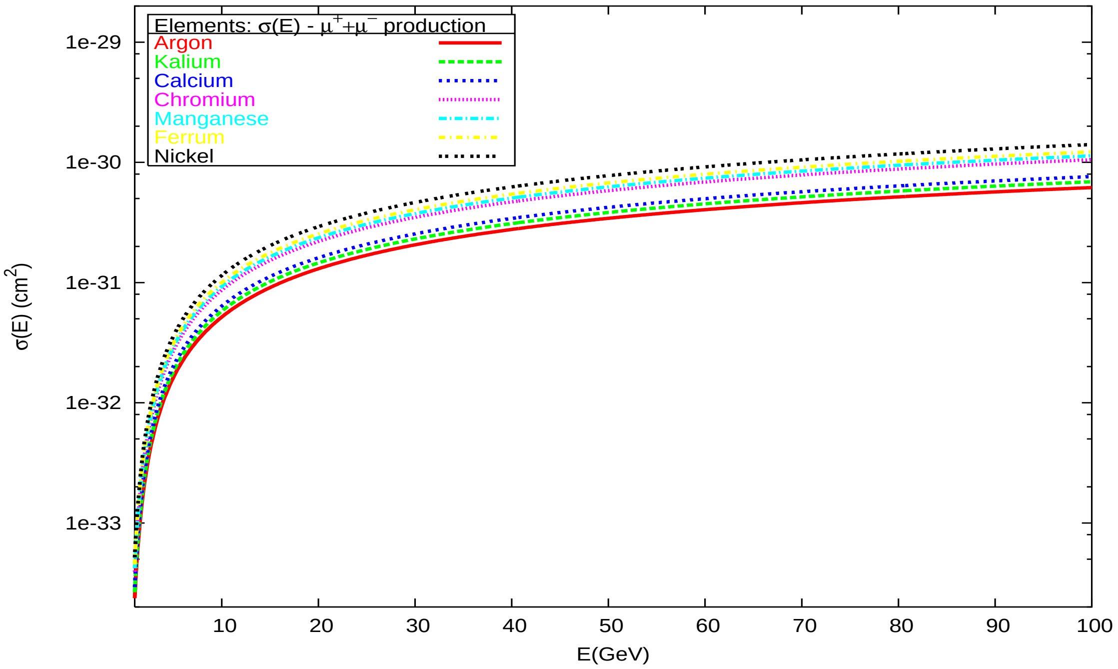

Figure 2.4: Muon trident cross-section per target nucleus, elements II.

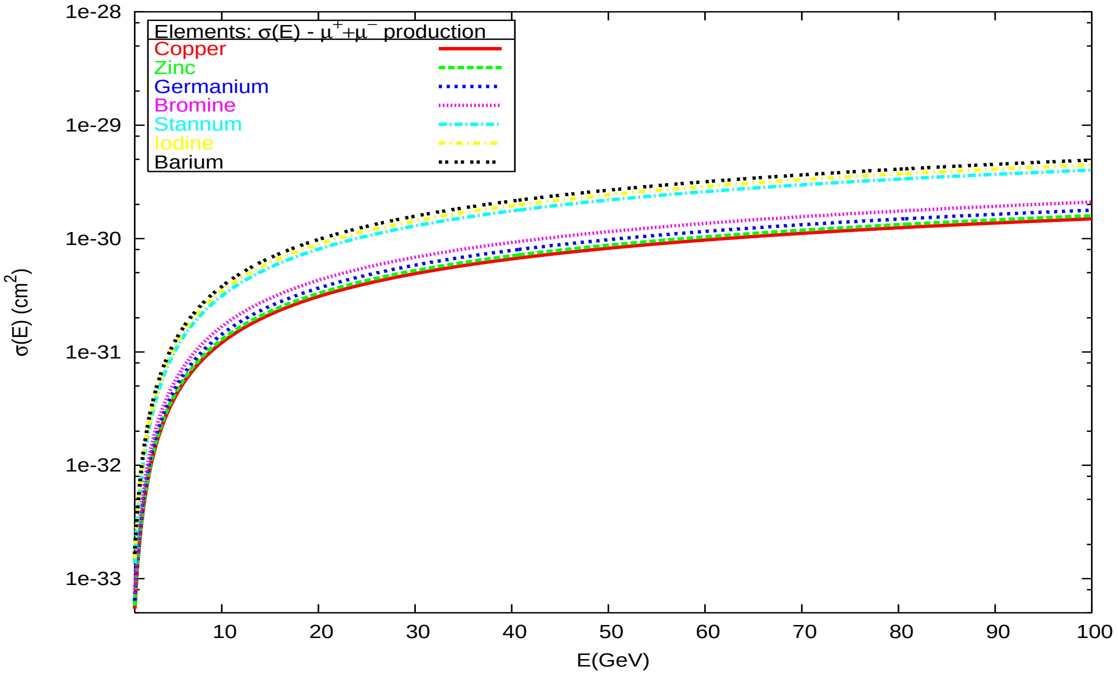

Figure 2.5: Muon trident cross-section per target nucleus, elements III.

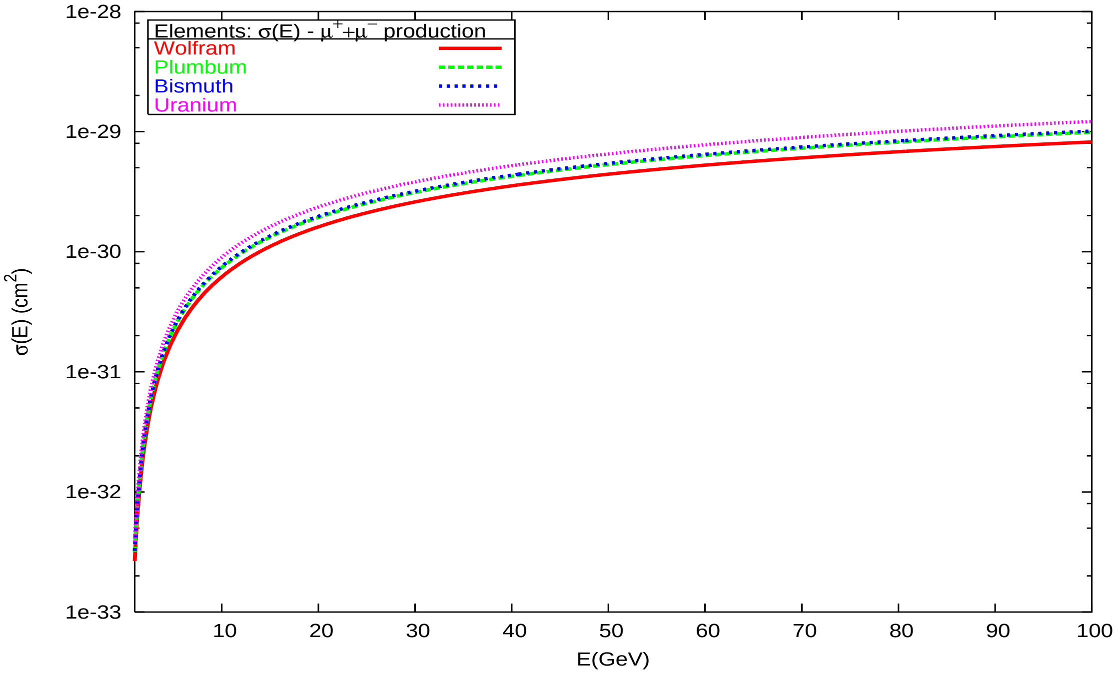

Figure 2.6: Muon trident cross-section per target nucleus, elements IV.

Chapter 3

ALEPH, CosmoALEPH

I do not feel obliged to believe that the same God who has endowed us with sense, reason, and intellect has intended us to forgo their use.
Galileo Galilei

3.1 ALEPH

ALEPH ([Gru96]) was located on the LEP ring at CERN, and it was one of the 4 detectors that detected particles produced in the e^+e^- collisions. It contains several subdetectors, each based on different conception and designed for different purpose. Only part of subdetectors are interesting, from point of view of atmospheric muon detection. Those are: - TPC or Time Projection Chamber, a cylindrical multi-wire detector, with very good time resolution (it allows track reconstruction and implicit momentum estimation, with high precision over broad energy range);
- ECAL or Electromagnetic Calorimeter , that was off during atmospheric muon measurements (it stops the electromagnetic components and thus must be counted);
- HCAL or Hadron Calorimeter (it stops Hadron showers and has track pattern for charged particles);
- Muon chamber (act as verifiers for muon ID).

3.2 CosmoALEPH

CosmoALEPH experiment is a somehow natural extension for ALEPH experiment, by extending the area of interest from beam events to outer-beam generated particles. The latter are atmospheric muons or particles from showers initiated by these muons.

The atmospheric muons are particles produced in cosmic particle induced atmospheric showers. The

Table 3.1: ALEPH subdetectors

Subdetector	main material
Time Projection Chamber (TPC)	Argon-Methane mixture
Electromagnetic Calorimeter (ECAL)	Lead 11.4 cm or 129.39 g/cm^2
Hadron Calorimeter (HCAL)	Iron 120 cm or 944.4 g/cm^2
Muon Chambers	$ArCO_2$ + Isobutane

Figure 3.1: ALEPH detector, view along beam axis

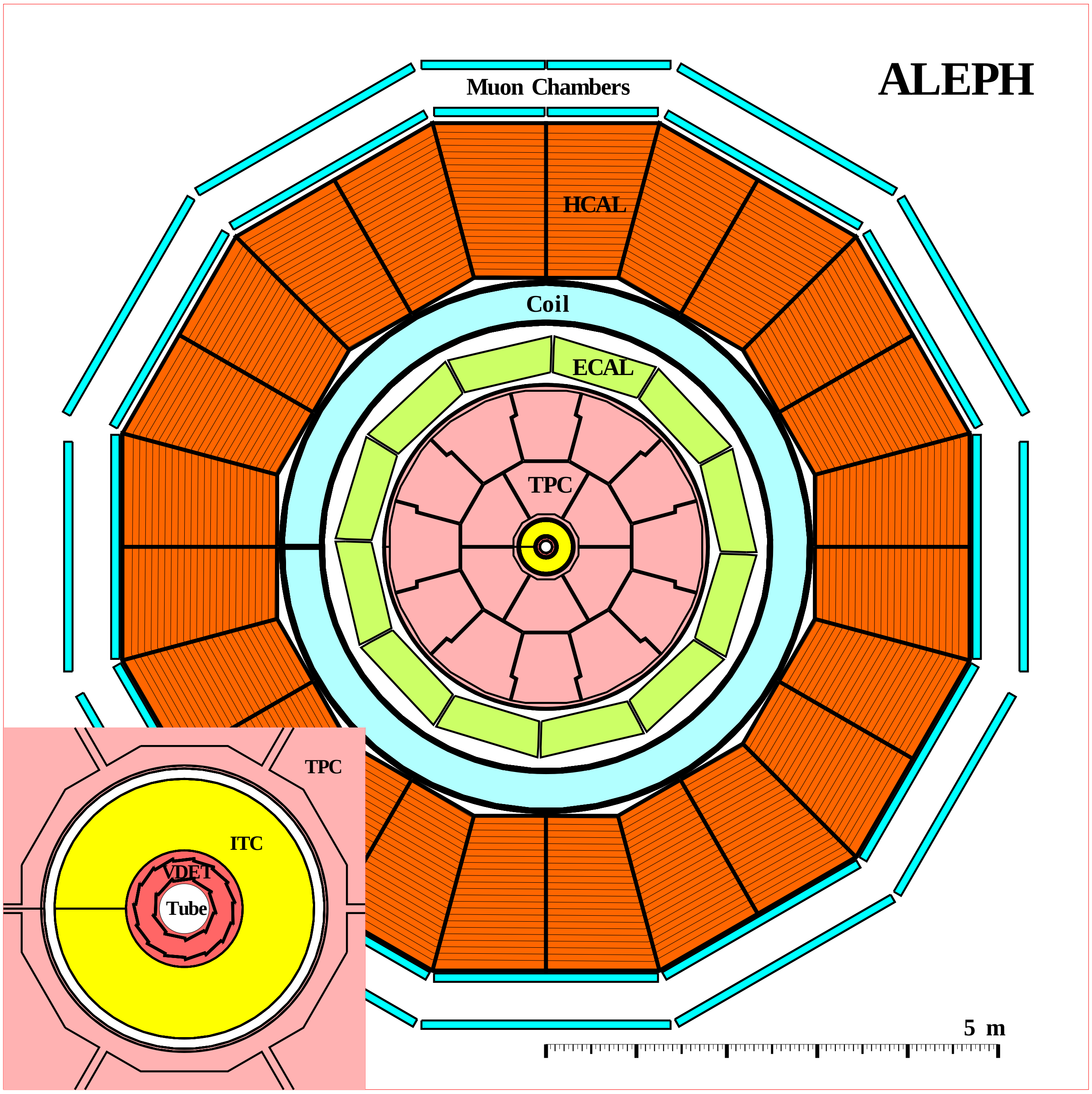

Table 3.2: CosmoALEPH numbers

Rate	2.6 events/second
Total No. events	1 397 015 events
Date	21.04.1999 - 29.04.1999
Fiducial Volume	(TPC) 47.745 m^3

primary particle, a heavy or light nucleus (in gamma astrophysics we can have gammas produced by Inverse Compton process and by synchrotron radiation emissions) produced in extragalactic or galactic outer space, is incident on top of atmosphere with energies up to 10^{21} eV. As the atmosphere becomes more dense, the cosmic primary is scattered by hard interaction and generates bundles of hadrons. The charged component produces an electromagnetic addition to the initiated shower of particles. The latter is not visible underground, because muons coming from $\gamma \to \mu^+\mu^-$ are slow. Only, muons coming from hadron decay are observed underground. These are the atmospheric muons, sometimes called cosmic muons.

CosmoALEPH used ALEPH to record atmospheric muon events. The beam was off during data taking. The period of measurements spanned between 21.04.1999 - 29.04.1999, 6.5 days.

Additional to ALEPH electronics-software, a muon trigger was introduced. HCAL has 23 layers of plastic streamer tubes, and the trigger condition requires 8 hits in one module of HCAL and 8 in one of the opposite three modules. It is a strong condition that rejects most of noise and gives an overall efficiency for muon detection of 80-90% (each layer of HCAL has an approximate 75% detection efficiency).

The CosmoALEPH data analysis tools are the same as those of ALEPH experiment. There is close resemblance between beam di-muon events and atmospheric muons. Muon pattern recognition is identical in both cases.

In contrast with ALEPH di-muons, we must deal with hadronic and electromagnetic showers in TPC. These are produced when a high energy muon penetrates the outer ALEPH layers and suffers bremsstrahlung or photonuclear interaction. Tagging of these events and subsequent separation from trident events are required.

The scope of this study is not to ascertain something about muon spectra underground or at surface, but, I am interested in possible interactions suffered by the penetrating muon. Especially, I am after $\mu^+\mu^-$ pair production by a primary muon.

In this frame, a study of an individual interaction was never tried.

Chapter 4

Energy loss in ALEPH as physical criterion for muon recognition

Few things are harder to put up with than a good example.
Mark Twain

ALEPH's TPC was designed to record the energy deposited by charged particles via ionization. We know that each charged particle with rapid movement relative to background produces ionization as a slowing-down mechanism. Generally, the Bethe-Bloch ionization model estimates the data with high accuracy. Yet, this model main formula gives mean value, and in reality the actual values can differ greatly (e.g. catastrophic energy loss by delta rays). This fact makes, generally, energy loss a not so reliable particle identification criterion.

TPC setup allows sampling of energy loss distribution, for one charged particle, in more than 300 points along the reconstructed track. This gives some degree of confidence to this procedure. There are cuts on raw energy loss estimates that reject part of noise and catastrophic cases. Due to these cuts, the recorded distribution has an unnormalized scale.

Average, model dependent, values can be given for each mass hypothesis. In figure 4.1, I plot the TPC measured values together with electron, muon, pion, kaon and proton average expected values.
Conclusion can be drawn regarding the capacity to identify particles, from energy loss distribution. We see that muon and pion distributions overlap, and can not be distinguished one from the other. The particle that can be separated by this method is electron (or its antimatter counterpart). This is useful to separate $\mu^+\mu^-$ pair productions from e^+e^- pair production.

The second conclusion is that: knock-out protons are visible on display. There seem to be a clear photonuclear signal in TPC energy loss distribution. Thus, the presence of photonuclear interactions (possible background to trident production) is ascertained.

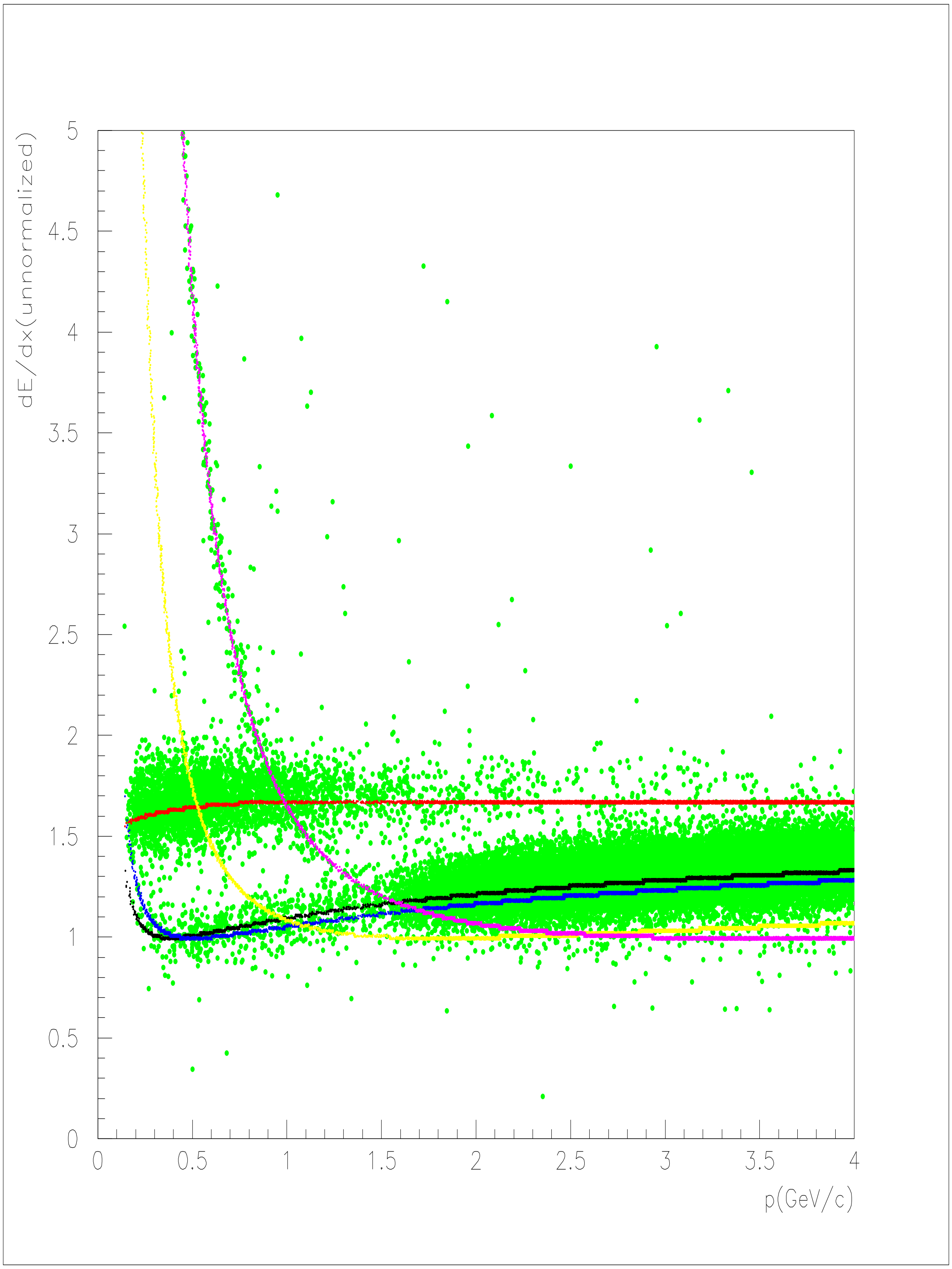

Figure 4.1: Colored diagram for energy loss $\frac{dE}{dx}$ distributions: green dots correspond to experimental values, red to electrons and positrons (expectation mean values), blue to pions, black to muons, yellow to kaons and violet to protons

Chapter 5

Candidate selection criteria

If you find something, it means
that you have not searched enough ...
Aglaja Veteranyi

5.1 Selection conditions

When looking for candidates, we had, at first, to consider the magnitude of muon events number. There are 1.3 million and close to 1 million events reconstructed. It is impossible to thoroughly analyze all, and thus, a preliminary cut on the sample is required. Since most of events are single muon events, we just cut these, and we are left with a multiple muon events sample. This sounds easy, but this cut depends on the efficiency of the algorithm that estimates muons multiplicities. At the moment of this analysis, there was no perfect choice for the reconstruction algorithm (also true in near future at least), and this being said, there could be some non-reconstructed trident events in the thrown-away sample.

The high muon-multiplicity sample is composed of 4091 events. There are: 3753 2-fold multiplicity tagged events, 246 3-fold multiplicity tagged events, 62 4-fold multiplicity tagged events, 13 5-fold multiplicity tagged events, 11 6-fold multiplicity tagged events, 4 7-fold multiplicity tagged events and 2 9-fold multiplicity tagged events. For ALEPH run and event numbers see listing in Appendix. The above numbers must be considered only quantitatively, because the real muon multiplicity in TPC is subject to fluctuations. An initial sample with 131 events was also included in final analysis. This time, each event has only 3-fold multiplicity tag (some of the events are present in both samples).

After selection we are left with two samples of high multiplicity events. To further sift the remaining sample events, I had to remove the events with clear secondaries or shower remnants but without corresponding HCAL hits (only the incident muon has HCAL hits, or the pattern in HCAL is to chaotic to have clear single charged particle ID). The sample removed by this cut should contain: all the e^+e^- pair production events, all the pure electromagnetic showers remnants and a part of the hadronic showers remnants.

Why should be the upper statement correct? It is simple. If we require that any charged track from TPC should have clear track in HCAL, this means the charged particles observed in TPC must pass through ECAL (11 cm of lead plus other material) or an equivalent layer of 21.48 radiation lengths. This will definitively stop electrons, positrons and γ's. The probability to have an unscattered γ or $e^{\pm}$ in HCAL is approximately 10^{-9}. Hadrons can in principle punch through, yet some are stopped or lose energy by hadronization. Indication of a hadronic shower in HCAL would tag a particle leaving ECAL as pion or a heavy hadron (knock-out protons are present, evidence from TPC $\frac{dE}{dx}$ distribution). ECAL is equivalent with a layer of 1-1.3 λ_{int} for a 5 GeV pion (see [Bow95] for details). The muons, as heavy leptonic particle, can scatter in lead only by electromagnetic interactions (the weak interactions can not be considered, "only" for 11 cm of lead). The average energy loss in ECAL for a muon with energy up to several hundred GeV is lower than 0.5 GeV. Since we look for muons with a reconstructed energy higher than 1 GeV, almost all muons (providing there is no catastrophic energy loss) will pass through ECAL.

To separate between cosmic muon triads (coincidences of three muons in TPC) and muon tridents, I look for events with evidence of a vertex (convergence of tracks to a single point). This eliminates events with vertex in overburden. The latter events will, nevertheless, be included in Monte Carlo - they could produce an observable effect in the muon multiplicity distribution of individual events. The upper cut will accept only tridents produced in HCAL iron and ECAL lead.

For end, to separate between hadrons and muons, and remain with events having clear vertex and three or two evident muons, we require that at least two charged particle go through HCAL unscattered. HCAL is equivalent to a 1.2 m iron layer or minimum 7.16 λ_{int} interaction lengths (for pions at 5 GeV). This tags muons in ALEPH with an efficiency of close to 100 % . This cut is applied selectively, and muons with low energy (lower than 2.5 GeV, the energy required to punch through) are still included if they fulfill the other conditions.

These cuts should eliminate all possible sources of background, except muon deep-inelastic scattering followed by decay of pions to muons in flight.

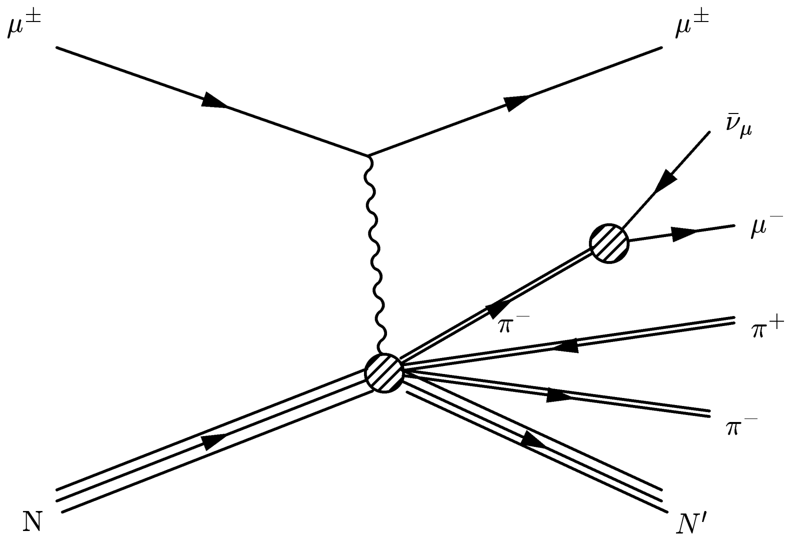

These type of interaction should provide the main source of background for $\mu^+\mu^-$ muon pair production in the field of the nucleus. To separate between contributions, I shrink the sample of candidates, to those events that pass all cuts. Next, I search for hadronic components in TPC or HCAL (for this purpose TPC $\frac{dE}{dx}$ info is useful and also HCAL rim layers, where pions have low probability to reach). Also, if large number of tracks are present in TPC and they converge, this is evidence of showering in upper part of ALEPH. The simultaneous appearance of a muonic triplet or doublet together with evidence of hadronic shower, would rule out trident hypothesis, because deep-inelastic scattering (mainly photonuclear) and tridents are low probability events and, thus, the probability to have both interactions in the same event is negligible. Of course this is not true for $\mu^+\mu^-$ pair production with large momentum and energy transfers to nucleus, where hadronic jets can result, leading to hadronic showers. However this type of interaction is improbable because of two reasons. The incident muon must strike not only the field of nucleus, but individual components within and the Form Factor has lower value due to this localization. Also the virtual photon has to carry high energy and momentum. These facts lead to a severe decrease in the cross-section value. Based on the upper statements, we can assume deep-inelastic trident cross-section to be negligible in our context.

To back up our assumptions we have to see what are the efficiencies for each subdetector.

5.1.1 Hadron calorimeter efficiency

There are 23 planes in the hadron calorimeter, each with close to 75% trigger efficiency ([Bow95]). If we consider the lowest energy muon - 1 GeV - that is considered in TPC, the mean energy loss in ECAL is close to 0.3 GeV. Normally, we should have a penetrating muon in HCAL iron at a depth of $130g/cm^2$ [1]. This corresponds to lower limit of 3 planes of HCAL crossed. The probability to have a pattern in HCAL is 45 % . For 4 planes crossed , this number increases to 75 %. For 5 planes $P = 0.75^5 + 5 \times 0.75^4 \times 0.25 + 10 \times 0.75^3 \times 0.25^2 = 0.90\%$ probability to have pattern in HCAL. For a particle of 1.5 GeV in TPC, the probability to have a track in HCAL (at least 3 hits in HCAL) is (taking the number of transversed planes to be 7):

$$P_{\text{pattern}} = 0.75^7 + 7 \times 0.75^6 \times 0.25 + 21 \times 0.75^5 \times 0.25^2 + 35 \times 0.75^4 \times 0.25^3 + 35 \times 0.75^3 \times 0.25^4 \approx 0.987 \quad (5.1)$$

Only one muon, in 100 muons of 1.5 GeV, will have no distinctive track in HCAL. In principle, for muons with energies higher than 1.5 GeV and with tracks orientated to match a full track in HCAL barrel, we can consider HCAL to be 100% efficient. Pions are subject to strong interaction and this account for higher energy loss of pions in ECAL and HCAL. Practically all pions should stop in HCAL. The only way for a pion to exit ALEPH is by decay to muon.
TPC is considered with an efficiency of 100% and muon chambers act as verifiers.

5.2 Possible candidates

By applying the cuts presented in the previous section, we end up with 13 possible candidates. These are given in tables 5.1 and 5.2. In the same tables there are given possible values of momenta for possible tridents. Each table gives output values of different algorithms. The second algorithm (based on ALEPH software, Julia) is much more robust in multiplicity estimates. Scanning of each event justifies the values of Julia output, within [0.3GeV,100 GeV] range. The first algorithm appears to be less robust from point of view of error and track ID. During analysis I have chosen to use the values provided by Julia if the energies involved were lower than 100 GeV (at low energy the tracks are rejected by 1 GeV cut, see 5.1). Sometimes, if the event has a complex "topology" (hadronic shower with multiple components in TPC), it is impossible to find a right choice for trident primary and secondaries, and in this case the momenta values are missing. Also, for cases when the number of fit points is small and/or the values of particle

[1] ECAL has $x = 129g/cm^2$ and energy loss $\frac{dE}{dx} \approx 0.002GeV/g/cm^2$. HCAL has 1.2 m of iron and an equivalent of $944.4g/cm^2$. Energy loss is, again, close to $0.002GeV/g/cm^2$. This gives an average energy loss in HCAL-iron close to 2 GeV, and a 0.1 GeV per HCAL-plane. A muon with 0.7 GeV should cross in average 6 planes of HCAL before coming to rest. The curvature of track radius should decrease this number , but a lower limit of 3 planes is resonable assumption.

Table 5.1: Events that exhibit some of the characteristics required by tridents ID conditions. Reconstructed momenta for possible secondaries and primaries are listed; first reconstruction algorithm results

run	event	multiplicity	momenta no.	$P_{max}(\frac{GeV}{c})$	$P_1(\frac{GeV}{c})$	$P_2(\frac{GeV}{c})$
49050	9642	5	5	14.0 ± 0.4	9.57 ± 0.01	2.6 ± 0.02
49055	6580	2	4	40.2 ± 0.2	1.625 ± 0.010	1.5 ± 0.2
49056	20965	2	3	40.4956 ± 0.0003	1.211 ± 0.005	-
49061	18897	3	4	183 ± 18	25 ± 3.0	-
49066	2909	2	3	81.821 ± 0.002	1.48 ± 0.10	1.3081 ± 0.0006
49068	14055	5	5	-	-	-
49082	22181	4	4	59.211 ± 0.002	6.708 ± 0.006	1.997 ± 0.005
49089	34710	3	3	77.585 ± 0.003	12.956 ± 0.003	2.290 ± 0.005
49092	15133	2	2	473 ± 1.2	14.4 ± 0.2	-
49093	15966	(1)3	3	473 ± 183	3.86 ± 571	2.32 ± 571
49097	13832	3	3	-	-	-
49100	9231	1(3)	2	45.8 ± 4.0	-	$1.267 \pm 26.$
49155	5401	5	5	-	3.08 ± 0.02	-
49155	17356	4	4	165.71 ± 0.06	10.84 ± 0.06	1.26 ± 0.2

energy too high, estimated relative errors higher than 100% can arise.

As we shall see in the next section from the upper sample only two candidates will fulfill all condition (close to 100% probability for trident ID). The last cut for background rejection, must sift tridents from deep-inelastic photonuclear interaction with muons as remnants. To be able to apply this cut, we have to identify hadronic showers. This is done by: counting the number of charged particle in TPC, analyzing $\frac{dE}{dx}$ information and estimating the fraction of tracks with extensions in HCAL. ECAL penetrating particles are heavy mass particles (muons, pions, kaons). The electrons and positrons of an electromagnetic shower should be all stopped within lead layers of ECAL. Gammas initiate electromagnetic shower that would have only shallow penetration length in HCAL (first two layers).

Images 5.1 and 5.2 display a muon photonuclear interaction followed by hadronic shower in TPC and, possibly, electron-positron production in the silicon layer that covers the beam pipe (ALEPH vertex detector). This event is tagged as hadronic shower by: the multitude of charged particles 17 ± 3 (there could be some electromagnetic processes in Inner Track Detector) of the shower, the fact that most for charged tracks in TPC have shallow track extension in HCAL, and more, these extensions lack the single-track pattern, resembling hadron showers produced by hadrons in HCAL iron. The particles that penetrate deeply in HCAL seem to produce secondary particles, too. Even though most of the charged particles in TPC pass the energy criterion to punch through HCAL, they just stop in HCAL, pointing in this way to an additional energy loss mechanism (production of hadrons by hadrons) that is not probable in lepton propagation. $\frac{dE}{dx}$ info for this event is not as conclusive as for other cases. It is not possible to reject hadronic or electromagnetic hypothesis based on TPC energy loss information, yet quantitatively, the hadron hypothesis seem favored. There is no evidence to support electromagnetic hypothesis, thus the shower must be tagged as hadron shower with photonuclear vertex in ECAL.

Other hadron events are displayed in Appendix.

Table 5.2: Events that exhibit some of the characteristics required by tridents ID conditions. Reconstructed momenta for possible secondaries and primaries are listed; second reconstruction algorithm results.

run	event	multiplicity	momenta no.	$P_{max}(\frac{GeV}{c})$	$P_1(\frac{GeV}{c})$	$P_2(\frac{GeV}{c})$
49050	9642	12	12	160 ± 58	17.4 ± 0.66	6.55 ± 0.11
49055	6580	7	7	28.5 ± 41	3.6 ± 1.4	1.57 ± 0.3
49056	20965	7	7	32 ± 11	1.72 ± 0.07	1.21 ± 0.03
49061	18897	8	8	29 ± 15	9.5 ± 2.3	7.6 ± 0.31 or 6.3 ± 0.23
49066	2909	5	5	106 ± 96	3.33 ± 0.78	1.05 ± 0.01
49068	14055	17	17	27.5 ± 2.4	1.07 ± 0.01	-
49082	22181	4	4	63 ± 12	6.9 ± 0.6	1.98 ± 0.04
49089	34710	3	3	89.2 ± 21.1	13.40 ± 0.46	2.26 ± 0.04
49092	15133	3	3	366 ± 695	32 ± 16	12.3 ± 0.9
49093	15966	4	4	196 ± 236	3.15 ± 0.3	2.3 ± 0.02
49097	13832	16	16	331	1.325 ± 0.007	-
49100	9231	3	3	45.8 ± 4.4	10.16 ± 0.33	1.26 ± 0.02
49155	5401	9	9	258 ± 178	3.18 ± 0.08	2.215 ± 0.014
49155	17356	7	7	484 ± 953	10.67 ± 0.36	1.96 ± 0.02

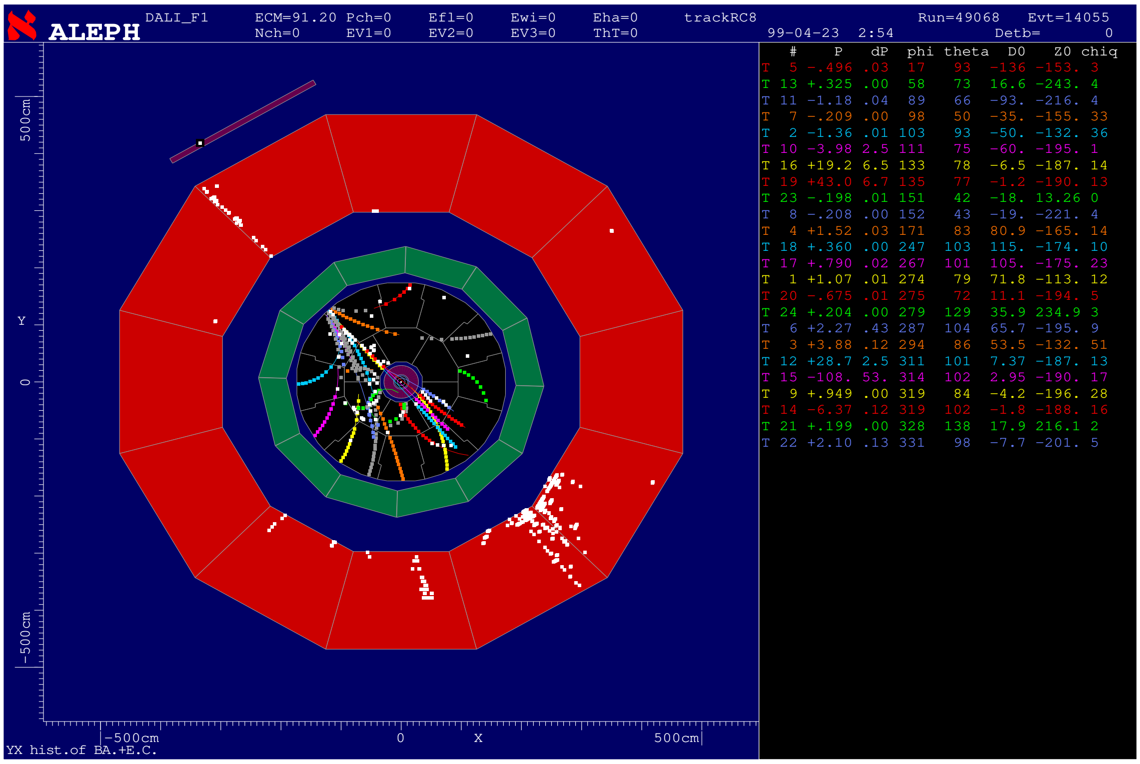

Made on 4-May-2004 19:49:58 by maciuc with DALI_F1.
Filename: DC049068_014055_040504_1949.PS

Figure 5.1: First hadronic event with vertex in HCAL or ECAL

End of tracks

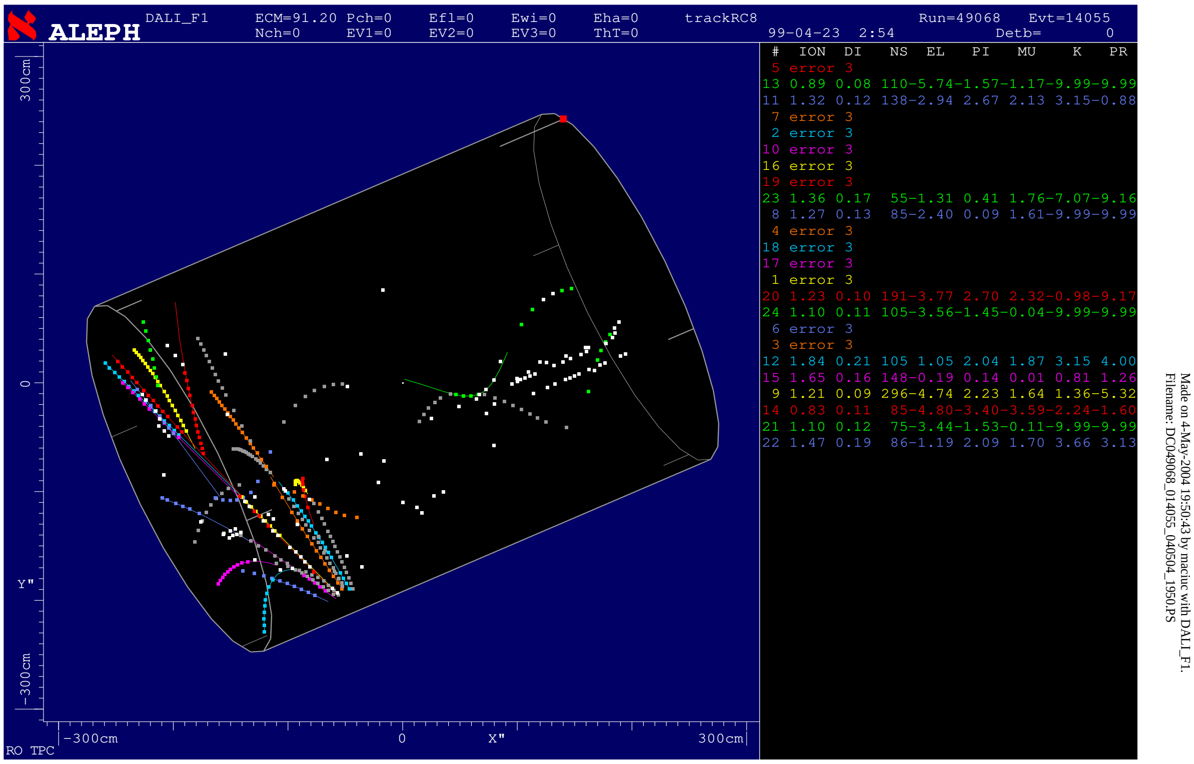

Figure 5.2: First hadronic event with vertex in HCAL or ECAL; $\frac{dE}{dx}$ is not reconstructed in some cases, generating "error 3" label (missing bank for energy loss info)

5.3 Final sample of Candidates

Two events can be explained only by $\mu^+\mu^-$ production by muon in detector layers or some other lower probability mechanism (arrival of three muons on same path, photonuclear interaction with production of three rapidly decaying pions, etc). These events have the distinct features that we would expect for tridents:
• convergence to a possible vertex;
• three charge particle tracks with opposite charge for the less energetic particles;
• only one visible track in HCAL upper side;
• HCAL tracks for all three particles on the lower side of HCAL (rules out low mass leptons);
• the energy loss and/or track length in HCAL is consistent with muon hypothesis;
• muon chambers trigger for at least one of the alleged secondaries (for primary as well but the primary has, usually, clear cut double HCAL track ruling out any doubts);
• for each track, $\frac{dE}{dx}$ info favors or is neutral towards muon hypothesis;
• absence of hadronic shower;
• high energetic alleged primary, low energetic alleged secondaries relative to primary energy;
• well reconstructed tracks (no erratic behavior for TPC reconstructed dots), for very high energy, problems with momenta estimates will be acceptable;
• after a blind analysis (removal of hadronic events, from real data, was done posteriorly to Monte Carlo analysis), **agreement with Monte Carlo values** (see chapter 7), at level of trident number, particles energies and vertex positions, was found.

5.3.1 First $\mu^+\mu^-$ pair production event

The first event is composed of three very high energy particles. All three particles have tracks in HCAL, and all reach the other side of ALEPH, triggering the muon chambers. There is high degree of collinearity for the tracks, two tracks being almost indistinguishable. Due to this, the presumed primary track is only half reconstructed. This causes problems with momentum estimates because only one half of TPC track can be used to estimate the dynamical attributes of the particle. $\frac{dE}{dx}$ distribution is reconstructed only for the low energy particle. The reconstructed energies (momenta, but for this values they are equal) are:
- primary with 366 ± 695 GeV , we have no reliable estimate for primary track because of very high momentum and the low sampling points number in TPC;
- higher energy secondary $31.9 \pm 16.$ GeV with only one segment (half of TPC) giving momentum error estimate, the second segment is reconstructed, but gives no error estimate;
- lower energy secondary has a track, that is fully reconstructed, each segment in TPC gives 9.78 ± 2.1 GeV and 12.9 ± 0.98 GeV with a weighted average of 12.3 ± 0.9 GeV.

For last track, $\frac{dE}{dx}$ is generated and in agreement with pion or muon hypotheses (higher mass and lower mass hypotheses appear to be rejected). There is lack of any hadronic evidence in HCAL, no perturbation in HCAL tracks of the particles are seen. The extensions of the muon tracks in HCAL are clear and the reconstruction dots are collinear. Given a width of 8.5 radiation lengths for 5 GeV pion in ECAL-HCAL combined layer, the probability that two particles from the triad are pions is close to 5×10^{-8}. Probability that all are muons is close to 100%. Some remnant noise plagues the event, yet, the reconstructed positions are far from tracks and have no impact on track reconstruction.

It is reasonable to assume pion decay hypothesis as having negligible probability for this particular event. At these energies $E_1 \approx 32$ GeV and $E_2 \approx 12.3$ GeV - here only the assumed secondaries - we have

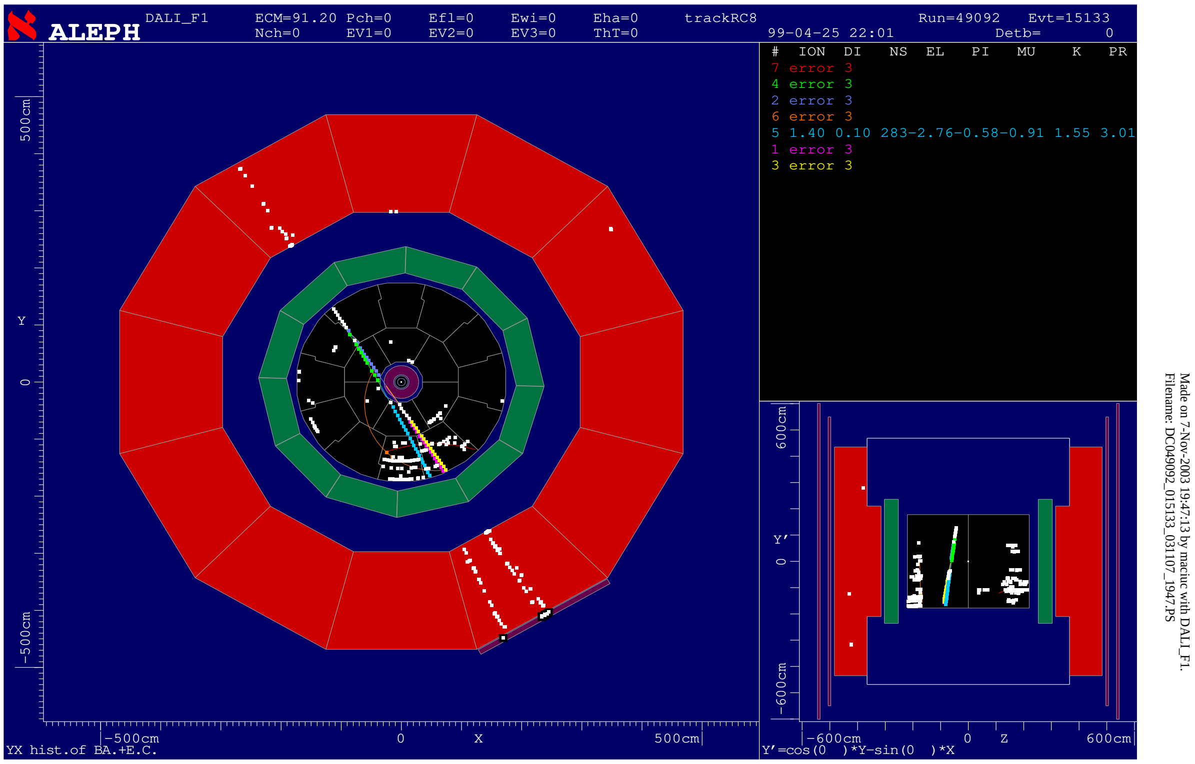

Figure 5.3: First trident event with vertex in HCAL or ECAL: sectional view

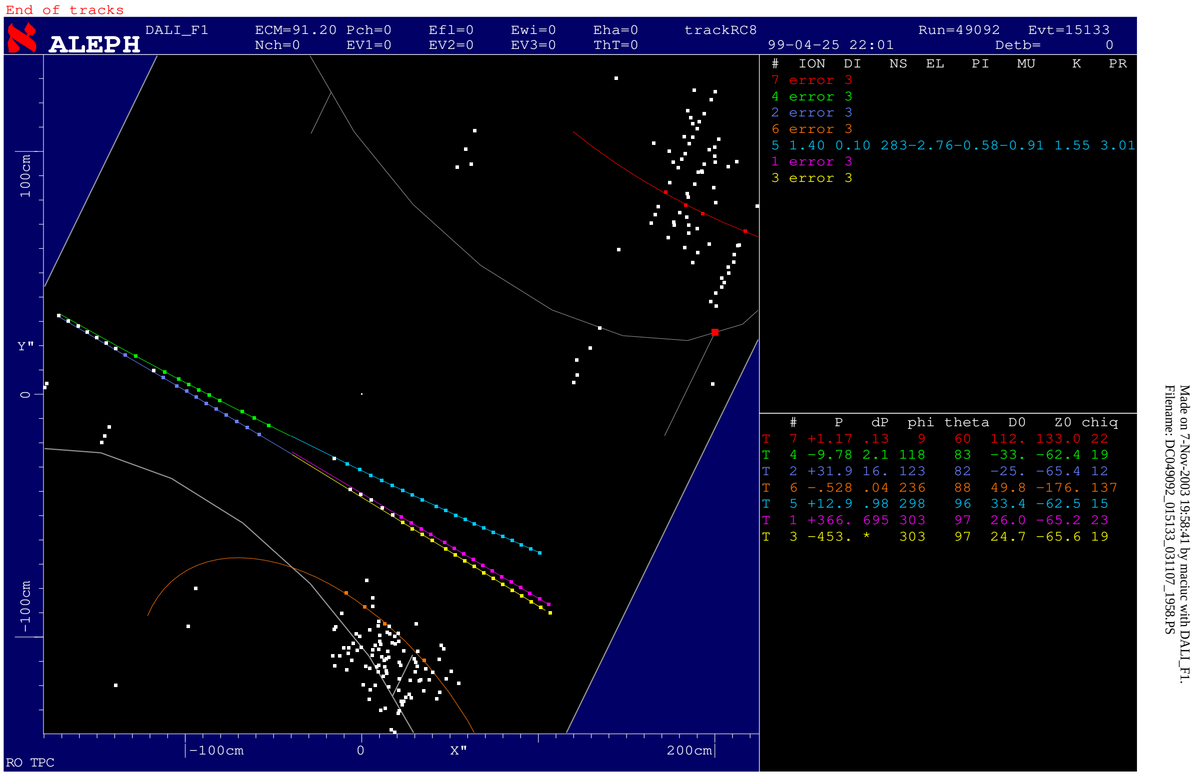

Figure 5.4: First trident event with vertex in HCAL or ECAL: 3d view

$\gamma_1 = 239$ and $\gamma_2 = 92$ respectively. The equivalent life times, for pions, are $6.2\mu s$ and $2.4\mu s$ respectively (rest frame lifetime close to 26 ns). The time needed by a particle, with velocity close to light speed, to cross ALEPH is of the order of 20ns. We can safely forget about pion hypothesis in this peculiar case.

Common origin or vertex location could be in HCAL, ECAL or proximity of ALEPH (due to high energy of the observed trinity, it may be only one incident track at ALEPH point of entry).

Unless by a strange coincidence there are three atmospheric muons coming on same path through overburden (hard to imagine, because of the radiative processes that dominate the energy loss at these energies), event 15133 of run 49092 is a trident or a $\mu^+\mu^-$ pair production by an atmospheric muon.

5.3.2 Second $\mu^+\mu^-$ pair production event

The second muon event contains a triad of charged particles fully consistent with muon triple coincidence in TPC. The tracks have all the features expected for a trident:
- opposite charge for low energy particles;
- HCAL tracks consistent with energy loss and two punch through tracks;
- convergence to a common vertex in HCAL;
- absence of hadronic features, facts that reject hadronic hypothesis (e. g. absence of hadron production in HCAL in conjunction with high energy for at least two particles, crystal clear and highly linear tracks in HCAL);
- good quality reconstructed $\frac{dE}{dx}$ distribution for two segmented tracks, that is consistent with pion and muon hypothesis, one $\frac{dE}{dx}$ distribution appear to favor an electron hypothesis, but the energy domain corresponds to overlap of distributions;
- two triggered muon chambers for two distinctive tracks;
- one low energy track that stops in HCAL and has overall energy loss in concordance with muon energy loss for the same path;
- there is absolutely no evidence for other particles in TPC.

This event has only negligible noise, and mostly, it is connected with space points that do not count in reconstruction algorithm. More, those reconstructed points associated with noise, lay on the subsequent reconstructed path of the particles (it happens when two or more tracks overlap).

Dynamic properties of particles are:
- for primary particle Julia reconstruction algorithm provides three segments, each with reconstructed momentum of 45.8 ± 4.4 GeV/c, $74.8 \pm 62.$ GeV/c and 3.39 ± 2.2 GeV/c respectively (the large difference is normal because the last segments are reconstructed based on low number of sampling point - the last event on 4 sampling points, whereas helix fit need at least 5 points);
- I consider the energy of primary to be 45.8 ± 4.4 GeV;
- high energy secondary has a TPC track that is partitioned, again, in three segments 10.2 ± 0.33 GeV, 9.16 ± 1.7GeV and 4.67 ± 3.6 GeV (last segment with only 5 reconstruction points);
- the energy for first secondary can be estimated from weighted average of the segment energies (excluding a segment without large number of reconstruction points) 10.2 ± 0.33 GeV - same as first segment energy;
- the last secondary has only one segment, with 1.26 ± 0.02 GeV reconstructed energy.

We have a shift in directions of two tracks, at the membrane between TPC halves. This is due to an absolute time difference between one side of TPC and other. It is a common characteristic of CosmoALEPH runs.

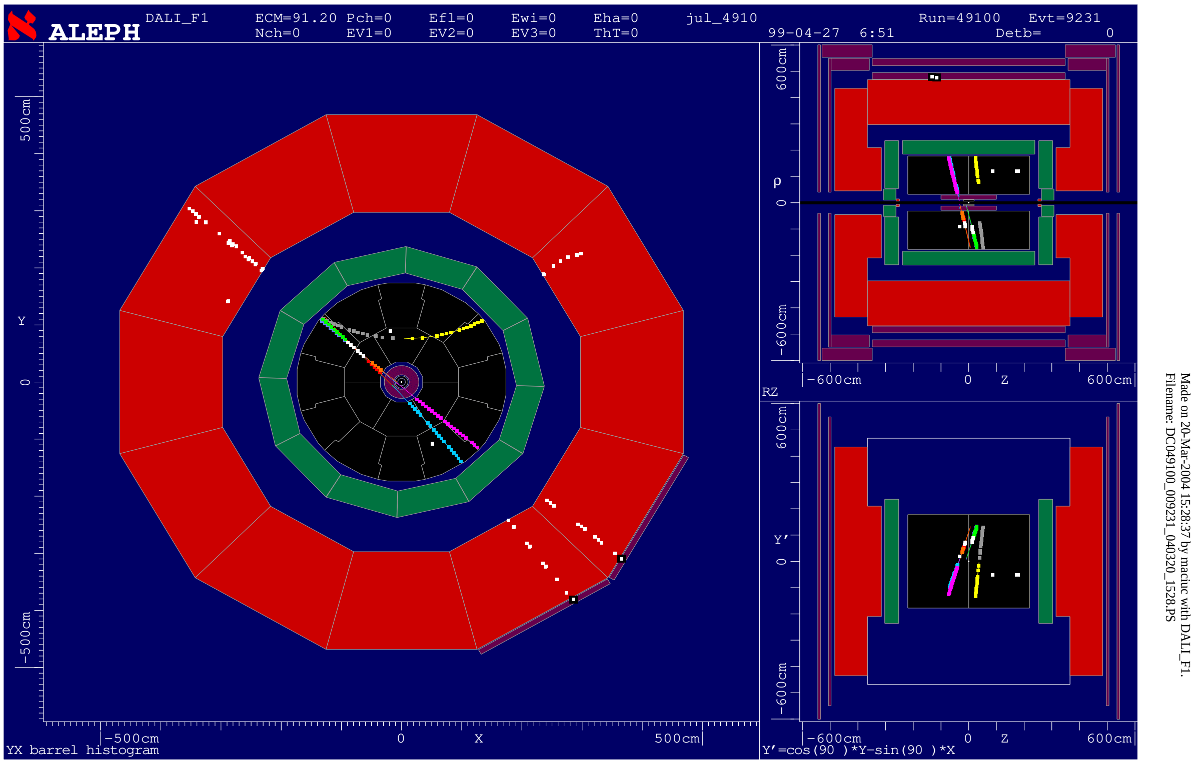

Figure 5.5: Second trident event with vertex in HCAL or ECAL: sectional view

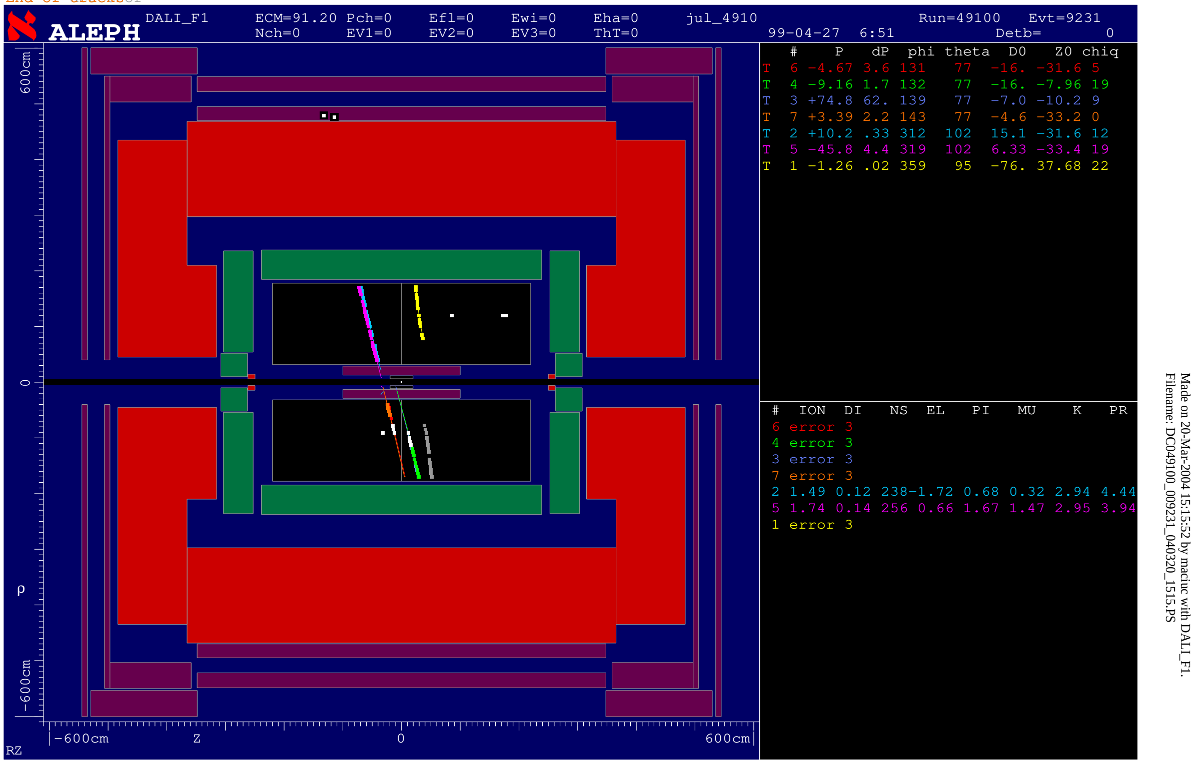

Figure 5.6: Second trident event with vertex in HCAL or ECAL: 3d view

5.4 Experimental cross-section

The following deductions should be taken qualitativley and not "ad literam". They regard a physical quantity, that is not exactly an observable for CosmoALEPH framework. The cross-sections should be gauged in experiments with constant $\sqrt{s}$, were the energy distribution, in center of mass, is equal to Dirac distribution.

In our case, we have a continuum, and more, the atmospheric muon energies span a very large domain. Here, a cross-section estimate must be qualitative, due to non-liniar composition between muon spectrum and interaction probability, the latter is function of muon energy. There are, as it will be seen below, technical dificulties too.

In this section, I use some of the results of an extrapolation procedure presented in chapter 6. The procedure estimates the spectrum of muons at different boundaries: TPC rim (the experimental data), ECAL rim (values extrapolated through ECAL), HCAL rim (spectrum of muons incident in ALEPH), soil-molasse separation zone (the values of muon energies extrapolated to this level), ground level (muon spectrum at surface). The overburden thickness is round 18500 g/cm^2 for a molasse layer and 11500 g/cm^2 for a soil layer. The energy loss, for each muon, is calculated by an iterative method, and the energy values are updated at each sub-layer (a choice of 1000 sub-layers, for each overburden layer, was considered here). The results of this procedure are plotted in the compound graph 5.7. For now, the values of interest are: the average energy for muons incoming in HCAL of 68$\pm$99.8 GeV and the number of detected muons (close to 950000). It can be seen, that even average energy is an elusive concept in present case (because of the spectrum shape). However, I consider the muon energy to be, successively, 40 GeV, 70 GeV and 100 GeV.

To deduce an estimate for the trident cross-section, I make use of the following relations:

$$\Phi(cm^2/g) = \frac{N_A}{A}\sigma \times \epsilon = \frac{\text{number of observed events}}{\text{number of projectiles}} \frac{1}{\text{target thickness}} \tag{5.2}$$

where: Φ rate of interaction, ϵ overall efficiency, N_A Avogadro number, A atomic weight of target material (HCAL iron) and σ value to be estimated. The parmeter ϵ is function of muon energy.

Now we know the number of observed tridents to be 2. As first approximation we take $\epsilon \lessapprox 1$. The estimate of interaction rate is: $\Phi = \frac{2}{9.5 \cdot 10^5 \cdot 944 g/cm^2} = 2.2 \times 10^{-9} \mathrm{g/cm^2}^{-1}$. Thus, the cross-section estimate is: $\sigma = 2.1 \times 10^{-31}$ cm. Here the thickness of target is considered HCAL radial thickness of 944 g/cm^2, ECAL will be neglected, but only in this section.

The theoretical values for cross-section are: $5.4 \times 10^{-31}\,\mathrm{cm}^2$ for 40 GeV muons, $9.1 \times 10^{-31}\,\mathrm{cm}^2$ for 70 GeV muons and $1.2 \times 10^{-30}\,\mathrm{cm}^2$ for 100 GeV muons.

To get a better estimate of ϵ, I have run the Monte Carlo program of chapter 6 with all muons set to 40 GeV, 70 GeV and 100 GeV (again this only for this section, later the full observed spectrum will be used). The fraction of the real events (2 observed events) to total MC estimate, represents an estimate of efficiency. The numbers are: 13 tridents in HCAL for 40 GeV muons, 17 tridents for 70 GeV muons and 28 tridents in HCAL for 100 GeV muons. The estimates for efficiency are: 0.15 ± 0.08 at 40 GeV, 0.12 ± 0.06 at 70 GeV and 0.07 ± 0.036 at 100 GeV. In view of the selection procedure and imposed cuts of candidate events, these values for efficiency appear to be not unrealistic.

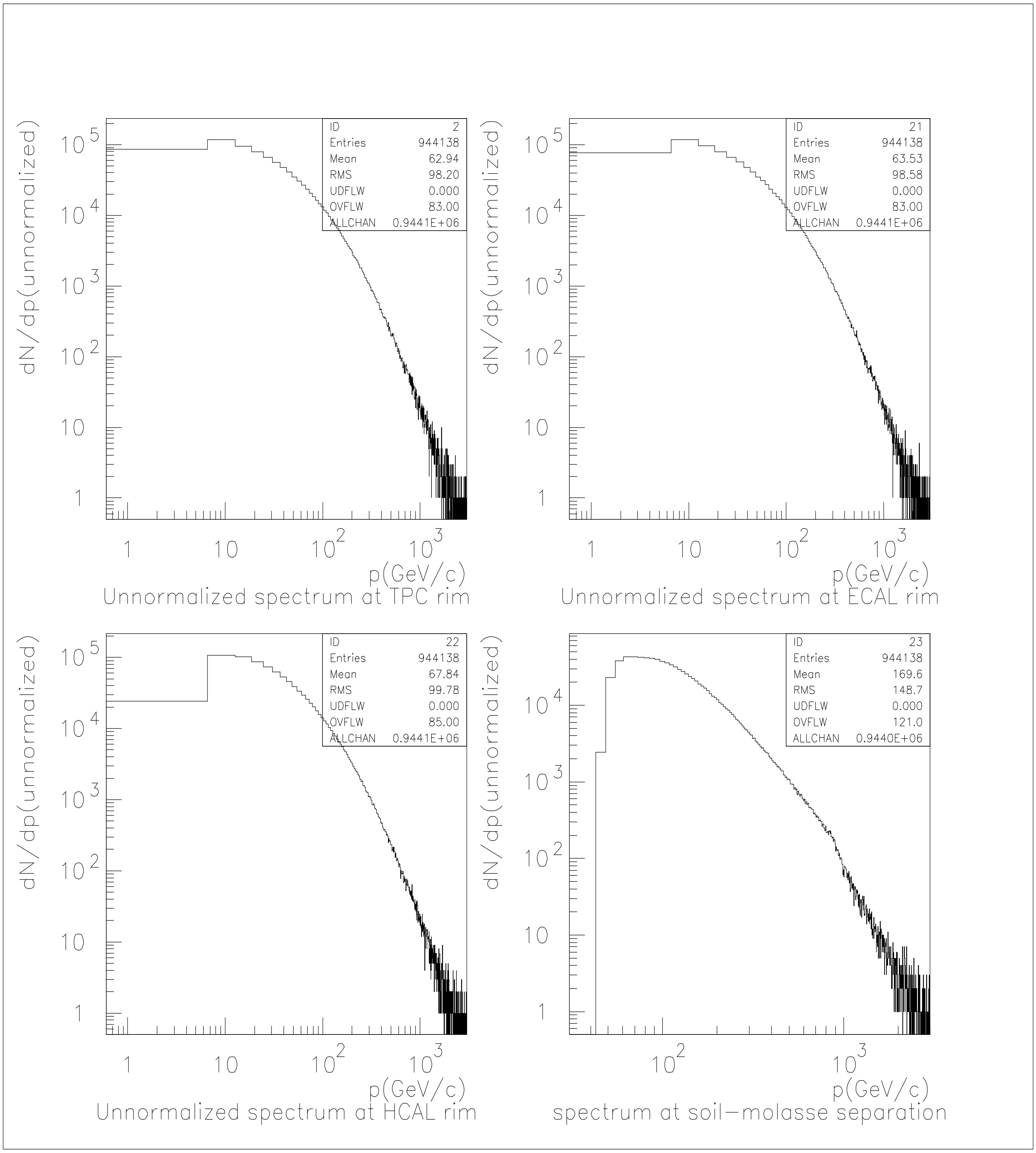

Figure 5.7: Unnormalized muon spectrum at layers separation boundaries: estimated values after extrapolation from ALEPH level to surface (results of extrapolation procedure)

The new estimates for trident cross-section are: $1.4 \pm 1.22 \times 10^{-30}$ cm^2 for 40 GeV, $1.75 \pm 1.52 \times 10^{-30}$ cm^2 for 70 GeV and $3 \pm 2.61 \times 10^{-30}$ cm^2 for 100 GeV. Error propagation analysis takes into account: the thickness error (≈ 0.5 or 50% relative error, due to slant thickness), the efficiency error (an underestimate probably, ≈ 0.5 or 50%), the error in number of observed events (conservatively set to 50%) and the number of incident muons that is considered with negligible error.

The latter assumption, is based on several underlying facts: close to 100% efficiency in ALEPH fiducial volume (the trigger efficiency can be neglected here because we are interested only on those events where the primary muon is "seen"), high reconstruction efficiency for events with one muon and energy above 5GeV (99.5 % of total sample), negligible contribution from low energy part of spectrum (improbable tridents) and inverse power law distribution for events with very high energy (above 100 GeV).

To speed up the precedent calculation, I have neglected the correlation factor between efficiency and number of observed events, because it is proportional to the inverse of Monte Carlo number: 1/13, 1/17 and 1/28. The error introduced in error estimate should be much smaller than the cross-section error.

In figure 5.8 the extrapolated surface spectrum is displayed. There are two estimates here: for muon energy extrapolated numerically and for muon extrapolated by an energy loss formula (see formula 5.3 below).

$$\frac{dE}{dx} = b \times E + a \Rightarrow E_{surface} = E_{ALEPH} \times exp\left(x_{depth} b\right) + \frac{a}{b}\left[exp\left(x_{depth} b\right) - 1\right] \tag{5.3}$$

here a, b are taken as constants (rough approximation, they are normally functions of energy) $a = 0.0022\mathrm{GeV/g/cm^2}$ and $b = 4 \times 10^{-6}\left(\mathrm{g/cm^2}\right)^{-1}$, and x_{depth} is the ALEPH depth level (≈ 320 m.w.e or meter water equivalent for vertical atmospheric muons).

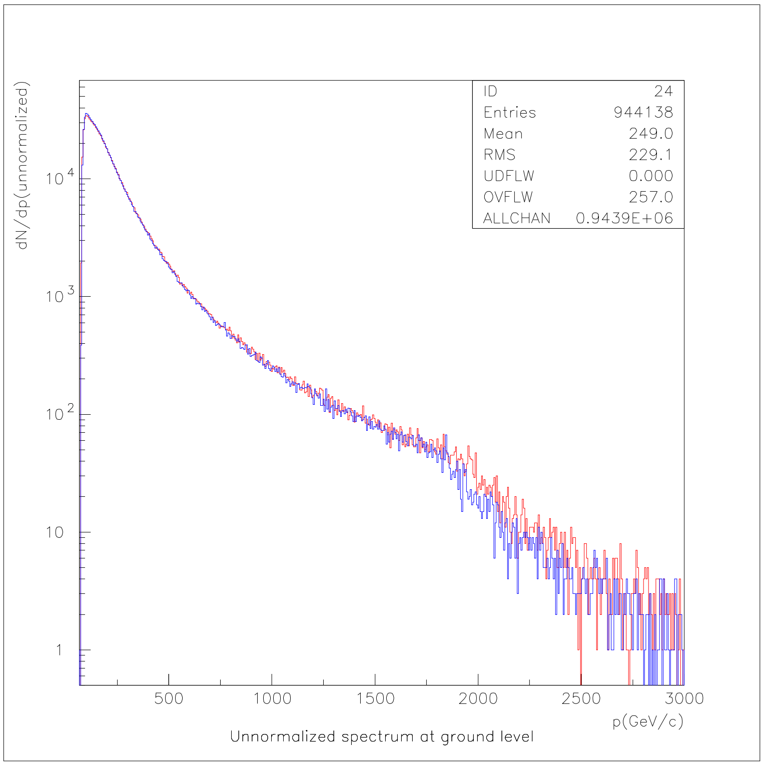

Figure 5.8: Unnormalized muon spectrum at surface: red is the extrapolation procedure result and blue is the estimation based on parameterized energy loss formula

Chapter 6

Monte Carlo

A nous deux maintenant!
Rastignac
(in *Le père Goriot*
by Honoré de Balzac)

As stated in introduction, the lack of a professional Monte Carlo that includes $\mu^+\mu^-$ pair production imposes development of a new Monte Carlo that would include besides usual interactions a wholly or partially stochastic trident process.

Other interactions relevant for energy loss mechanism, are: ionization, bremsstrahlung, e^+e^- pair production and photonuclear.

The upper interactions are treated as continuous energy losses, thus, we simply take mean values of energy loss contributions. Of course, as we shall see, this is not exactly justified for bremsstrahlung and photonuclear interactions. Yet, given the limited time allocated to this study, we have no alternative but to suppose that lack of stochasticity will not ultimately affect the physical results. The upper Ansatz is posteriorly checked. In any case, Monte Carlo method is just a checkup of experimental data consistency and coherence.

6.1 Physics of muon transport in materials

Muons are experiencing two types of interaction, one with electrons of atoms and one with the field of nucleus. The latter interactions are the so called radiative processes. An incident muon strikes the virtual photon cloud surrounding nucleus, leading to formation of secondary particles (for photonuclear processes, the virtual cloud of incident muon interacts with nucleons). Radiative energy loss in compound/mixture materials is simply superposition of individual element contributions.

In case of ionization, the targets are essentially atomic electrons. Because of Ionization Potential term, (see 6.1 formula), energy loss in compound/mixture should be computed non-linearly from the contribution of each element.

6.1.1 Ionization produced by muon in elements, compounds and mixtures

Ionization is the dominant energy loss mechanism for muons with energy below critical energy E_c. E_c is a material dependent parameter, and generally has a magnitude of hundreds GeV. At this energy the

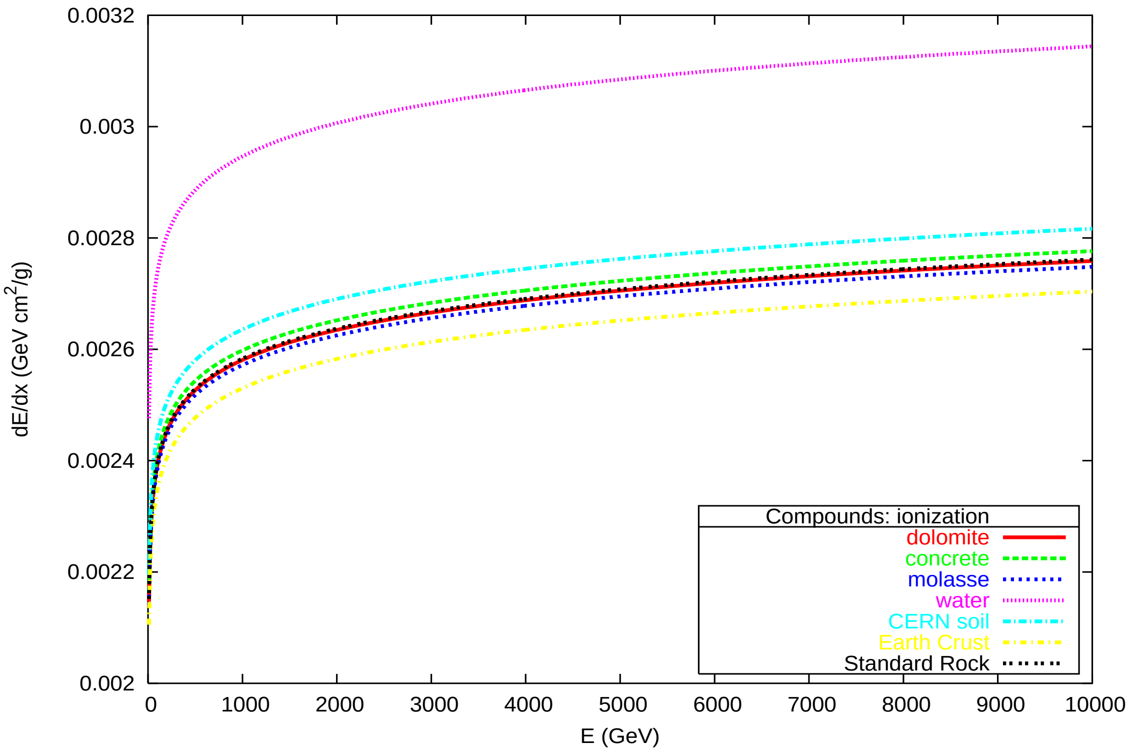

Figure 6.1: Muon energy loss by ionization in 7 compounds

energy loss of muon by ionization equals in value the radiative counterpart.

For an ultra-relativistic muon ([WLV85]):

$$\frac{dE}{dx} = 2\pi\alpha^2 N_A \lambda_e^2 \frac{Zm_e}{A\beta^2}\left\{ln\frac{2m_e\beta^2\gamma^2E'_m}{I^2(Z)} - 2\beta^2 + \frac{E'^2_m}{4E^2} - \delta(\gamma)\right\} \tag{6.1}$$

Bethe-Bloch formula for a muon with energy between 1-10000 GeV, $E > m_\mu$. For explicit form and definition of parameters see appendix.

The density correction δ and Ionization potential $I(Z)$ are the non-trivial parts of Bethe-Bloch formula. Density corrections are necessary for high energy muons due to polarization of media under the influence of the relativistically "compressed" muon field. Ionization potentials are larger in compounds than in simple elements.

For compounds and mixtures the straightforward generalization of 6.1 leads to:

$$\left\langle\frac{Z}{A}\right\rangle = \frac{\langle Z\rangle}{\langle A\rangle} = \frac{\sum_i Z_i w'_i}{\sum_j A_j w'_j} = \sum_i \frac{Z_i}{A_i} w_i \tag{6.2}$$

where w'_i is the number fraction for each element and w_i is the weight of each element in compound/mixture;

$$\langle I\rangle = exp\left[\frac{\sum_i w_i \frac{Z_i}{A_i} ln\,(I_i)}{\langle\frac{Z}{A}\rangle}\right] \tag{6.3}$$

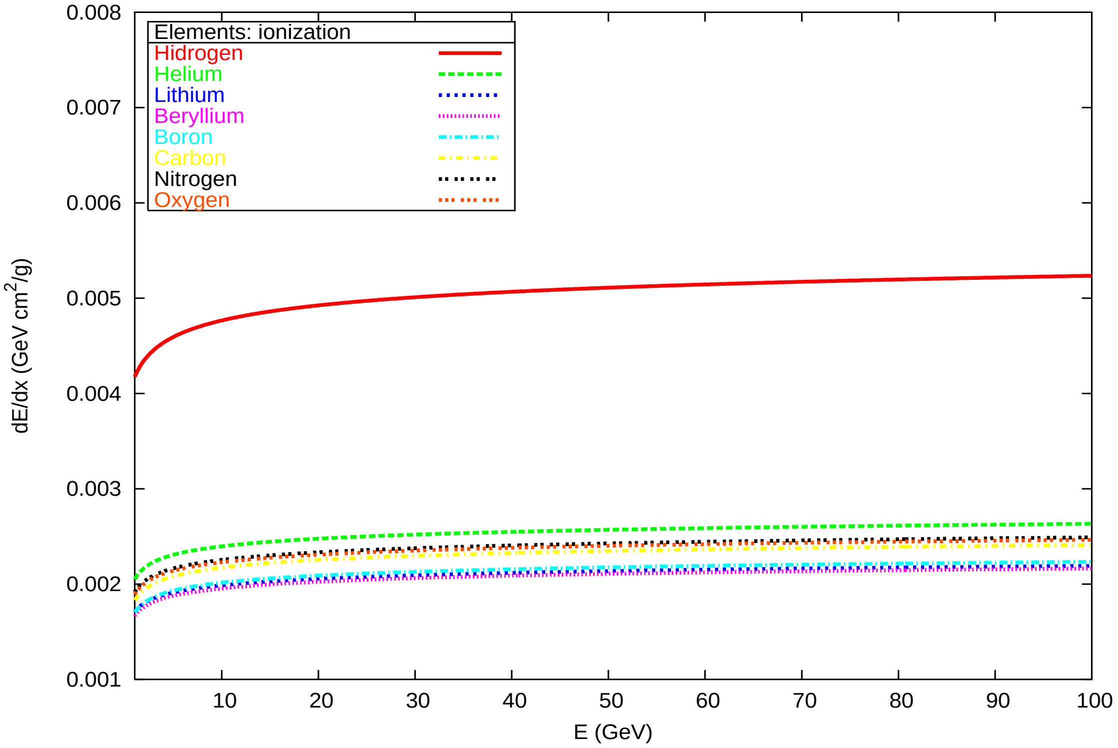

Figure 6.2: Muon energy loss by ionization in elements I. (for other elements see appendix)

$$\langle \delta \rangle = \sum_i \frac{Z_i}{A_i} \delta_i w_i \tag{6.4}$$

Using these estimates we can virtually compute the energy loss for any material. Yet, the upper formulae are sometimes generating large difference (higher than 10%) with respect to energy loss true values. Based upon chapter 26.2.4. of [Gro98] (web version) and [Cra95] we can use an alternative way:

$$\left(\frac{dE}{dx}\right)_{\text{ionization}} = \sum_i \left(\frac{dE}{dx}\right)_i w_i \quad , \tag{6.5}$$

plus 13% rule, that is we take for each element of compound a value of ionization potential $I_{eff} = I_{element} \times 1.13$. This is a phenomenological artifice to account for difference between ionization potential of the atom in bulk element and the bound atom in some molecular configuration.

This Monte Carlo includes ionization information for 34 elements plus 7 compounds and mixtures.

6.1.2 Bremsstrahlung

Bremsstrahlung interaction leads to high energy photons, thus the incident muon loses a great deal of its initial energy. The cause is easy to prove just by looking at the two main Feynman diagrams:

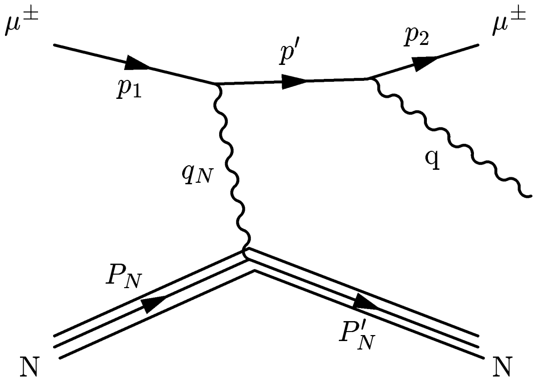

Bremsstrahlung Feynman diagram I
(leading term)

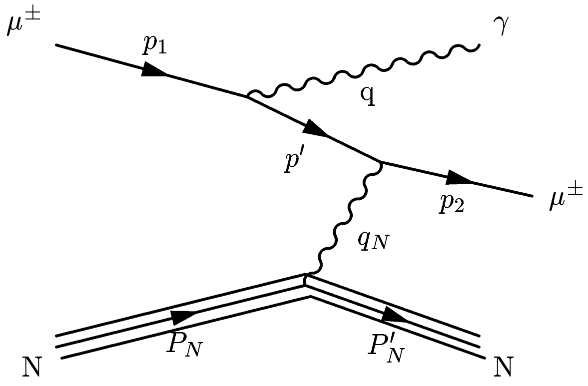

Bremsstrahlung Feynman diagram II
(leading term)

These diagrams contain a real photon, q. We see that there is no requirement in diagram construction for small q and large p'. The probability for radiating a photon with momentum q, is, for soft part of bremsstrahlung spectrum [PS95]:

$$d(prob) = \frac{d^3q}{(2\pi)^3} \sum_{\lambda} \frac{e^2}{2q} \left| \epsilon_\lambda \left(\frac{\mathbf{p}'}{p' \cdot q} - \frac{\mathbf{p}}{p \cdot q} \right) \right|^2 \tag{6.6}$$

This leads to a $\frac{1}{q}$ dependence, a very soft one. On average, this assures large energy transfers, thus, it increases the probability of stochastic process in simulation.

To simulate muon energy loss by Monte Carlo we use the parameterized formula (valid over all available phase space - see [WLV85]or [SKP95]):

$$\frac{d\sigma}{dv} = \alpha^3 Z(Z+1) \left(2\bar{\lambda}_e \frac{m_e}{m_\mu} \right)^2 \frac{1}{v} \left(\frac{4}{3} - \frac{4}{3}v + v^2 \right) \phi(\delta) \tag{6.7}$$

here, $v = \frac{q}{E}$ is the fraction of incident energy taken by photon (for explicit description of formula see Appendix). In Monte Carlo I use the integrated formula:

$$\frac{dE}{dx} = E \frac{N_A}{A} \int_{v_{min}}^{v_{max}} v \frac{d\sigma}{dv} dv \tag{6.8}$$

This average value is considered, instead of splitting the phase space in a continuous region and a stochastic one. Kinetic limits are: $v_{max} = 1 - \frac{3}{4}\sqrt{e} \left(\frac{m_\mu}{E} \right) Z^{1/3}$, $v_{min} = 0$, the latter is not a kinematic result, but involves careful consideration upon Form Factor.

In case of compound target material, the energy loss value for any radiative process is deduced by applying:

$$\frac{dE}{dx} = \sum_i \left(\frac{dE}{dx} \right)_i w_i \tag{6.9}$$

with w_i the weights of elements in compounds.

At this point, it is appropriate to make some statements regarding the compounds. The average values of A and Z are important for qualitative analysis and understanding of energy loss mechanism via different processes. The formulae for $< A >$ and $< Z >$ are:

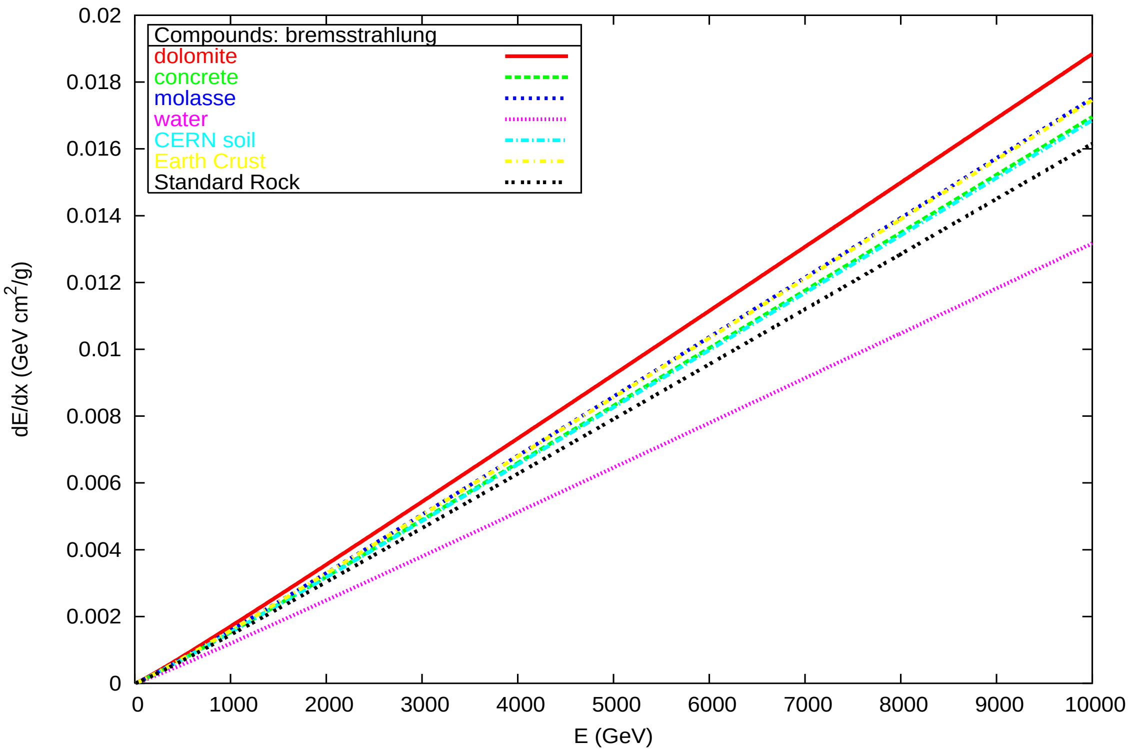

Figure 6.3: Muon bremsstrahlung energy losses in 7 Compounds

$$
\begin{aligned}
< A > &= \sum_i A_i w_i' \\
< Z > &= \sum_i Z_i w_i'
\end{aligned} \tag{6.10}
$$

where A_i,Z_i, w_i' are atomic number, element number, and number fraction of element in compound or mixture see table 6.1.

Table 6.1: mean Z and A for 7 compounds

Compound	Z	A	$\frac{Z}{A}$	$\rho(g/cm^3)$
Water (H_2O)	3.3	6.0	0.56	1.
Dolomite($CaCO_3$)	10.0	20.0	0.5	2.8
Concrete	8.6	17.1	0.5	2.2
Molasse	10.1	20.2	0.5	2.4
CERN Soil	7.2	14.2	0.51	2.4
Standard Rock	11.0	22.0	0.5	2.65
Earth Crust	10.2	20.6	0.5	3.3

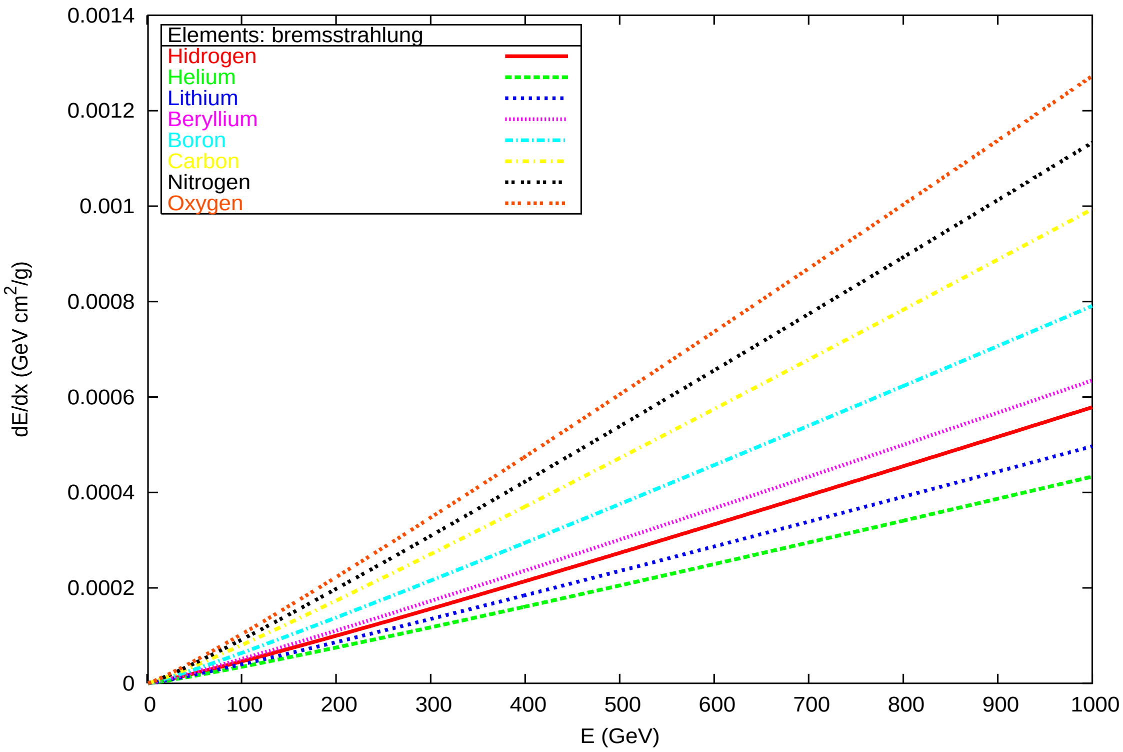

Figure 6.4: Muon bremsstrahlung energy losses in elements I. (for other 26 elements see appendix)

Using literature references [SR00], [WLV85], [Ser71](for molasse and CERN soil), [WC99], we can create a model of different materials[1]. The so called "Earth Rock" is an average over mantle rock composition), see [Mur], the composition is not to be taken "ad litteram", it is just for qualitative analysis (the reference is didactical, even though it is in agreement with a MINOS report, the latter was removed from circulation).

6.1.3 Pair production by high energy muons

From CERN Yellow report ([WLV85]):

$$\frac{d\sigma}{dv d\rho} = \alpha^4 \frac{2}{3\pi} Z(Z+1)\,(\lambda_e)^2\,\frac{1-v}{v}\left[\phi_e + \left(\frac{m_e}{m_\mu}\right)^2 \phi_\mu\right] \tag{6.11}$$

This function has a almost $\frac{1}{v^\alpha}$ dependence , with $\alpha \gtrsim 2$. The ρ dependence is relatively flat, with slow decrease to 0 in the upper part of interval. There is similarity between e^+e^- pair production and its pure muonic counterpart, yet, the value of higher momentum transfer, in case of latter channel, leads to cross-sections smaller than just $\left(\frac{m_e}{m_\mu}\right)^2$ times the electron-positron pair production cross-section. This is due to a greater importance of the nuclear structure.

[1]Here Dolomite is in fact Calcium carbonate $CaCO_3$ and not $CaCO_3(MgCO_3)$, and, concrete is ordinary not shielding concrete

Table 6.2: Elements mass weights in compounds

Element	Concrete	Water	Dolomite($CaCO_3$)	Earth Rock	Soil	Molasse
H	0.01	0.11	-	-	0.021	-
C	-	0.89	0.12	-	0.011	0.049
O	0.529	-	0.48	0.466	0.565	0.492
Na	0.016	-	-	0.028	0.005	0.006
Mg	-	-	-	0.021	0.015	0.035
Al	0.034	-	-	0.081	0.035	0.064
Si	0.337	-	-	0.277	0.125	0.198
K	0.013	-	-	0.026	0.003	0.019
Ca	0.044	-	0.40	0.036	0.024	0.093
Mn	-	-	-	-	-	0.002
Fe	0.014	-	-	0.05	0.027	0.041

Table 6.3: Elements number fraction in compounds

Element	Concrete (Ordinary concrete)	Water	Dolomite($CaCO_3$)	Earth Rock	Soil	Molasse
H	0.169	0.67	-	-	0.297	-
C	-	-	0.2	-	0.013	0.083
O	0.564	0.33	0.6	0.605	0.501	0.624
Na	0.012	-	-	0.025	0.003	0.005
Mg	-	-	-	0.014	0.009	0.029
Al	0.022	-	-	0.062	0.019	0.048
Si	0.205	-	-	0.205	0.125	0.143
K	0.005	-	-	0.018	0.003	0.01
Ca	0.019	-	0.2	0.019	0.024	0.047
Mn	-	-	-	-	-	0.001
Fe	0.004	-	-	0.019	0.007	0.015

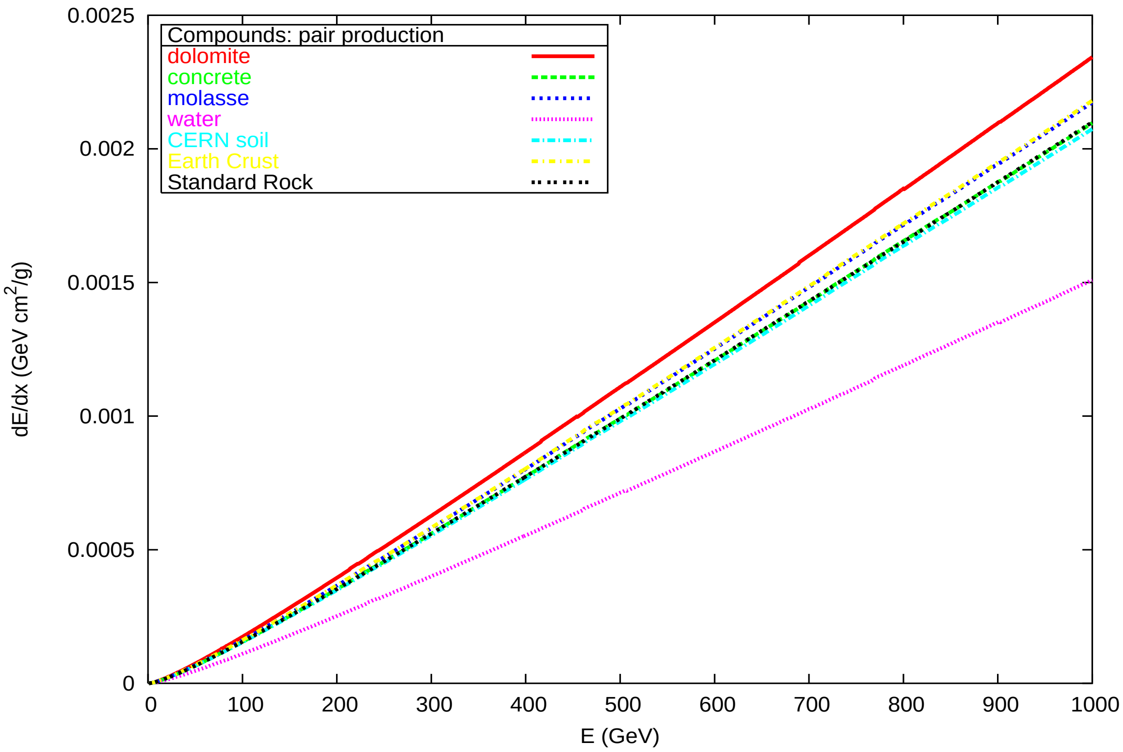

Figure 6.5: Muon energy losses via pair production in 7 Compounds

To get an estimate of the muon energy loss via pair production we use the double integration of formula 6.11. Integration limits are:

$$\frac{4m_e}{E} \leq \quad v \quad \leq 1 - \frac{3\sqrt{e}m_\mu}{4E} Z^{1/3} \tag{6.12}$$

$$0. \leq \quad |\rho| \quad \leq \left[1 - \frac{6m_\mu^2}{E^2(1-v)}\right] \sqrt{1 - \frac{4m_e}{Ev}} \tag{6.13}$$

In 6.12 the lower limit is not the kinematic limit but an arbitrary limit (twice the kinematic limit), chosen to accommodate the 6.11 parameterization. This parameterization is based upon the ultra-relativistic limit, and twice the kinematic limit is a reasonable choice. Upper limits in 6.12 and 6.13 are model dependent (via Form Factor and 6.11 parameterization) similar to the bremsstrahlung case.

To integrate I have used alternatively two adaptive integration methods. Both are based on the Gauss-Lagrange methods with adaptive integration sampling. For details on integration algorithm and numerical methods see [CER] or [WPF92] . The integration is performed according to:

$$\frac{dE}{dx} = 2E\frac{N_A}{A}\int_{v_{min}}^{v_{max}} v \int_0^{\rho_{max}} \frac{d^2\sigma}{dvd\rho} d\rho dv \tag{6.14}$$

the 2 factor was fitted in because of space inversion symmetry in ρ space.

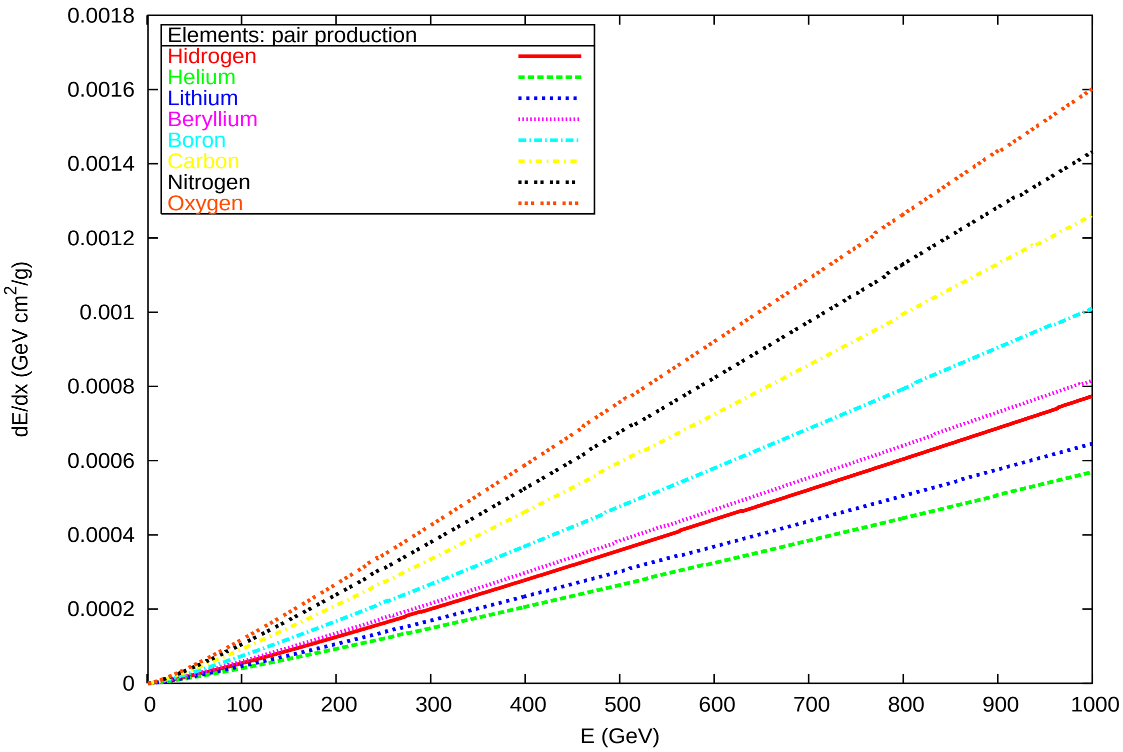

Figure 6.6: Muon energy losses via pair production in elements I. (for other 26 elements see appendix)

Both bremsstrahlung and pair production are radiative processes. The Bragg law of addition 6.9 remains valid for pair production.

6.1.4 Photonuclear interaction

This interaction is less understood and conflicting values for photonuclear cross-section exist in the literature. There is particular doubt regarding the extrapolation of models towards the very high energy domain, were there are no experimental measurements. All this is evident if we consider the very nature of this interaction. Previously we were dealing with interactions that were not changing the nuclear state, and the only worry was to quantize the nuclear charge density in form of a Form Factor. This time the interaction can split the nucleus down to its constituents or/and create hadronic secondary particles like pions, kaons, etc, or even light elements. This is deep-inelastic scattering. Since the complexity of hadronic channels can be extreme, providing there is sufficient energy to pass the threshold, photonuclear interaction can not be reduced to "simple" Feynman diagram calculus. It requires phenomenological modeling and this splits the field in competing models without an overall answer.

Due to upper stated reasons I consider two alternative parameterizations (each based on the same model) of photonuclear cross-section. The first parameterization is given by Bezrukov and Bugaev in [BB81] with further references in [WLV85], [DR] and [IASK01]. The last two references are muon propagation Monte Carlo manuals. The second parameterization is due to Borog and Petrukhin, and it is the parameterization used by Geant 4, [Gea04]. Without describing the underlying model (Vector Dominance Model), we can note: the model assume the virtual exchanged photon can be treated as real. For analytic expressions see appendix.

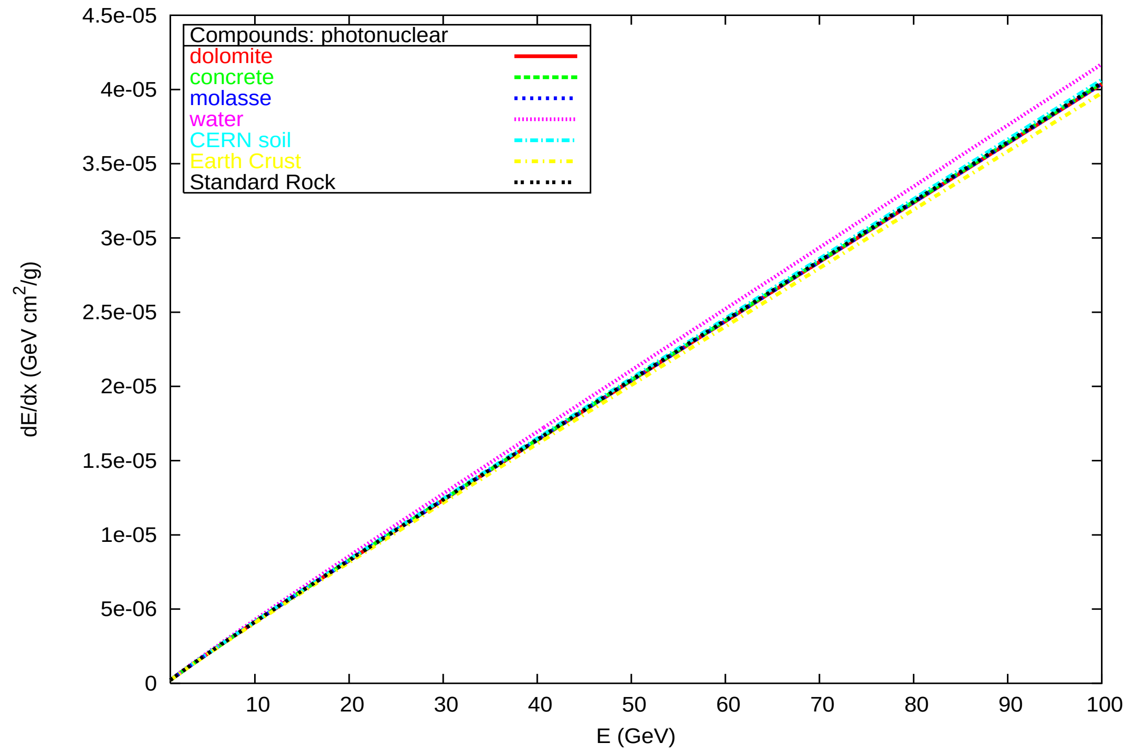

Figure 6.7: Muon energy losses via photonuclear interaction in 7 Compounds

6.1.5 $\frac{dE}{dx}$ overall conclusions

The energy loss of a single muon is a superposition of individual contributions:

$$\frac{dE}{dx} = \left(\frac{dE}{dx}\right)_{\text{ionization}} + \left(\frac{dE}{dx}\right)_{\text{bremsstrahlung}} + \left(\frac{dE}{dx}\right)_{\text{pairprod}} + \left(\frac{dE}{dx}\right)_{\text{photonuclear}} \tag{6.15}$$

In pictures 6.9 and 6.10, I plot the the energy loss in 8 elements for different energy domains: [0,100] GeV and [0,1000] GeV. These domains correspond to different regimes for the energy loss mechanism: at lower energy there is the ionization dominant regime and at higher energy (above certain critical energy) the radiative processes takeover. These facts are easily recognized from graphs, in 6.9 the higher energy loss is exhibited by lighter elements and there is consistency with the $\frac{Z}{A}$ dependence. At higher energy, were radiative processes have high probability to occur, the dependence on element numbers changes to $\frac{Z^2}{A}$, and this is easy to spot in 6.10.

For mixtures and compounds, in 6.11 graph, we have ionization dominant behavior for low energy and radiative domain at high energy. Calcium Carbonate $CaCO_3$ has highest energy loss and water lowest energy loss in high energy domain. At low energies the reverse is true. All facts displayed in graph are in complete agreement with the upper stated dependencies at high and low energy, this time the element numbers are replaced by compounds effective Z_{eff} and A_{eff}, see table 6.1.

I take standard rock as archetype of overburden and reference material. To check the validity of one of the initial assumptions upon which the transport and generation algorithm is founded, we weight all interactions strengths. This is displayed: for standard rock (as approximation for overburden layer

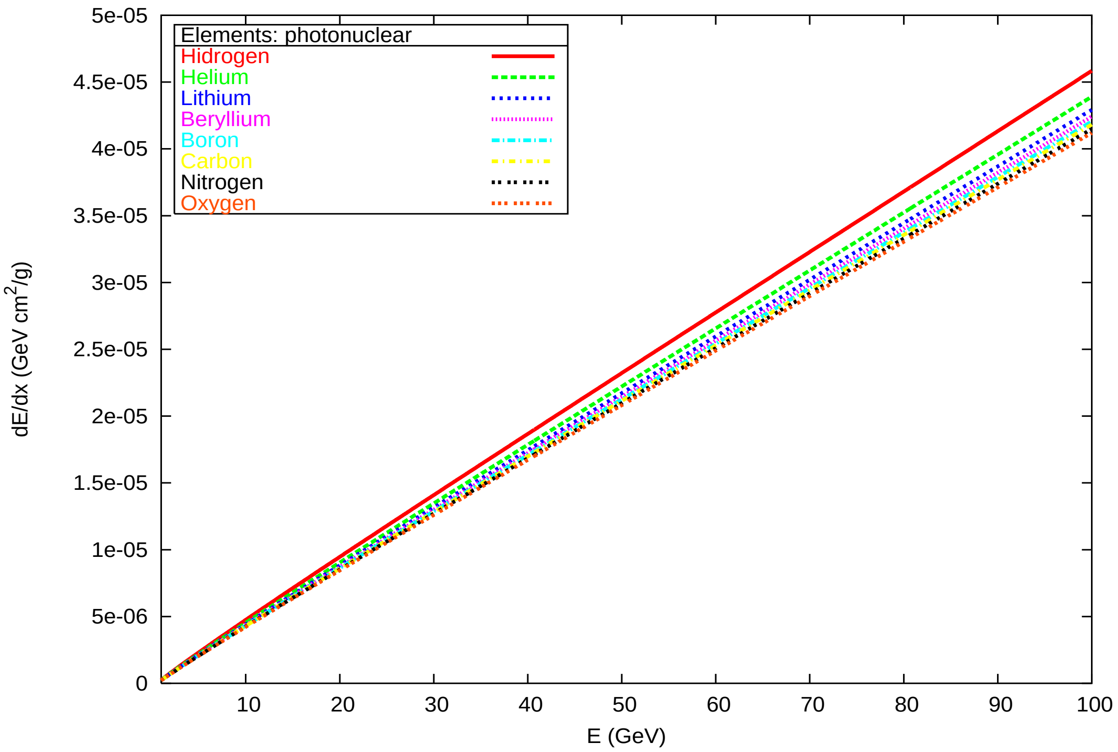

Figure 6.8: Muon energy losses via photonuclear interactions in elements I. (other 26 elements in appendix)

materials) 6.12, for iron (HCAL) 6.13 and lead (ECAL) 6.14.

When building a Monte Carlo for muon propagation and trident generation, I have included a deep-rooted assumption: **Within our framework, it is possible to consider predominantly stochastic processes, bremsstrahlung and photonuclear interactions, as continuous energy loss contributions**, without substantial change in final results. Graph 6.12 shows that continuous-like energy loss processes, ionization and pair production dominate the total energy loss mechanism and the stochastic-like processes are having small contributions to energy loss of muons. The photonuclear interaction can be for most cases neglected, see graphs 6.13 and 6.14. Bremsstrahlung has $\frac{dE}{dx}$ contribution of same order in value with the pair production energy loss contribution. The large transfers to bremsstrahlung photon, means that the cross-section or occurrence probability are much smaller in bremsstrahlung case than pair production (bremsstrahlung $\frac{1}{v}$ versus pair production $\frac{1}{v^2}$, with v the transferred energy to secondary or secondaries). The lower relative probability for muon bremsstrahlung in detector layers, and the large width of overburden layer should combine to lower the fluctuational tendency associated with stochastic bremsstrahlung. This would hold true for each individual muon in TPC with exceptions.

Weighting everything stated, and adding the fact that the electromagnetic and hadronic showers (remnants of bremsstrahlung and photonuclear interactions in HCAL or ECAL) are seldom occurring, I conclude that the assumption is, from point of view of physics, sound. From experience, after sifting a sample that should contain most (if not all) events with track multiplicity higher than 2, I can say that bremsstrahlung and photonuclear processes seen in TPC are in combined number close to 40. This is smaller than e^+e^- pair production (even though, for e^+e^- production, only the separation layer between

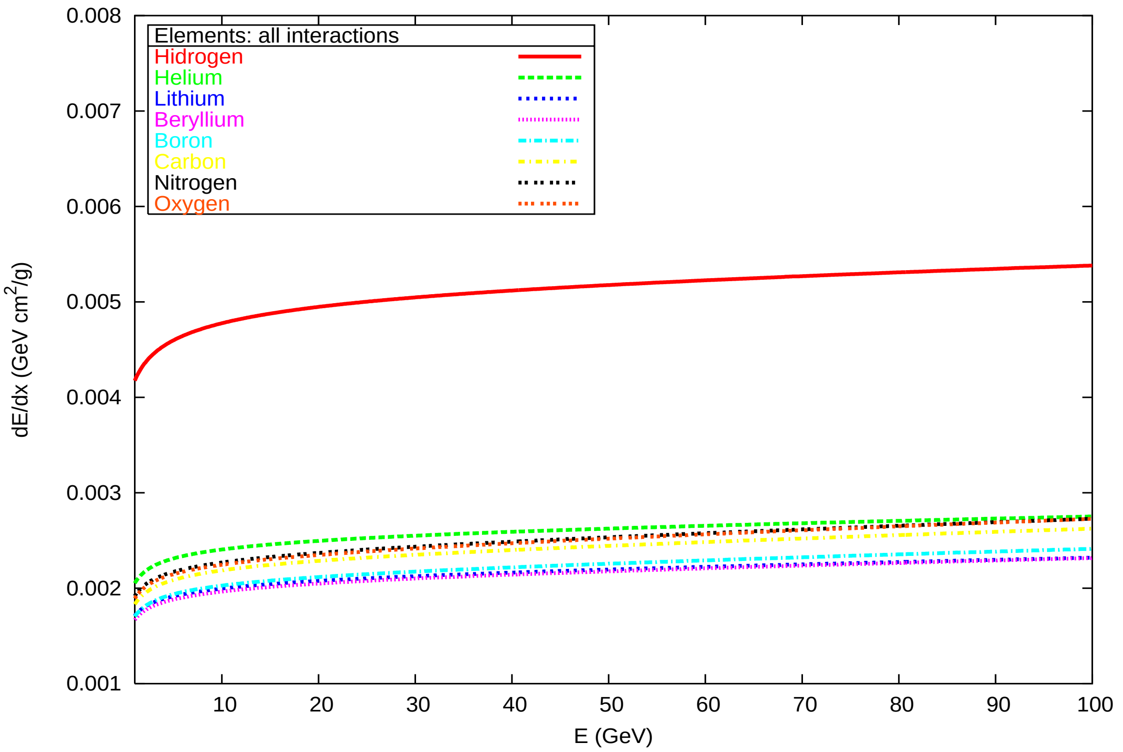

Figure 6.9: Toatl muon energy loss in elements I, low energy range

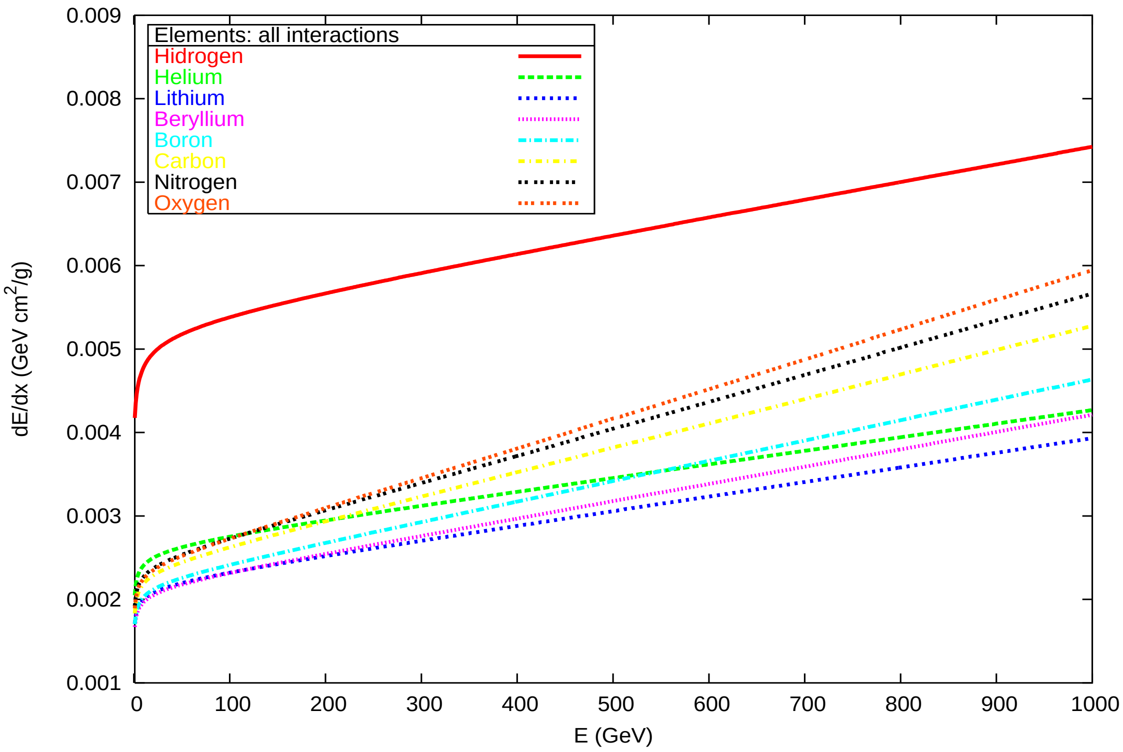

Figure 6.10: Toatl muon energy loss in elements I, intermediate energy range

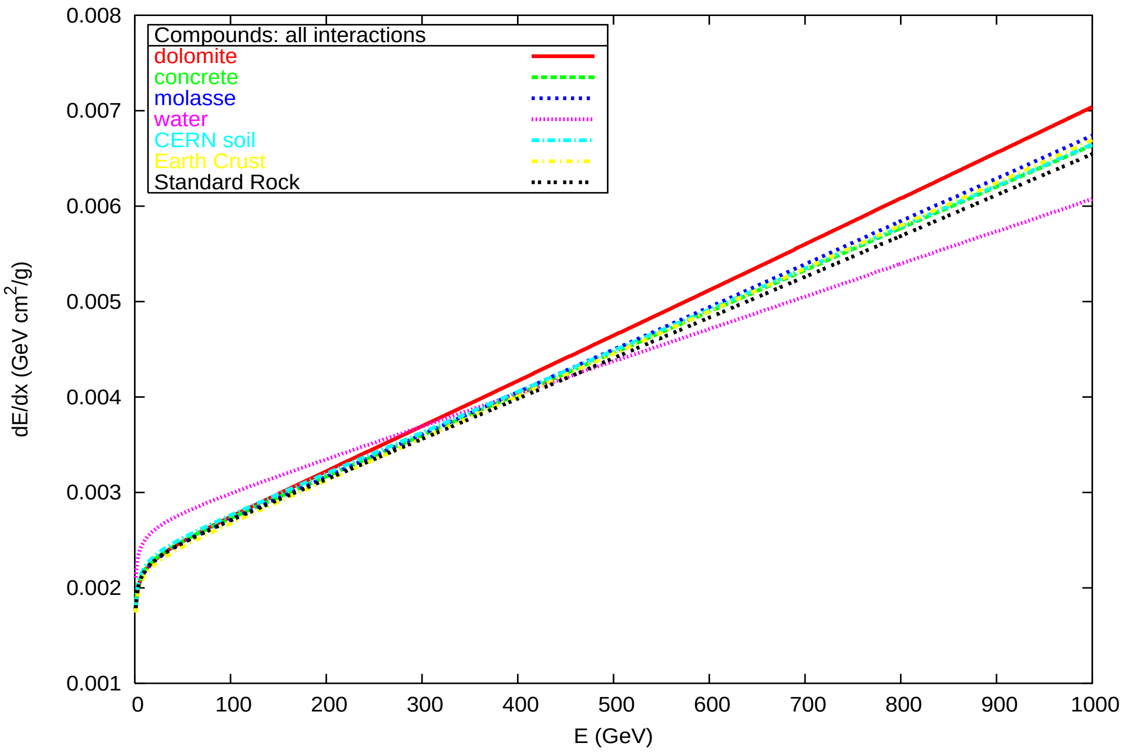

Figure 6.11: Total muon energy loss in 7 compounds.

TPC and ECAL or inner layers of ECAL give contribution) and negligible compared with total number of multiple chance coincidences (coincidences of two or more atmospheric muons), and this without speaking of the number of total muons in TPC, which is close to a 6 digits number.

6.2 Algorithm and Tools

I have named my Monte Carlo HMDMC (Home MaDe Monte Carlo). To achieve a fully functional status for this transport-generation code the following steps were sequentially implemented:
- the parameterized formulae for energy losses and cross-sections were numerically integrated by various integration algorithms;
- a the library that cumulates enough sampling points to reconstruct energy loss distributions and trident cross-section for 34 elements and 7 compounds, also the energy loss is structured in individual interaction contributions;
- in library a step size for the energy of muons is 0.1, 1, and 10 GeV respectively, with alternate highest energy of 100 GeV, 1 TeV, 10 TeV respectively (3000 sapling points for each element-interaction combination);
- geometry of ALEPH and ALEPH proximity is implemented;
- to prevent inconsistency in energy loss estimates, the partitions in layers are: 1000 sub-layers for soil layer, 1000 sub-layers for molasse part of overburden, 200 sub-layers for HCAL iron layer, 129 ($1g/cm^2$) sub-layers for ECAL lead layer;
- an extrapolation method for muon energy to ground level is coded (the energy is numerically extrapolated by a backward propagation of muons in overburden and detector layers - reversed time);

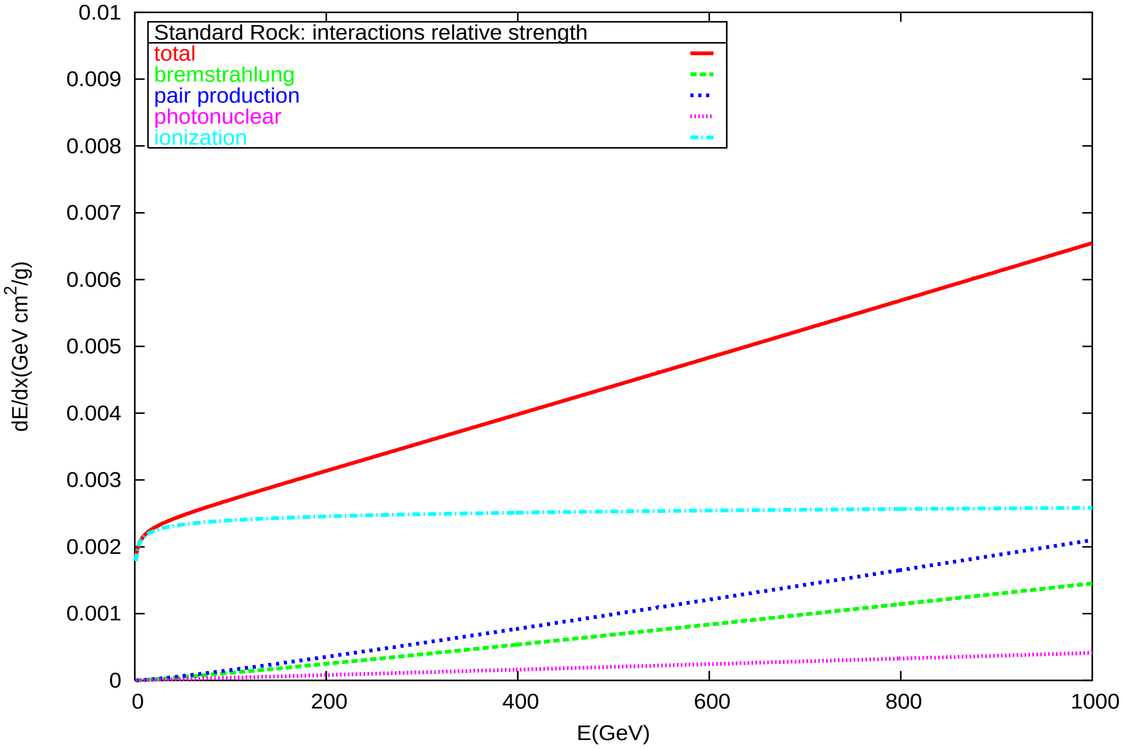

Figure 6.12: $\frac{dE}{dx}$, relative strength of interactions in Standard Rock

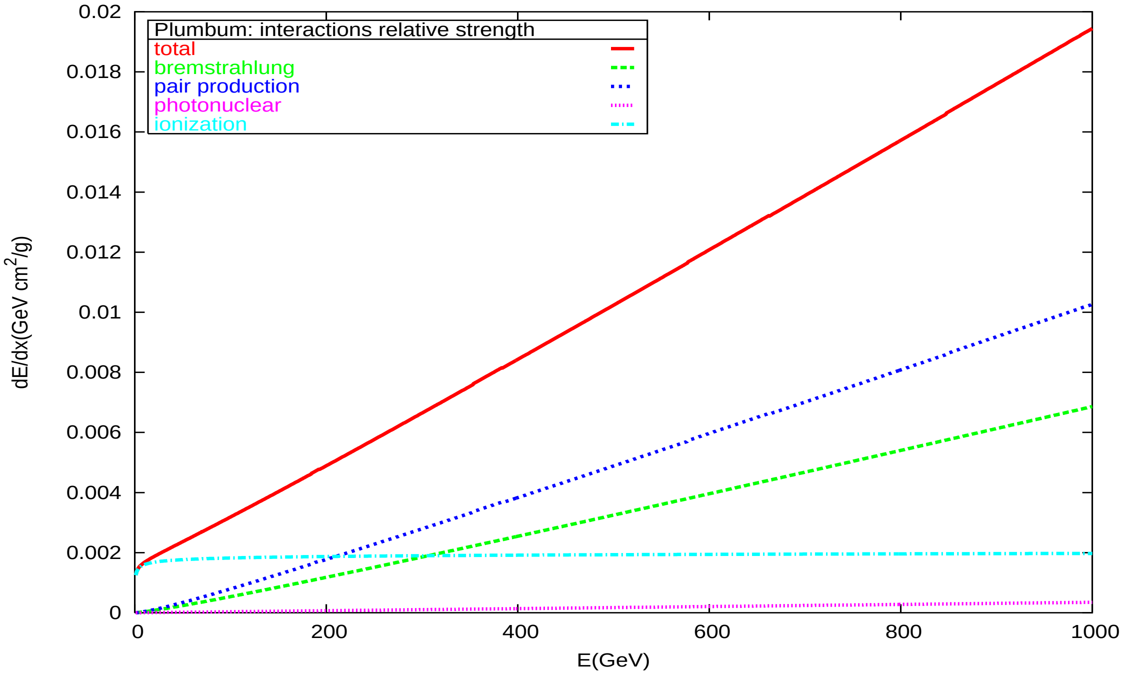

Figure 6.13: $\frac{dE}{dx}$, relative strength of interactions in lead - plumbum (Latin)

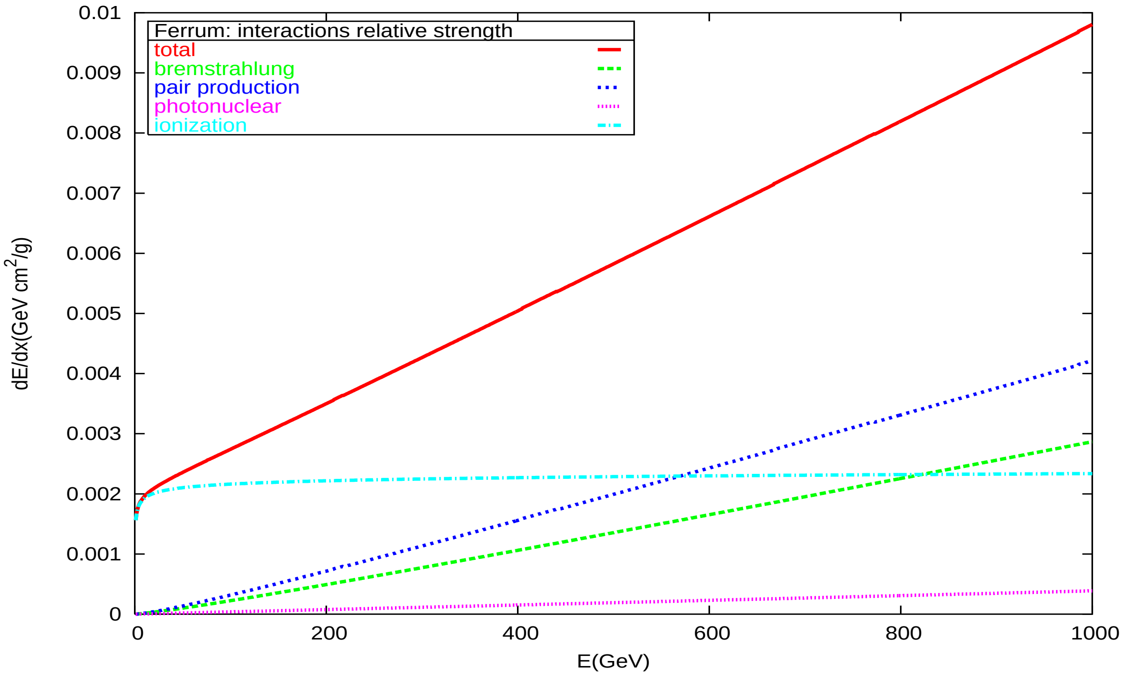

Figure 6.14: $\frac{dE}{dx}$, relative strength of interactions in iron - ferrum (Latin)

- a propagation algorithm is assembled, and it propagates muons with different zenith ($[0, 1.4]$ radians range) and azimuth (full range) angles
- inputs for the muon energies are the TPC reconstructed values after processing by the extrapolation subroutine, the latter shifts the values to a ground level estimate;
- to avoid the systematic error propagation in the code, a Monte Carlo production of trident vertices is enabled directly in the extrapolation procedure;
- for each vertex two secondaries are produced and the extrapolation of primary is stopped;
- the ground level muons and the muons generated at trident vertices are propagated back to ALEPH level;
- information on number of vertices, positions, muon energies at physical significant locations and directions of muons are stored.

The algorithm implementation is in FORTRAN language and several CERNLIB procedures were used. The program runs under True Unix and under LINUX. It is portable among workstations that run under UNIX and LINUX and where CERNLIB is installed.

Chapter 7

Results of simulations, comparison with data

It's kind of fun to do the impossible.
Walt Disney

7.1 First results

Just for observation, the program is not a Fast Monte Carlo, there are no parameterizations of muon flux, but, each individual muon from the experimental data is used as input to program.

To be able to draw some conclusions on most probable and average values of the observables, the simulation was carried out several times, each time with experimental data as input. A statistically significant sample was collected and the resulting values binned in histograms. Statistic analysis was performed.

I begin by listing those values, that are not explicitly connected with observables. These are: total number of tridents produced in each layer, energies for secondaries and primary at vertex. I give in tables 7.1 and 7.2 the number of expected events and particle spectra, in absence of cuts. The most probable energy for a primary is close to 100 GeV and the secondaries have spectra consistent with power laws (see graph 7.2). The most probable number of tridents in HCAL and ECAL are 11 and 3 respectively, these without energy requirements or other cuts. There is a difference of two orders of magnitude between average energy of primary and the sum of the secondaries energies. This justifies, one more time, a physical assumption on which MC is based: **the energy of primary muon is only negligibly modified by a trident event**.

We can see (graph 7.1) that compared with numbers of $\mu^+\mu^-$ pairs produced in overburden, the

Table 7.1: Number of produced tridents per layer: the average values for the Monte Carlo samples

Layer	Mean Number	RMS	average deviation (adev)
Soil	261	14.3	11.6
Molasse	268	16.5	12.7
Iron	13	3.5	2.8
Lead	3.3	2.0	1.5

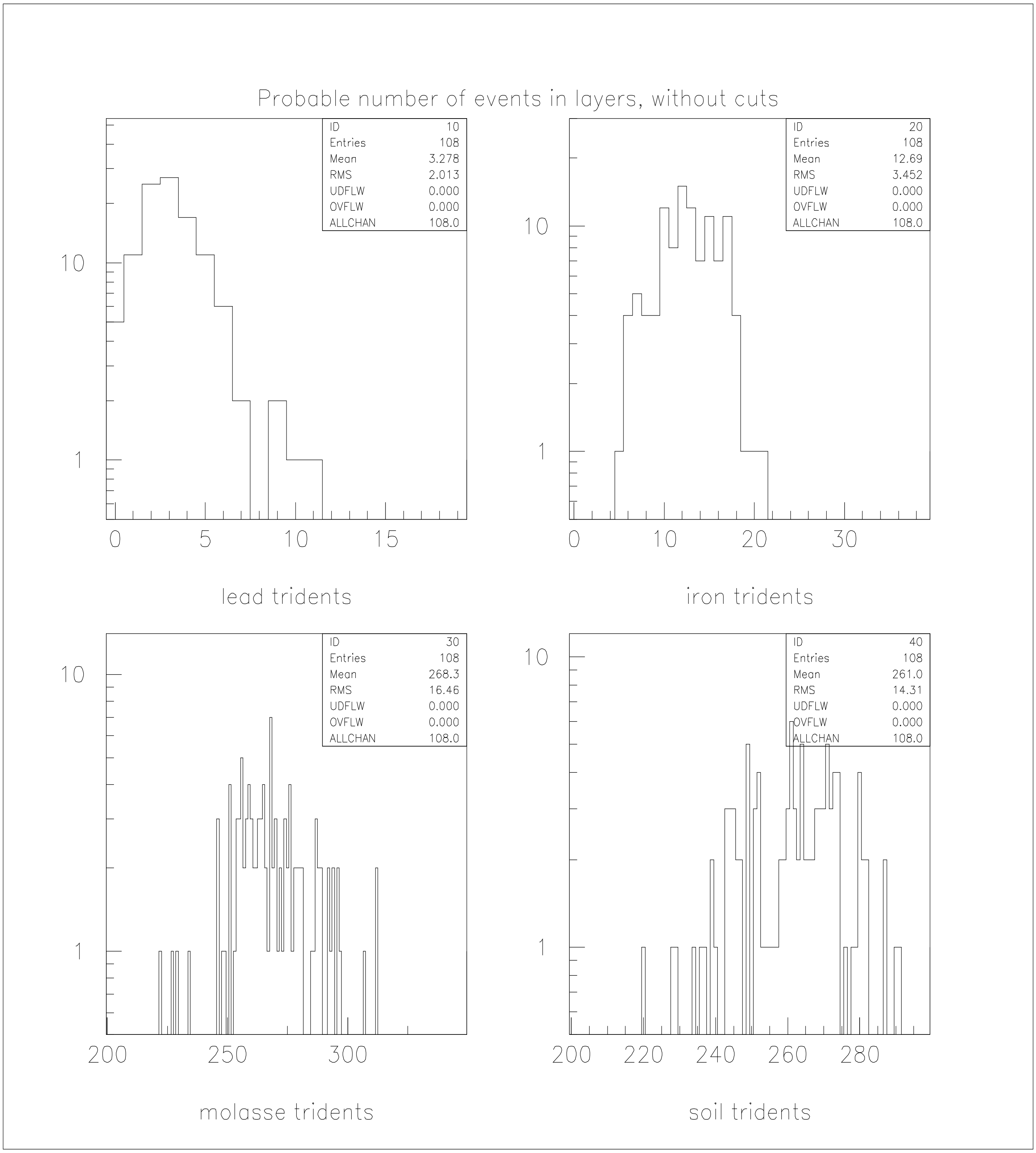

Figure 7.1: Distribution of the trident numbers per layer, all $\mu^+\mu^-$ events are considered

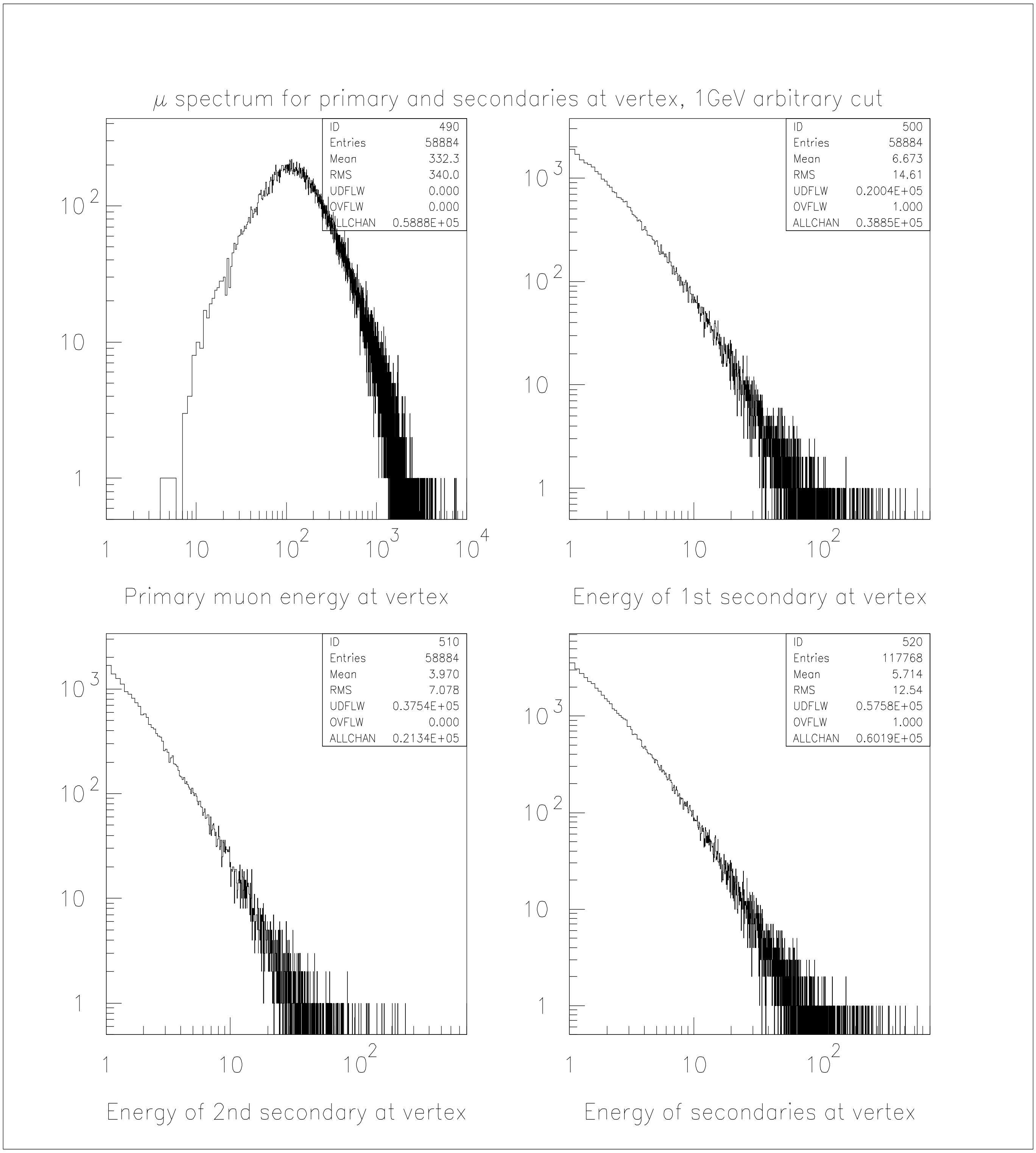

Figure 7.2: Spectra for primary and secondaries at vertex, with arbitrary 1 GeV cut

Table 7.2: Energy values at vertex: E' energy of primary muon, E_1 1st secondary muon and E_2 2nd secondary muon: MC results

Physical quantity	Average	adev (or average deviation)	sdev(or RMS)
E'	332	230.0	340.0
E_1	4.6	4.9	12.9
E_2	1.7	1.7	4.6
$E_{secondaries}$	3.2	3.5	9.8

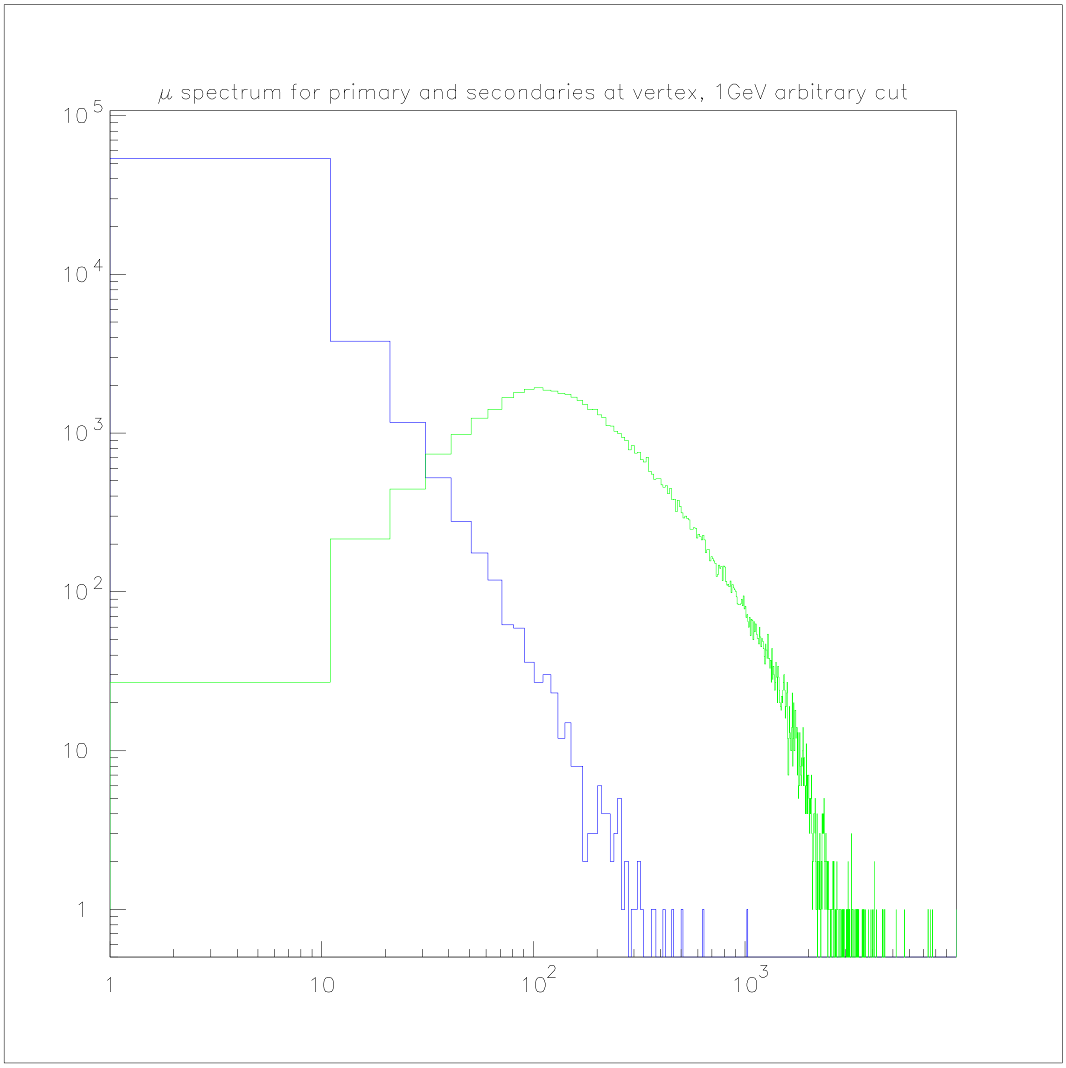

Figure 7.3: Comparison between spectra for primary and secondaries at vertex

Table 7.3: Number of trident events with exactly two tracks in TPC: MC results

Layer	Mean Number	adev	RMS
Soil	0.3	0.45	0.5
Molasse	3	1.5	1.9
Iron	2.5	1.6	1.3
Lead	1	1	0.75

Table 7.4: Number of trident events with all three tracks visible in TPC: MC results

Layer	Mean Number	RMS	adev
Soil	0.	0.	0.
Molasse	0.7	0.8	0.7
Iron	2.0	1.4	1.
Lead	1.7	1.3	1.0

number of pairs produced in ALEPH shells is insignificant. Yet, exactly this small fraction from total is expected to produce the highest observable contribution. This is due to power law dependence in secondary spectrum (graph 7.2) and propagation of secondary muons from vertex to TPC and even through ALEPH. The huge difference between primary and secondaries is evident in 7.3.

By propagating the generated muons from their vertex to TPC and imposing conditions on final multiplicity of the muons that reach TPC, we can estimate an observable. The numbers found by this method can not match the data, because there is no condition that muon should have double path through HCAL (the data analysis rejects events that had no double track in HCAL).

7.2 What may be observed in ALEPH

The expected numbers of observable tridents (full sample, the only rejected events are the ones that have only the primary track in TPC), are deduced from Monte Carlo (MC) after propagation of muons through overburden and outer detector shells.

A first set of values is given in table 7.3 and 7.4. However the same tables show very high error estimates and some times higher than the average number. This happens because standard deviation of sample is a not so robust estimate of fluctuation. The average deviation has higher confidence level in error estimate for the case at hand, but even this estimate has values equal to average values. The distributions plotted in 7.4 and 7.5 are highly peaked at low values or have broad tails to high values, and this explains the large values of sample RMS and sample average deviation. Due to this reason, I will not limit myself on usual statistical estimates.

Most probable values for number of “visible” events $\mu^+\mu^-$ in layers are:
- for 2-fold TPC coincidences, 0 in ECAL, 2 in HCAL, 2 in Molasse and 0 in Soil (exclusive 2-fold);
- for 3-fold TPC coincidences, 1 in ECAL, 2 in HCAL, 0 in Molasse and 0 in Soil.

Probabilities for each scenario are:
- 59% probability that there is one or more than one event in ECAL;

- for HCAL there is 11% probability for 0 events, 18 % for 1 event, 28 % for 2 events, 23% for 3 events, 11% for 4 events;
- in molasse overburden, the probabilistic weights are 5% for no events, 19% for 1, 25% for 2, 17 % for 3, 12% for 4, 11 % for 6 (we see only 2 or 3 events from HCAL);
- in soil there is 77% probability that no observable events occur. Already the muon tridents from detector shells dominate the “stage”. We should expect on average 3-4 double coincidences in TPC as shells contributions and 2-3 double coincidences from overburden.

For triple coincidences I estimate 1-2 observable tridents from ECAL (17% weighted probability for null case, 34 % for 1 event, 29% for 2 and 13% for 3 events), 2 observable tridents from HCAL (15% probability for null case, 25% for 1 event, 27% for 2, 18% for 3 and 14% for 4), 0 events from overburden (for molasse the probabilities are 49 % for null case and 51% for one or more events).

All quoted numbers are expected to be higher than data analysis results (blind analysis!!! the data prior-to-final sample is including hadronic component with an undetermined weight). To “close the gap” between simulation and reality, cuts must be applied in concordance with the cuts from data analysis. This is done in the next section.

This chapter ends with an immediate physical conclusion. The overburden has no impact on trident observables. An estimated number of overburden tridents seen in ALEPH TPC is close to 3(+2-1) and there is only a 50% probability for a single event with all three muon tracks in TPC. Even more, the expected overburden events, that have 2-fold multiplicity in TPC, should have one slow secondary muon and one very high energy primary. Thus, it is reasonable to assume non-collinearity between tracks in TPC. The 3 or 4 trident events with double track in TPC are engulfed by the number of double atmospheric muon coincidences in TPC , the latter is estimated to be close to 3750 events. Plus, there is some degree of overlap, from point of view of expected geometry, between atmospheric muon coincidences and overburden tridents. One fact emerges per se: it is apparent that no observable contribution comes from overburden. This holds true for the muon multiplicity distribution and also for the individual observed events (with tridents indistinguishable from double coincidences of atmospheric muons).

My findings appear to be in conflict with the results of MARCO collaboration (they observe a change in multiplicity distribution over small distances, because of muon tridents in overburden [Sio00], [01b], [Hon95], [Sca99]), however it is important to keep in mind the fact that CosmoALEPH is a shallow depth muon “observatory”, whereas MACRO is under 3150 to 7000 hg/cm^2 overburden thus 10 times deeper than ALEPH ($320 hg/cm^2$). This huge layer that muons must cross, accounts for a higher production rate of tridents and could explain the differences. Moreover, I do not include in the analysis events with closely spaced parallel tracks, like event 49086-4801 (display pictures 7.6 and 7.7) and which correspond to events weighted in MACRO's analysis. My choice is in agreement with the analysis performed by the Russian BARS group (includes Kelner, Kokoulin and Petrukhin, the KKP cross-section authors), where parallel tracks are rejected in analysis, see reference [01a] and especially Fig. 1 of this reference.

Even if two tracks are convergent to a point in HCAL or ECAL, I have rejected from data analysis all events with only double coincidences. This is the case of events 49087-19072 and 49094-30378 displayed in pictures 7.8, 7.9, 7.10 and 7.11. Event 49087-19072 seem more like a pion events, but 49094-30378 is very clean. Since nobody quantized for CosmoALEPH the chance coincidences probabilities of atmospheric muons, I must suppose that alternative scenarios besides trident production can take place for each double coincidence event. Most of these events will be atmospheric muon chance coincidences. Having

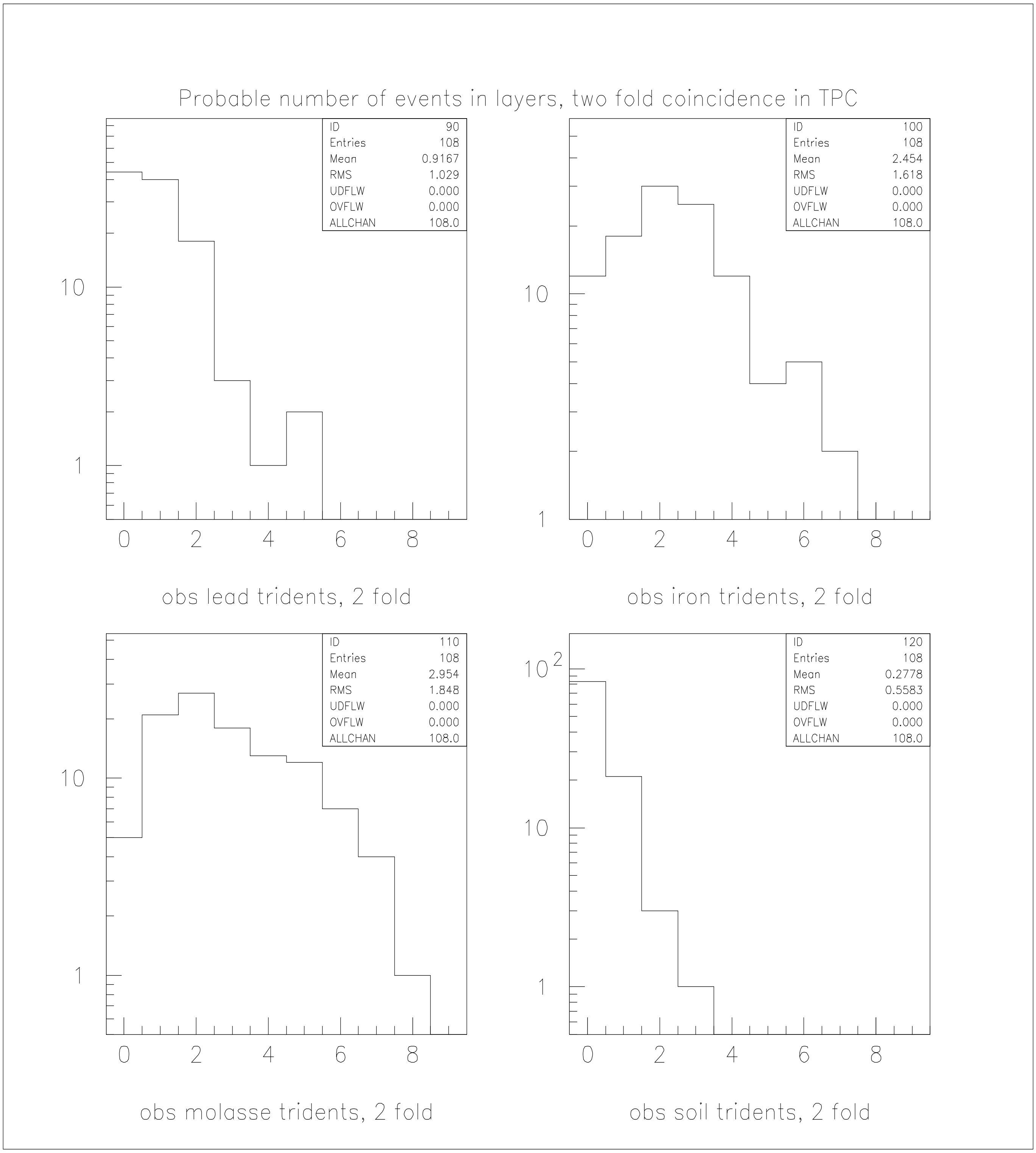

Figure 7.4: MC distribution of the tridents number per layers for double coincidences in TPC

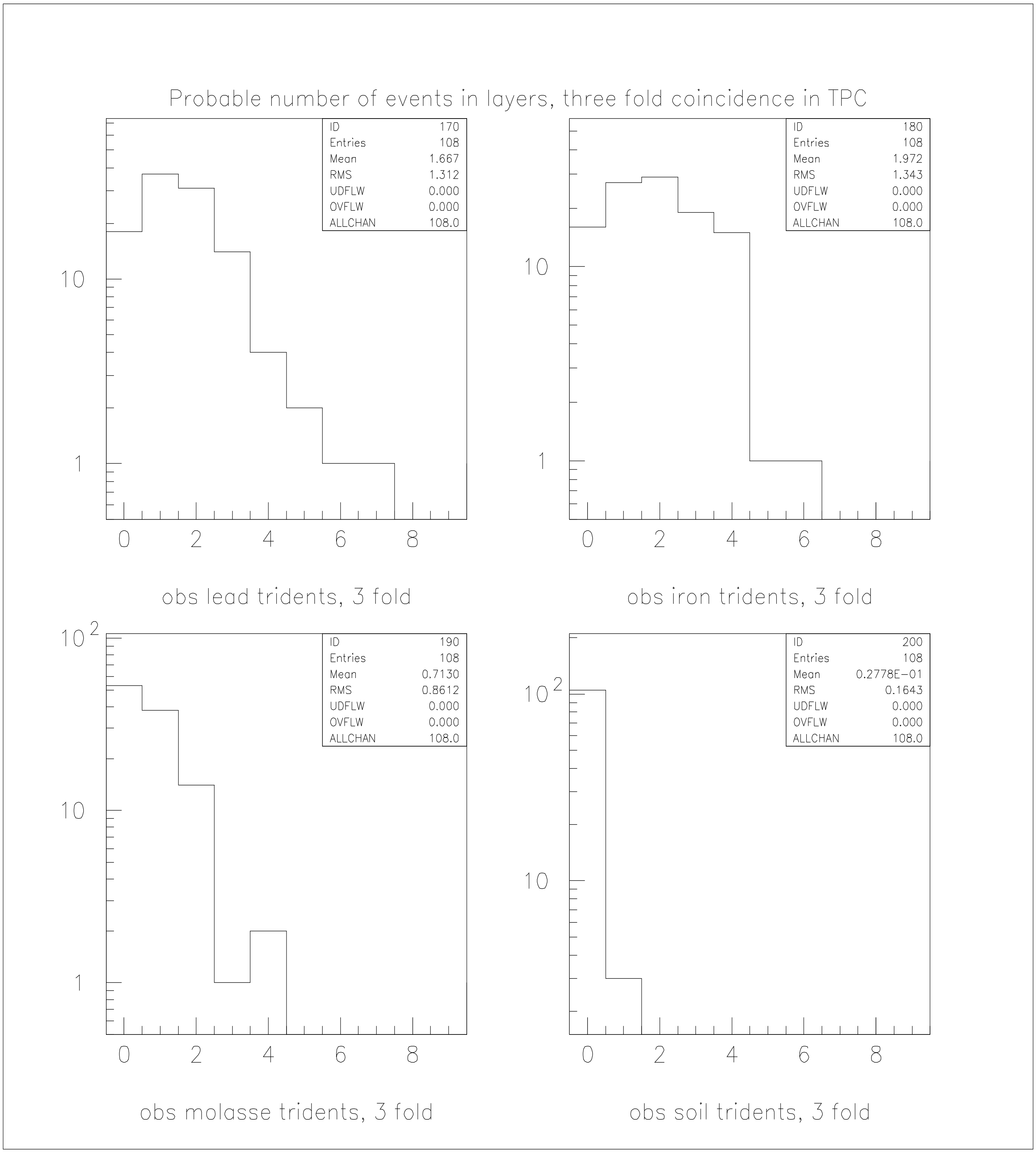

Figure 7.5: MC distribution of the tridents number per layers for triple coincidences in TPC

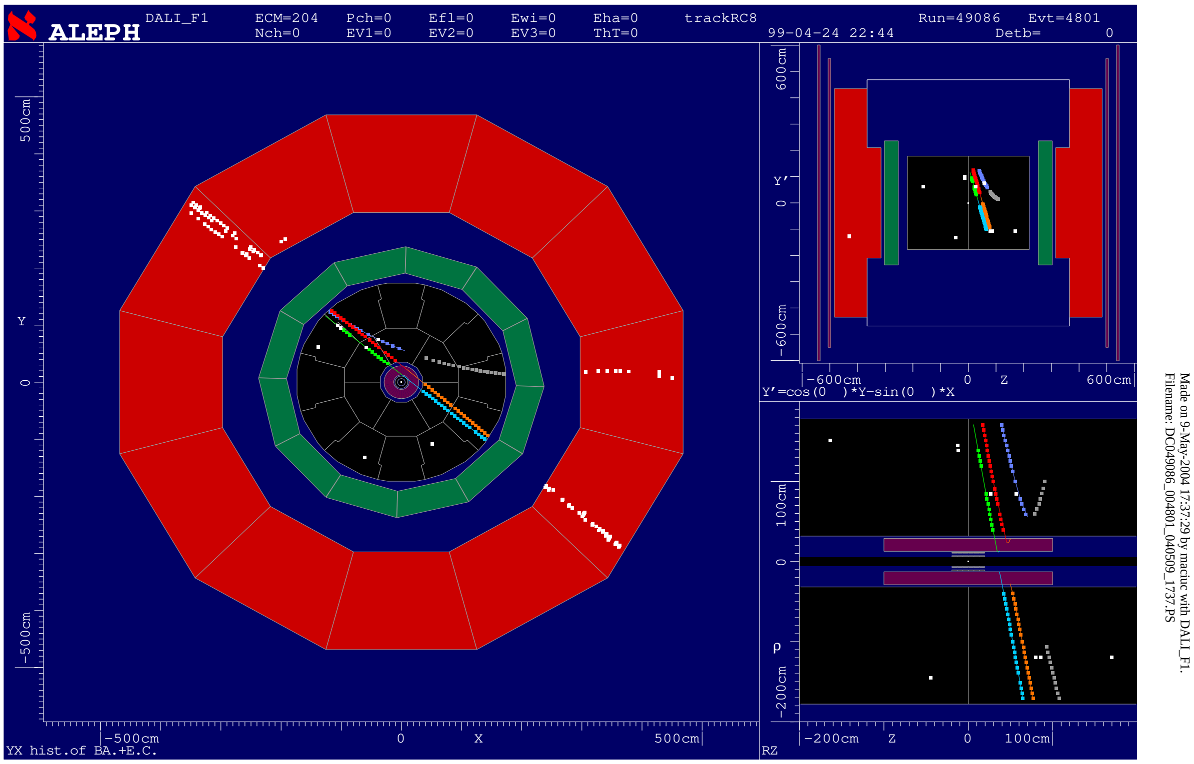

Figure 7.6: Triple coincidence of atmospheric muons or of trident muons in overburden I

End of tracks

no reliable way to fix a distance separation between individual tracks, under which value a muon trident is more probable than chance coincidence, I just state that the events shown are in apparent agreement with the predicted rate of trident double coincidences in TPC.

7.3 Trident sample after applying cuts that are in agreement with data analysis

The MC data was divided in events with secondary muon penetration in HCAL and events without. I am interested in latter case , because with a 100 % close trigger probability of HCAL, any secondary muon punching through ECAL and HCAL will tag an observable trident.

The MC final sample has the number distributions and spectrum distribution plotted in histograms 7.12, 7.13 , 7.14 and 7.15.

Again, I separate the sample in cases of double and cases of triple coincidences. Results of statistic significance are collected in tables 7.5 and 7.6.

Looking at the values in these tables the only conclusive info regards HCAL and molasse numbers. We would expect 1-2 events with tridents in HCAL and 2-3 events from Molasse. All these events will have only two complete tracks in ALEPH, and a secondary is stopping between vertex and ALEPH lowest layer. This is consistent with real event 49100-9231 (displayed in 5.5 and 5.6). The events from Molasse will not create recognizable pattern.

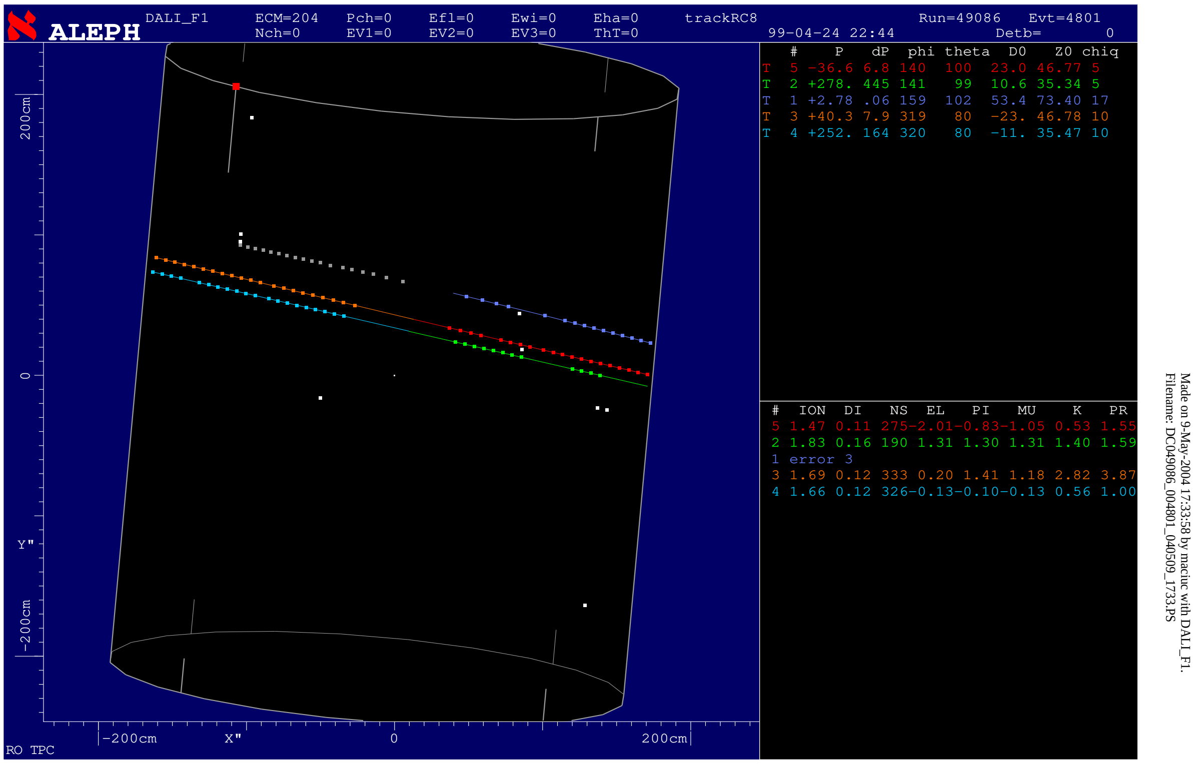

Figure 7.7: Triple coincidence of atmospheric muons or of trident muons in overburden II

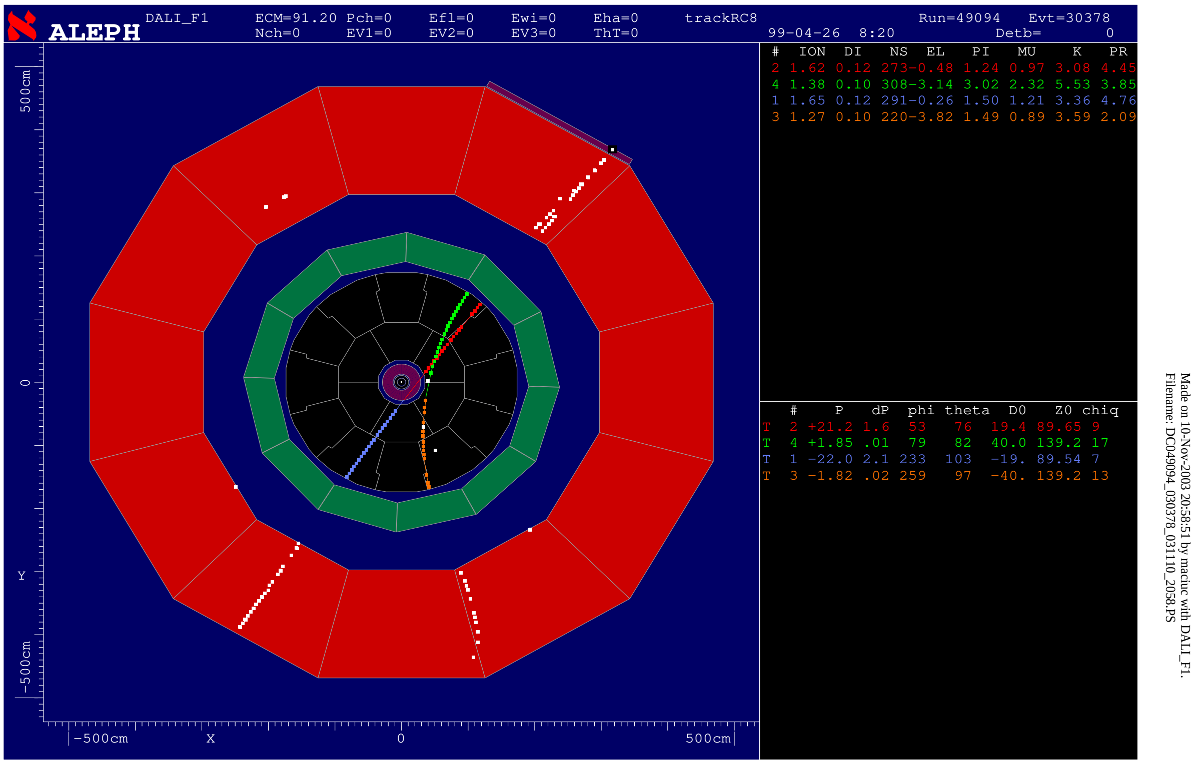

Figure 7.8: Double coincidence of atmospheric muons or trident in HCAL - I

End of tracks

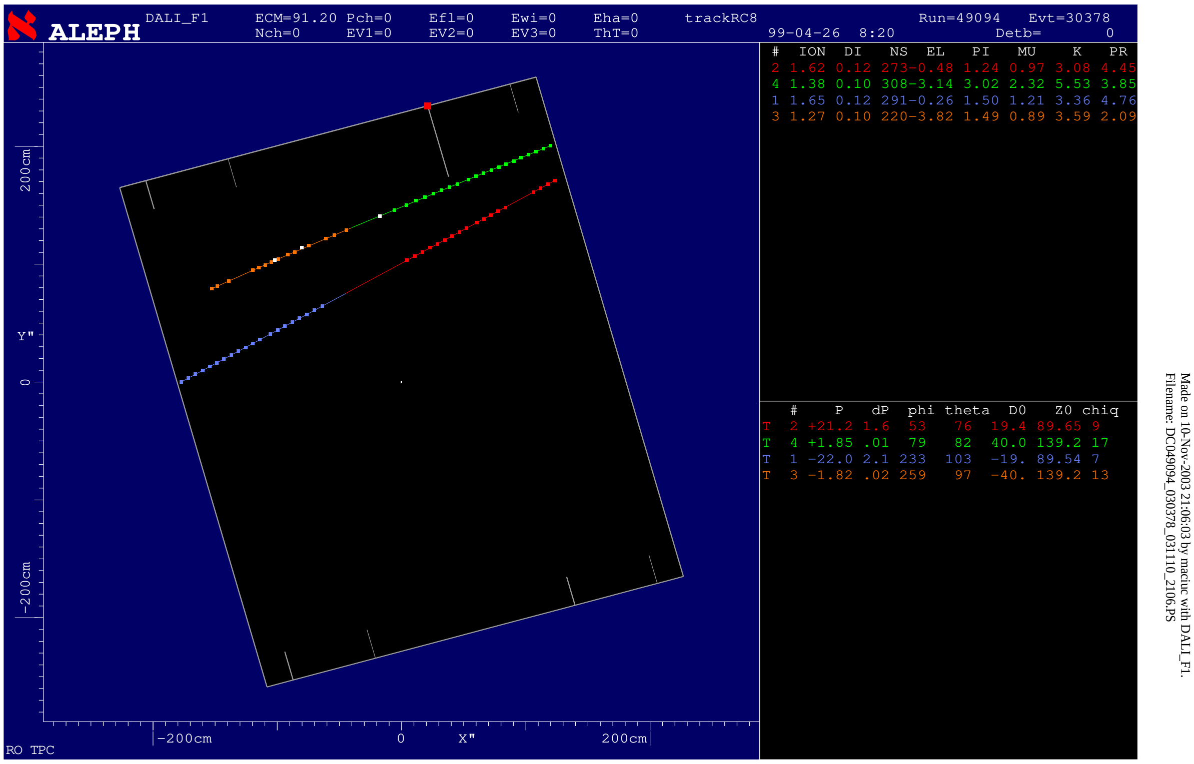

Figure 7.9: Double coincidence of atmospheric muons or trident in HCAL - II

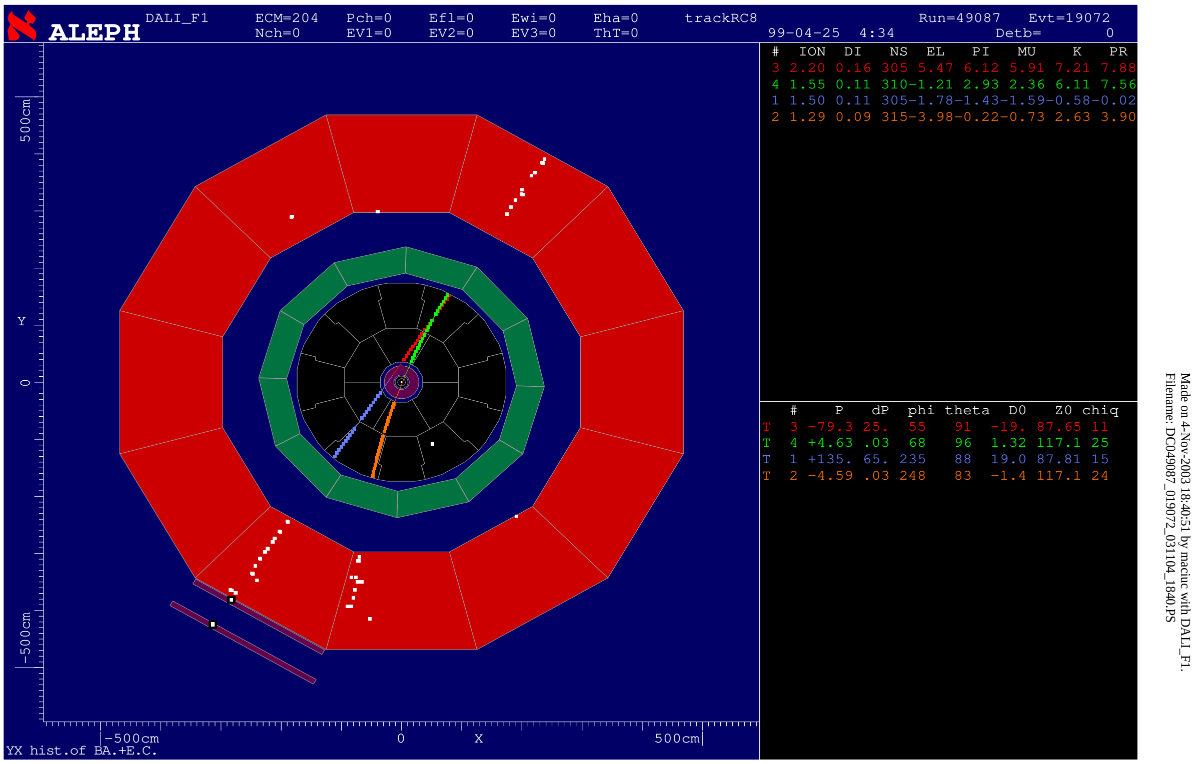

Figure 7.10: Pion photonuclear production or trident in HCAL - I

End of tracks

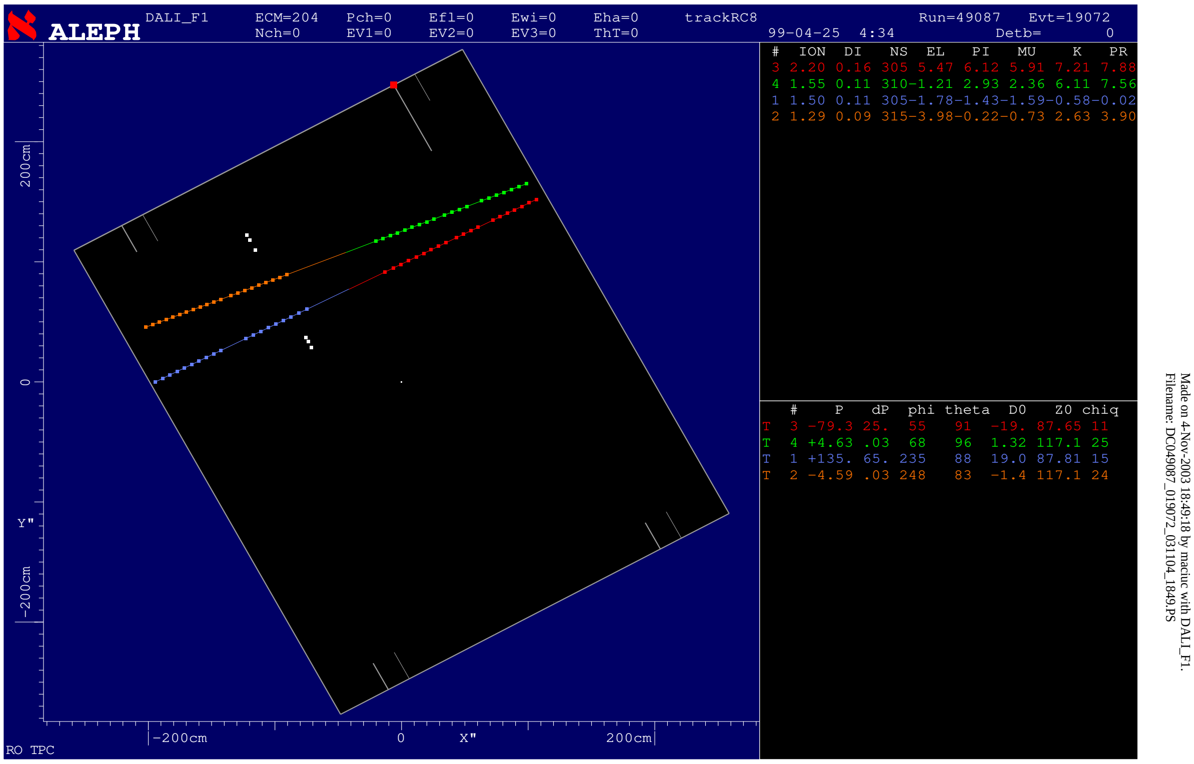

Figure 7.11: Pion photonuclear production or trident in HCAL - II

Table 7.5: MC number of events with primary and only one of secondaries going through ALEPH

Layer	average number	adev	sdev (RMS)
ECAL lead	0.52	0.60	0.69
HCAL iron	1.40	0.87	1.03
Molasse	2.10	1.31	1.66
Soil	0.24	0.38	0.52

Table 7.6: MC number of events with primary and all secondaries going through ALEPH

Layer	average number	adev	sdev (RMS)
ECAL lead	0.27	0.41	0.51
HCAL iron	0.50	0.61	0.72
Molasse	0.42	0.55	0.64
Soil	0.0	0.0	0.1

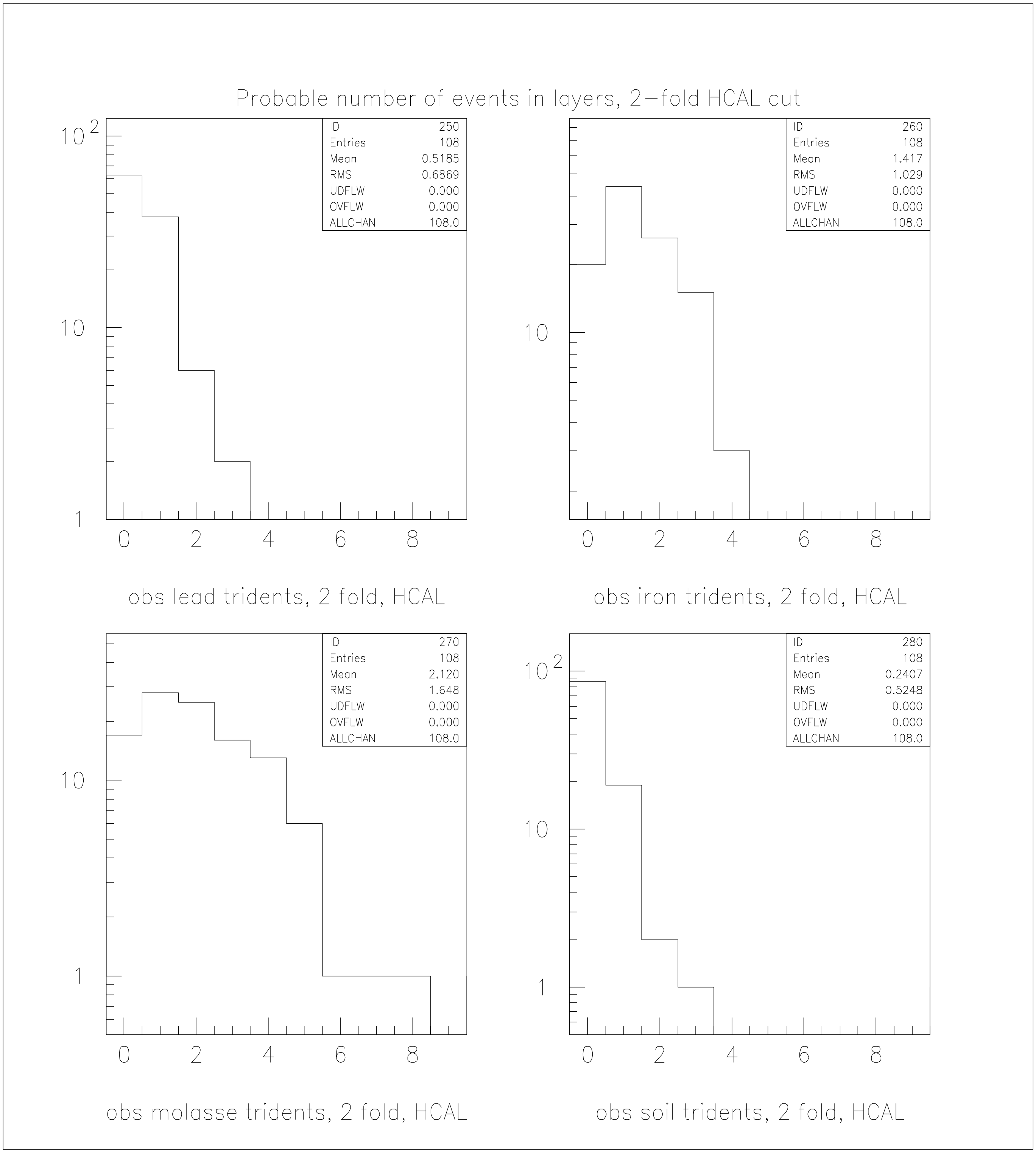

Figure 7.12: MC distribution of the trident numbers per layer, only $\mu^+\mu^-$ events with one secondary that punched through HCAL are included

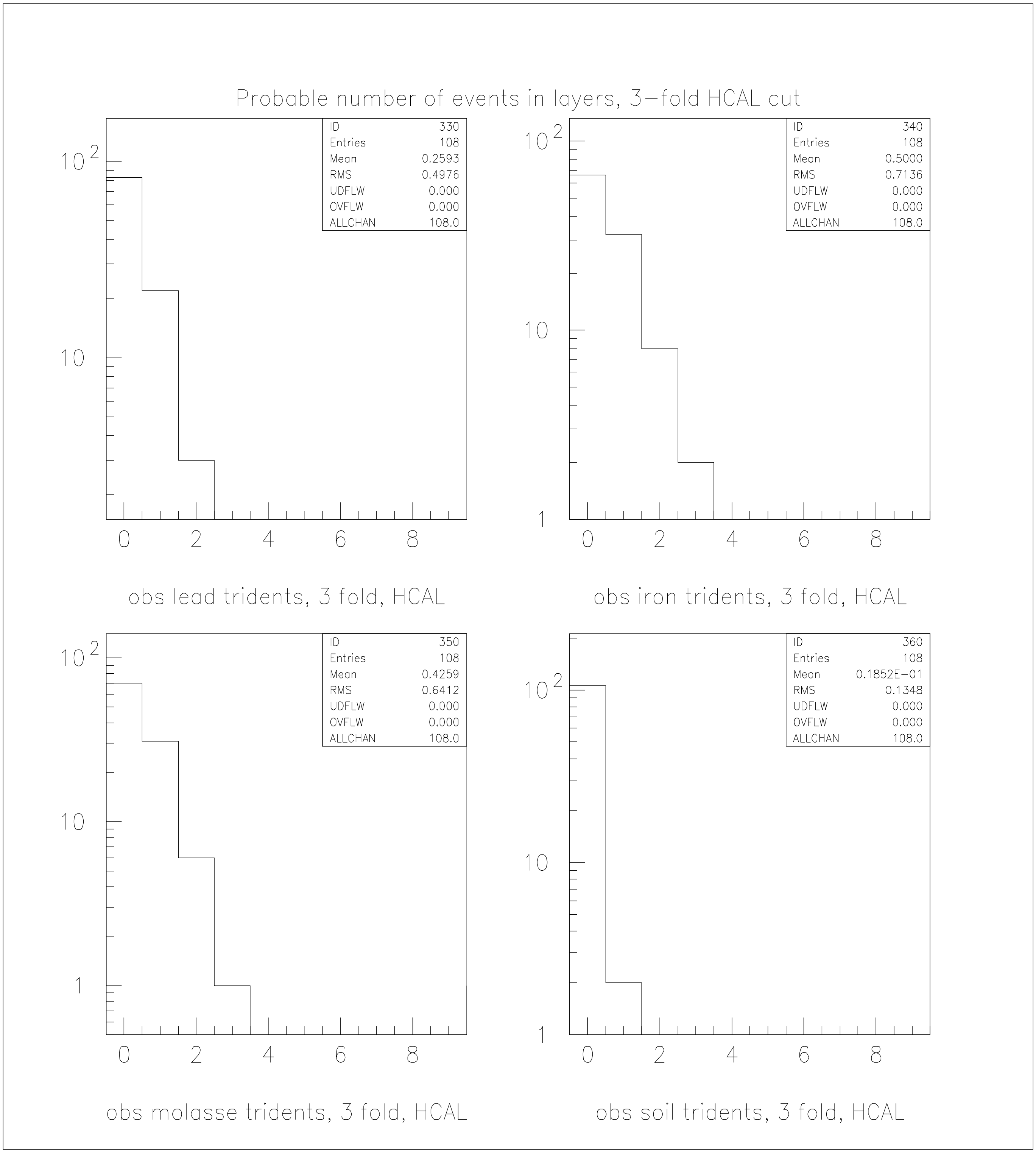

Figure 7.13: MC distribution of the tridents number per layers, only $\mu^+\mu^-$ events were a triad of tracks punched through HCAL

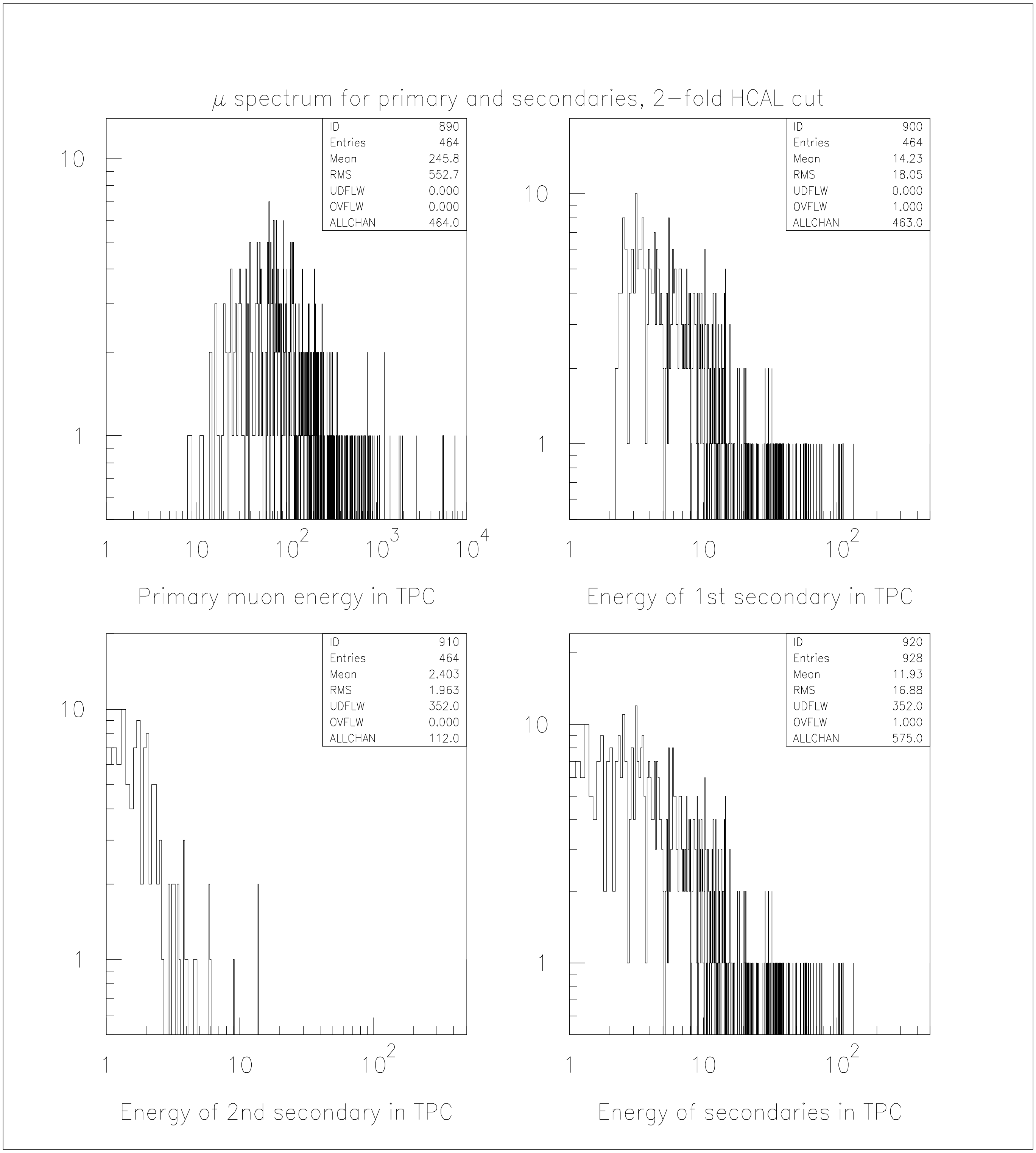

Figure 7.14: MC spectra of each trident component, only $\mu^+\mu^-$ events, with a punch-through HCAL secondary, were selected

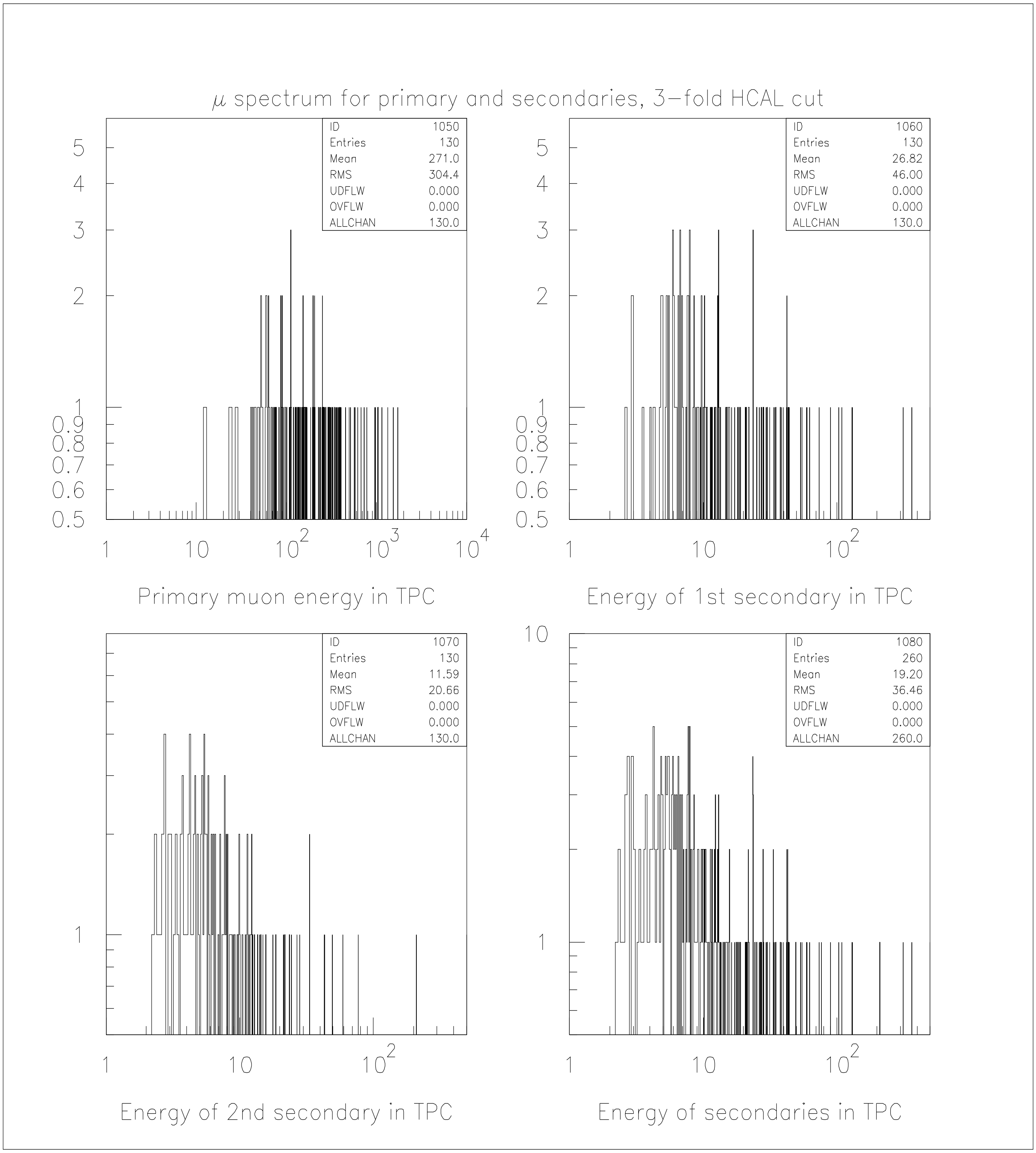

Figure 7.15: MC spectra of each trident component, only $\mu^+\mu^-$ events, where both secondaries punched through HCAL, have been selected

The values of table 7.6 are unsubstantial, thus some change in point of view is required. Of course, the values are suggesting a null event case for soil, molasse (we already knew that) and lead. An event could be expected (50 % probability) with a trident vertex in HCAL.

Considering only the ALEPH shells to be places of trident production, the combined HCAL-ECAL trident probability for a single event is 62 % . This is, again, consistent with event 49092-15133 (displayed in 5.3 and 5.4).

To check the upper conclusions I compare the expected spectra for observed tridents given in graphs 7.14 and 7.15 with the real data from 5.5, 5.6, 5.3 and 5.4. Concluding values are:
- for primaries the MC most probable values are close to 60 GeV (for 2 full tracks in HCAL) and 100 GeV (for 3 full tracks in HCAL);
- primaries real values are 46 ± 4.4 (2 full tracks in HCAL) and, an other, higher than 100 GeV (all 3 full tracks in HCAL) (consistent with large tail in 7.15);
- MC values for first secondary are 4 GeV (mean value of 14GeV - for 2-fold case) and mean value of 27 GeV (for 3-fold case);
- real values for first secondary muon are 10 GeV (for 2-fold case) and 32 ± 16 GeV (for 3-fold case);
- MC values for the last secondary are average value of 2.5 ± 2GeV (most probable value 1.3 GeV, this for 2-fold case) and average value of 12 ± 9 GeV (most probable close to 3 GeV, for 3-fold case);
- real values for last secondary are 1.26 GeV (2-fold) and 12.3 GeV (3-fold).

There seems to be a close match between expected spectra and data analysis values.

Chapter 8

Conclusions and envisaged improvements

The deepest sin against the human mind is to believe things without evidence. Science is simply common sense at its best – that is, rigidly accurate in observation, and merciless to fallacy in logic.
Thomas Huxley

This study of $\mu^+\mu^-$ pair production by atmospheric muons is concluded by the following statements:
• I found 2 close to perfect muonic candidates;
• the HMDMC code developed is consistent;
• the results of HMDMC agree to a high level of confidence with real data;
• there seems to be perfect agreement between KKP cross-section and CosmoALEPH physical results;
• overall the study is "bullet proof" in the sense of apparent lack of inconsistencies;
• the work invested (more than 10^5 lines of code, thousands hours of computer time, one full year of work) seems to have paid off.

To upgrade the present status of study some more additions are required. There is need of a hadronic simulation to estimate the level of background coming from photonuclear interactions. The code can be enhanced by refining the geometry setup of $\mu^+\mu^-$ pair production, and, also, of the detector. To achieve the latter, a full theoretical analysis of the exact $\mu^+\mu^-$ pair production cross-section is required.

For the future, I will increase the MC statistics. The runs were hampered till now by system and compiler bugs (they seldom appear in some of the runs, but since the output is common the file is corrupted, and all work is lost). The origin of this problem is known and the problem is fixed for future versions of Monte Carlo (HMDMC).

Bibliography

[BB81] L. B. Bezrukov and E. V. Bugaev. Nucleon shadowing effects in photonuclear interactions. *Soviet Journal of Nuclear Physics*, 5(33):635–641, May 1981.

[Bow95] C. Bowdery. ALEPH handbook. Technical report, ALEPH colaboration: CERN, 1995, http://aleph.web.cern.ch/aleph/handbook.

[CER] Cern computer library short write-ups, http://wwwasdoc.web.cern.ch/wwwasdoc/cernlib.html.

[Cra95] D. Crane. The length of the NuMI shield. Technical Report NuMI-B-121, NuMI, 1995, http://citeseer.ist.psu.edu/crane95length.html.

[DR] D.Chirkin and W. Rhode. Muon Monte Carlo: a new high-precision tool for muon propagation through matter, http://amanda.berkeley.edu/~dima/work/MUONPR/muon.ps.gz.

[Gea04] Geant4 physics reference manual, 2004, http://wwwasd.web.cern.ch/wwwasd/geant4/geant4.html.

[Gro98] Particle Data Group. Review of particle physics. *The European Physical Journal C*, 3, 1998, World Wide Web: http://pdg.lbl.gov/.

[Gru96] C. Grupen. *Particle detectors*. Cambridge University Press, 1996.

[Hon95] J. T. Hong. Multiple muon measurements with MACRO. arxiv: preprint, February 1995, arxiv.org/abs/hep-ex/9410001.

[IASK01] E. V. Bugaev I. A. Sokalski and S. I. Klimushin. MUM:flexible precise Monte Carlo algorithm for muon propagation through thick layers of matter, 2001, http://arxiv.org/abs/hep-ph/0010322.

[Kel67] S. R. Kelner. Pair production in collisions between a fast particle and a nucleus. *Soviet Journal of Nuclear Physics*, 5(5):778–783, November 1967.

[Mur] Kent Murray. Geology 118: Physical geology. Lecture on Geology: University of Michigan-Dearborn, http://www.umd.umich.edu/casl/natsci/geology/notes.html.

[PS95] M.E. Peskin and D.V. Schroeder. *An Introduction to Quantum Field Theory*. Westview Press, 1995.

[01a] Anikeev et al. Direct observation of muon pair production by cosmic ray muons. In *Proceedings of ICRC 2001*, pages 962–965. Copernicus Gesellschaft 2001, 2001, www.copernicus.org/icrc/papers/ici6561_p.pdf.

[01b] M. Amrosio et al. High statistics measurement of the underground muon pair separation at Gran Sasso. *Physical Review D*, 60, June 2001.

[RSB82] S.M. Seltzer R.M. Sternheimer and M.J. Berger. Density effect for the ionization loss of charged particles in various substances. *Physical Review B*, 26(11):6067–6076, December 1982.

[RSS84] M.J. Berger R.M. Sternheimer and S.M. Seltzer. *Atomic Data and Nuclear Data Tables*, 30:261–271, 1984.

[Sca99] E Scapparone. Review of cosmic ray experiments with underground detectors. arxiv: preprint, February 1999, `arxiv.org/abs/hep-ex/9902040`.

[Ser71] C. R. Serre. Evaluation de la perte d'energy unitaire et du parcours pour des mouns de la 2 a 600 GeV dans un abrosbant quelconque. CERN report 71-18, CERN, 1971.

[Sio00] M Sioli. Underground muon physics with the MACRO experiment. arxiv: preprint, February 2000, `arxiv.org/abs/hep-ex/0002051`.

[SKP95] R.P. Kokoulin S.R. Kelner and A. A. Petrukhin. About cross-section for high-energy muon bremsstrahlung. *Moscow:Preprint/MEPhI*, 024-95, 1995, `http://doc.cern.ch/cgi-bin/tiff2html?2/archive/electronic//scan/9510/SC%AN-9510048.tif`.

[SR00] S. Roesler S. Rokni, J.C. Liu. Initial estimates of the activation concentration of the soil and groundwater around the NLC Beam Delivery System Tunnel. SLAC RADIATION PHYSICS NOTE RP-00-04, SLAC, May 2000, `www-project.slac.stanford.edu/lc/local/Radphysics/BDSACTIVAATION.pdf`.

[SRKP99] R. P. Kokoulin S. R. Kelner and A. A. Petrukhin. Muon pair production by high energy muons and muon bundles underground. World Wide Web, `http://www.icrc1999.utah.edu/~icrc1999/root/vol2/h3_1_09.pdf`, 26th International Cosmic Ray Conference (ICRC 99), HE 3.1.09, 1999.

[Ste56] R.M. Sternheimer. Density effect for the ionization loss in various materials. *Physical Review*, 103(3):511–515, August 1956.

[Tit99] A. B. Titus. *Calcul numeric in C (in romanian).* Casa de Editura Albastra, Cluj-Napoca, 1999.

[Vis00] F. Vissani. Charm production by cosmic muons, 2000, hep-ph/0004073.

[WC99] A. Wehmann and S. Childress. Tritium production in dolomitic rock adjacent to NuMI beam tunnels. Technical Report NuMI-B-495, NuMI, 1999, `http://citeseer.ist.psu.edu/336170.html`.

[WLV85] R. Kopp W. Lohmann and R. Voss. Energy loss of muons in the energy range $1 - 10000\text{GeV}$. Yellow Reports 85-03, CERN, 1985.

[WPF92] W.T. Vetterling W.H. Press, S.A. Teukolsky and B.P. Flannery. *Numerical Recipes in C:The Art of Scientific Computing, Second Edition.* Cambridge University Press, Cambridge, 1992.

Chapter 9

Appendix

9.1 Parameterized formulae for different physical processes

9.1.1 Ionization energy loss

$$\frac{dE}{dx} = 2\pi\alpha^2 N_A \lambda\!\!\!^{-}_e{}^2 \frac{Zm_ec^2}{A\beta^2}\left\{ln\frac{2m_ec^2\beta^2\gamma^2E'_m}{I^2(Z)} - 2\beta^2 + \frac{E'^2_m}{4E^2} - \delta(\gamma)\right\}$$

Here: $\alpha = \frac{1}{137.036}$ is the fine structure constant,
$N_A = 6.022 \quad 10^{23}$ is Avogadro number,
Z, and A are atomic numbers, for compounds and mixtures, we have: $\frac{Z}{A} = \sum_i \frac{Z_i}{A_i} W_i$, W_i weight of individual element in compound,
m_e and m_μ are electron and muon masses,
$\beta = \frac{p}{E}$ where p muon momentum, $\gamma = \frac{E}{m_\mu}$
$\lambda\!\!\!^{-}_e = 3.8616 \times 10^{-11} cm$ is the Compton wavelength of electron divided by 2π,
$I(Z)$ is the ionization potential of medium, E'_m is the maximal energy transferable to electrons:

$$E'_m = 2m_ec^2\frac{p^2}{m_e^2c^2 + m_\mu^2c^2 + 2m_eE} \qquad ,$$

δ is the density correction with parameterization([RSB82]):

$$\begin{aligned} \delta(X) &= 4.6052X + a\,(X_1 - X)^m + C \qquad && X_0 < X < X_1 \\ \delta(X) &= 4.6052X + C && X > X_1 \end{aligned} \tag{9.1}$$

here $X = \lg(\beta\gamma)$ (in Rusian literature lg is $\log_{10}$ or log in anglo-saxon literature) , and the parameters for different elements, mixtures-compounds are found in literature ([RSS84],[Ste56],[RSB82]).

9.1.2 Bremsstrahlung Cross-section

$$\frac{d\sigma}{dv} = \alpha^3 Z(Z+1)\left(2\lambda\!\!\!^{-}_e\frac{m_e}{m_\mu}\right)^2\frac{1}{v}\left(\frac{4}{3} - \frac{4}{3}v + v^2\right)\phi(\delta) \tag{9.2}$$

the constants have the same meaning as in case of ionization, and function ϕ is:

$$
\phi(\delta) = \begin{cases} ln\frac{\frac{189 m_\mu}{m_e} Z^{-1/3}}{1+\frac{189\sqrt{e}}{m_e}\delta Z^{-1/3}} & \text{for} \quad Z \leq 10 \\ \\ ln\frac{\frac{2}{3}\frac{189 m_\mu}{m_e} Z^{-2/3}}{1+\frac{189\sqrt{e}}{m_e}\delta Z^{-1/3}} & \text{for} \quad Z > 10 \end{cases} \tag{9.3}
$$

with $\delta = \frac{m_\mu^2 v}{2E(1-v)}$ momentum transfer to nucleus.

9.1.3 Cross-Section of pair production by high energy muons

The following formulas are from [WLV85]:

$$
\frac{d\sigma}{dv d\rho} = \alpha^4 \frac{2}{3\pi} Z(Z+1)\left(\lambda\!\!\!^{-}_e\right)^2 \frac{1-v}{v}\left[\phi_e + \left(\frac{m_e}{m_\mu}\right)^2 \phi_\mu\right] \tag{9.4}
$$

$$
\phi_e = \left\{\left[\left(2+\rho^2\right)(1+\beta) + \xi\left(3+\rho^2\right)\right] ln\left(1+\xi^{-1}\right) + \frac{1-\rho^2-\beta}{1+\xi} - \left(3+\rho^2\right)\right\} \cdot L_e \tag{9.5}
$$

$$
\phi_\mu = \left\{\left[\left(1+\rho^2\right)\left(1+\frac{3}{2}\beta\right) - \frac{(1+2\beta)\left(1-\rho^2\right)}{\xi}\right] ln\,(1+\xi) + \right.
$$

$$
\left. + \frac{\xi\left(1-\rho^2-\beta\right)}{1+\xi} + (1+2\beta)\left(1-\rho^2\right)\right\} \cdot L_\mu \tag{9.6}
$$

$$
L_e = ln\frac{RZ^{-\frac{1}{3}}\sqrt{(1+\xi)(1+Y_e)}}{1+\frac{2m_e\sqrt{e}RZ^{-\frac{1}{3}}(1+\xi)(1+Y_e)}{Ev(1-\rho^2)}} - \frac{1}{2} ln\left[1+\left(\frac{3}{2}\frac{m_e}{m_\mu}Z^{\frac{1}{3}}\right)^2 (1+\xi)(1+Y_e)\right] \tag{9.7}
$$

$$
L_\mu = ln\frac{\frac{2}{3}\frac{m_\mu}{m_e} RZ^{-\frac{2}{3}}}{1+\frac{2m_e\sqrt{e}RZ^{-\frac{1}{3}}(1+\xi)(1+Y_\mu)}{Ev(1-\rho^2)}} \tag{9.8}
$$

$$
Y_e = \frac{5-\rho^2+4\beta\left(1+\rho^2\right)}{2(1+3\beta)\, ln\left(3+\frac{1}{\xi}\right) - \rho^2 - 2\beta\left(2-\rho^2\right)} \tag{9.9}
$$

$$
Y_\mu = \frac{4+\rho^2+3\beta\left(1+\rho^2\right)}{\left(1+\rho^2\right)\left(\frac{3}{2}+2\beta\right) ln\,(3+\xi) + 1 - \frac{3}{2}\rho^2} \tag{9.10}
$$

$$
\beta = \frac{v^2}{2(1-v)}, \quad \xi = \left(\frac{m_\mu v}{2m_e}\right)^2 \frac{1-\rho^2}{1-v} \tag{9.11}
$$

$$
\rho = \frac{E^+ - E^-}{E^+ + E^-}, \qquad v = \frac{E^+ + E^-}{E} \tag{9.12}
$$

Here Z(Z+1) was considered to account for the atomic electron contribution to the cross-section. The energy threshold for pair production on atomic electrons is 22.4 GeV, but, since this energy value is much smaller than critical energy (the energy from where the radiative processes become dominant), the formula was extended to low energy domain.

9.1.4 Photonuclear cross-section

Bezrukov and Bugaev parameterization of photonuclear cross-section

$$\begin{aligned}\frac{d\sigma}{dv} = \frac{\alpha}{2\pi} A\sigma_{\gamma N} v \Bigg\{ \frac{3}{4} G(x) \left[\kappa \quad ln\left(1+\frac{m_1^2}{t}\right) - \frac{\kappa m_1^2}{m_1^2+t} - \frac{2m_\mu^2}{t} \right] \\ + \frac{1}{4}\left[\kappa ln\left(1+\frac{m_2^2}{t}\right) - \frac{2m_\mu^2}{t}\right] + \\ \frac{m_\mu^2}{2t}\left[\frac{3}{4}G(x)\frac{m_1^2}{m_1^2+t} + \frac{m_2^2}{4t} ln\left(1+\frac{t}{m_2^2}\right)\right]\Bigg\}\end{aligned} \tag{9.13}$$

where:

$$\begin{aligned} G(x) &= \frac{3}{x^3}\left(\frac{x^2}{2} - 1 + e^{-x}(1+x)\right) \quad , \quad x = 0.00282 A^{1/3}\sigma_{\gamma N}(\epsilon) \\ \sigma_{\gamma N}(\epsilon) &= 114.3 + 1.647 ln^2(0.0213\epsilon)(\mu b) \quad , \\ t &= \frac{m_\mu^2 v^2}{1-v} \quad , \qquad \kappa = 1 - \tfrac{2}{v} + \tfrac{2}{v^2} \\ m_1^2 &= 0.54\,\mathrm{GeV}^2 \qquad m_2^2 = 1.8\,\mathrm{GeV}^2 \end{aligned} \tag{9.14}$$

and ϵ is the photon energy in GeV, $v = \frac{\epsilon}{E}$.
$\sigma_{\gamma N}$ is the total photonuclear cross-section per nucleon. A and α have the same meaning as in previous sections.

This analytic formula was integrated (an adaptive step Romberg formalism was used) to get the muon average energy loss and the formula is the same as for bremsstrahlung. There are singularities in 9.13 for 0 and 1, but this is easy to cure, by restricting the integration range to a kinematic and model dependent interval.

$$m_\pi + \frac{m_\pi^2}{2M} < v < E - \frac{M}{2}\left(1 + \frac{m_\mu^2}{M^2}\right) \tag{9.15}$$

M is the nucleon mass (proton mass). Even though, normally, the upper formulae are restricted to a range $\epsilon \in [10, 10^6]$, extrapolation of the formula to lower energies will not affect the energy loss estimate. This is consistent, since ionization dominates the lower energy interval.

Borog and Petruckhin parameterization of photonuclear cross-section

Borog, Petruckhin parameterization [Gea04] is valid at energies higher than 10 GeV (yet, it is not harmful to extrapolate to lower energies, since radiative processes are negligible in that range). Results of this formula are in agreement within 5% ([Gea04]) with energy loss average estimation of 9.13.

$$
\begin{aligned}
\frac{d\sigma}{d\epsilon}(\epsilon, E) &= \Psi(\epsilon)\Phi(E, v) && (9.16)\\
\Psi(\epsilon) &= \frac{\alpha}{\pi}\frac{A_{eff}N_A}{A}\sigma_{\gamma N}(\epsilon)\cdot\frac{1}{\epsilon} && (9.17)\\
\Phi(e, v) &= v - 1 + \left[1 - v + \frac{v^2}{2}\left(1 + \frac{2m_\mu^2}{\Lambda^2}\right)\right]\cdot ln\left\{\frac{\frac{E^2(1-v)}{m_\mu^2}\left[1 + \frac{m_\mu^2 v^2}{\Lambda^2(1-v)}\right]}{1 + \frac{Ev}{\Lambda}\left[1 + \frac{\Lambda}{2M} + \frac{Ev}{\Lambda}\right]}\right\} && (9.18)
\end{aligned}
$$

where: ϵ(GeV) is the energy lost by muon, $v = \frac{\epsilon}{E}$ is fraction of energy transfered to photon (approximated to be real), M is the proton mass, $\Lambda^2 = 0.4\,\mathrm{GeV}^2$ is Vector Dominance Model parameter (part of a Form Factor formula). A_{eff} is to take into account shadowing:

$$A_{eff} = 0.22A + 0.78A^{0.89} \tag{9.19}$$

An alternative cross-section for photon absorption by nucleon (compare to 9.14) is:

$$\sigma_{\gamma N}(\epsilon) = 49.2 + 11.1\cdot ln(\epsilon) + \frac{151.8}{\sqrt{\epsilon}} \quad (\mu b) \tag{9.20}$$

The limits of integration can be arbitrarily chosen: $\epsilon_{min} = 0.2$ GeV this lower limit has less influence upon the final numerical value, and, $\epsilon_{max} = E - \frac{M}{2}$.

9.1.5 $\frac{dE}{dx}$ picture gallery

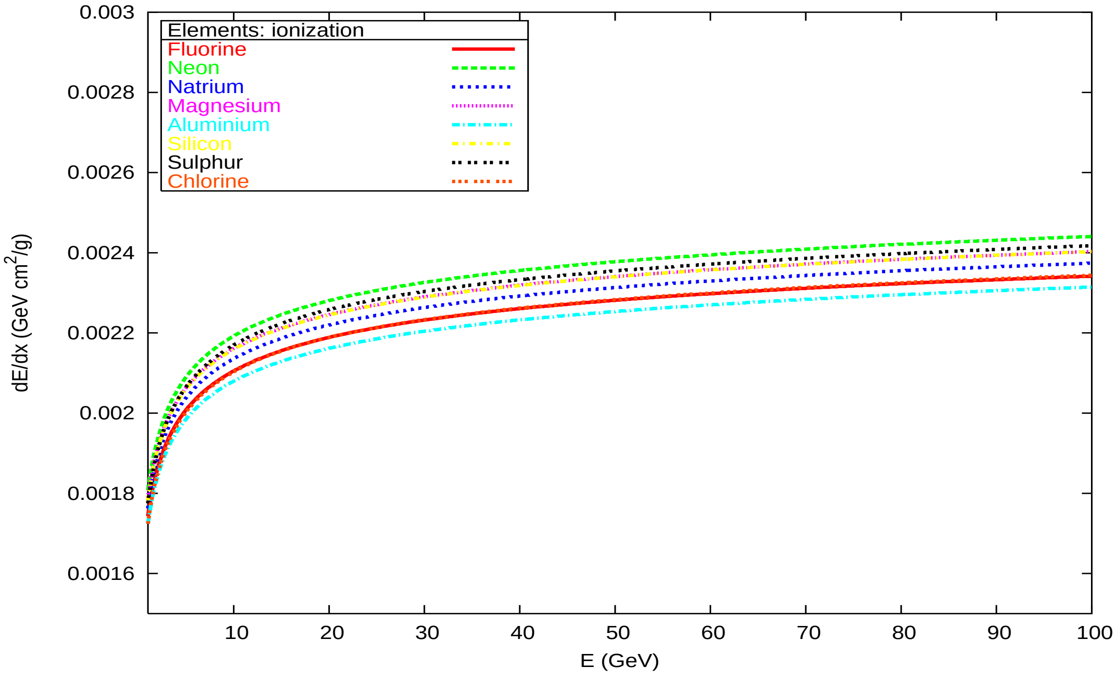

Figure 9.1: Muon energy loss by ionization in elements II

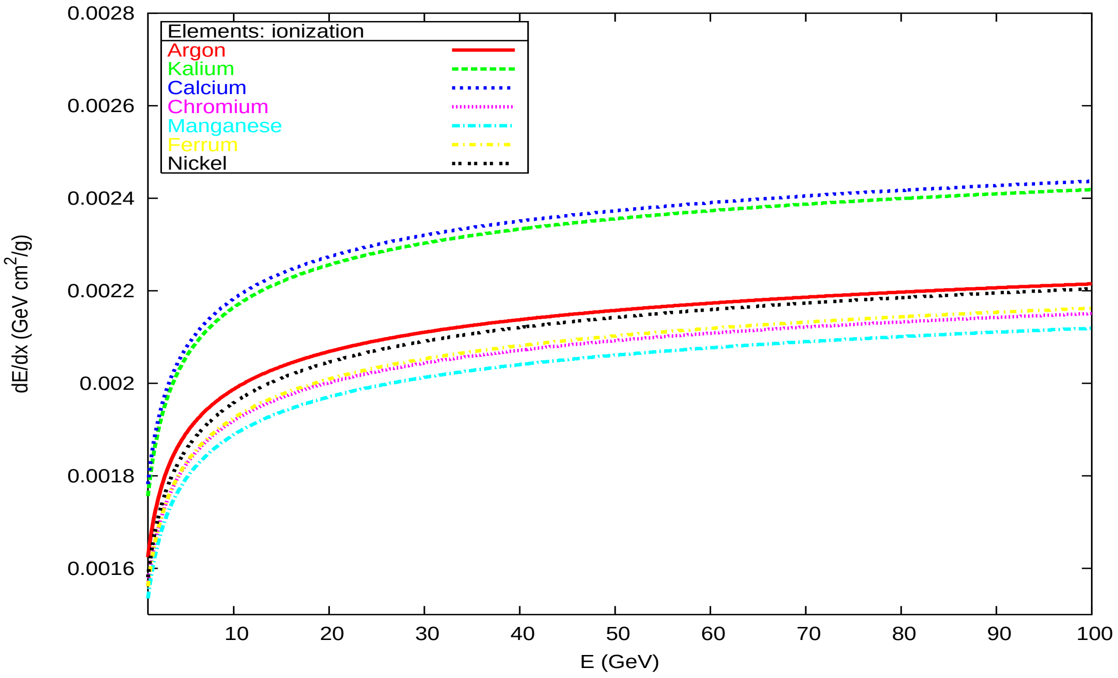

Figure 9.2: Muon energy loss by ionization in elements III

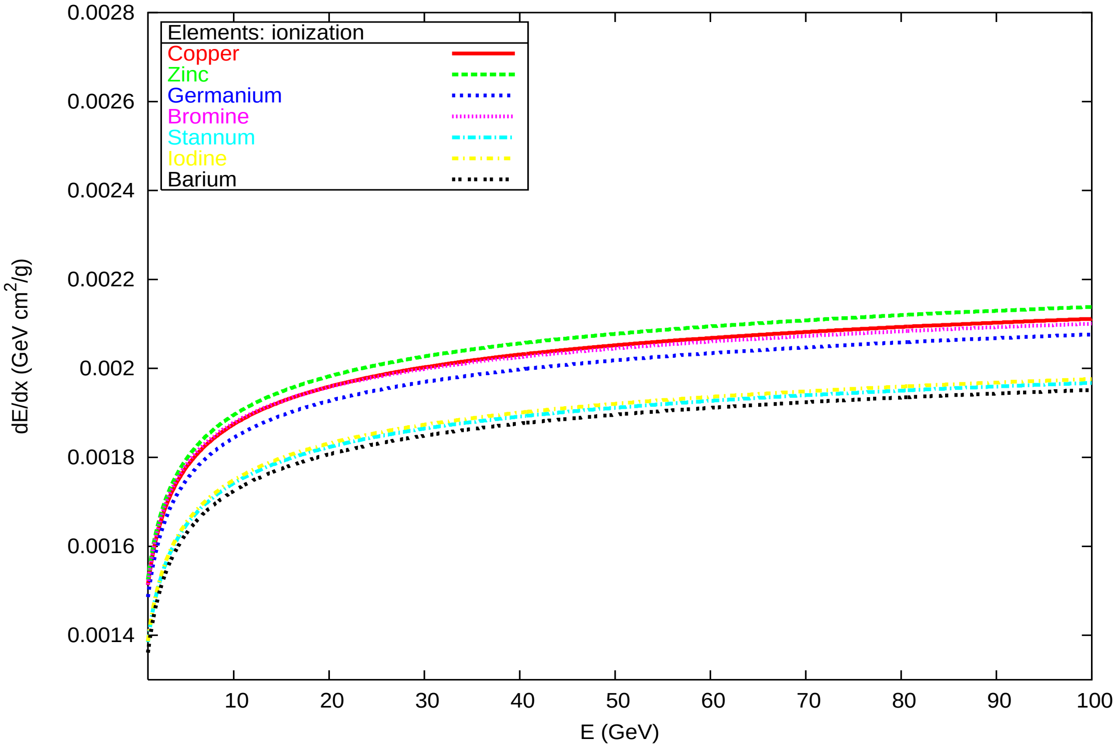

Figure 9.3: Muon energy loss by ionization in elements IV

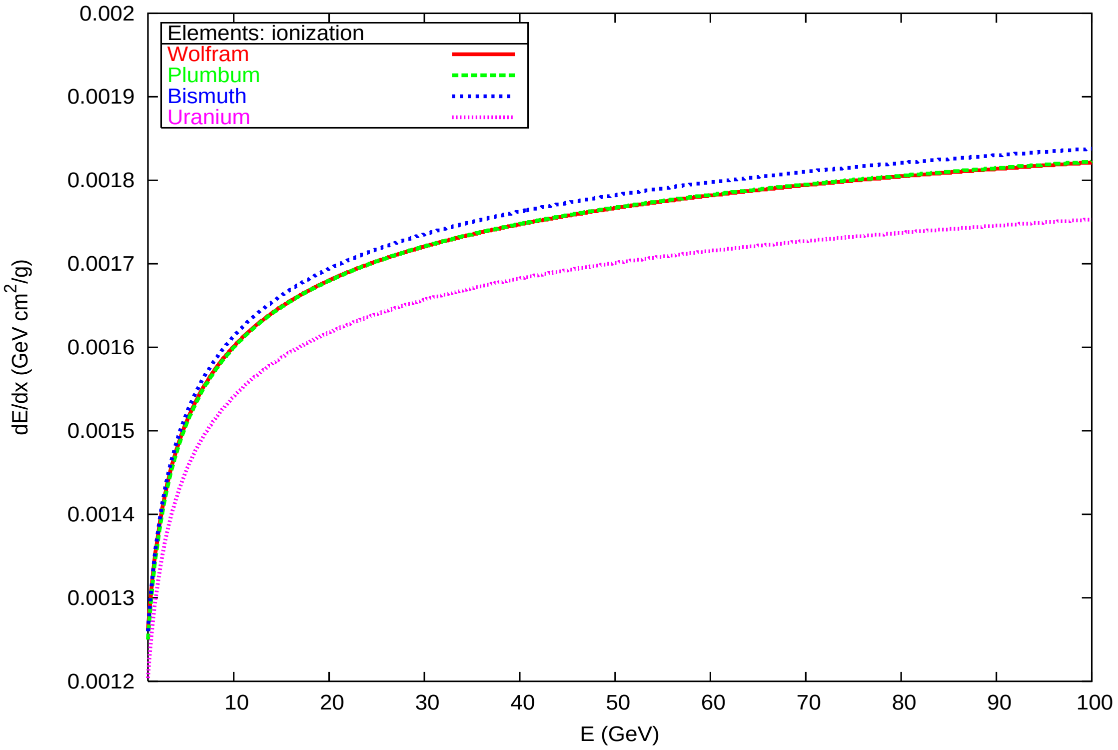

Figure 9.4: Muon energy loss by ionization in elements V

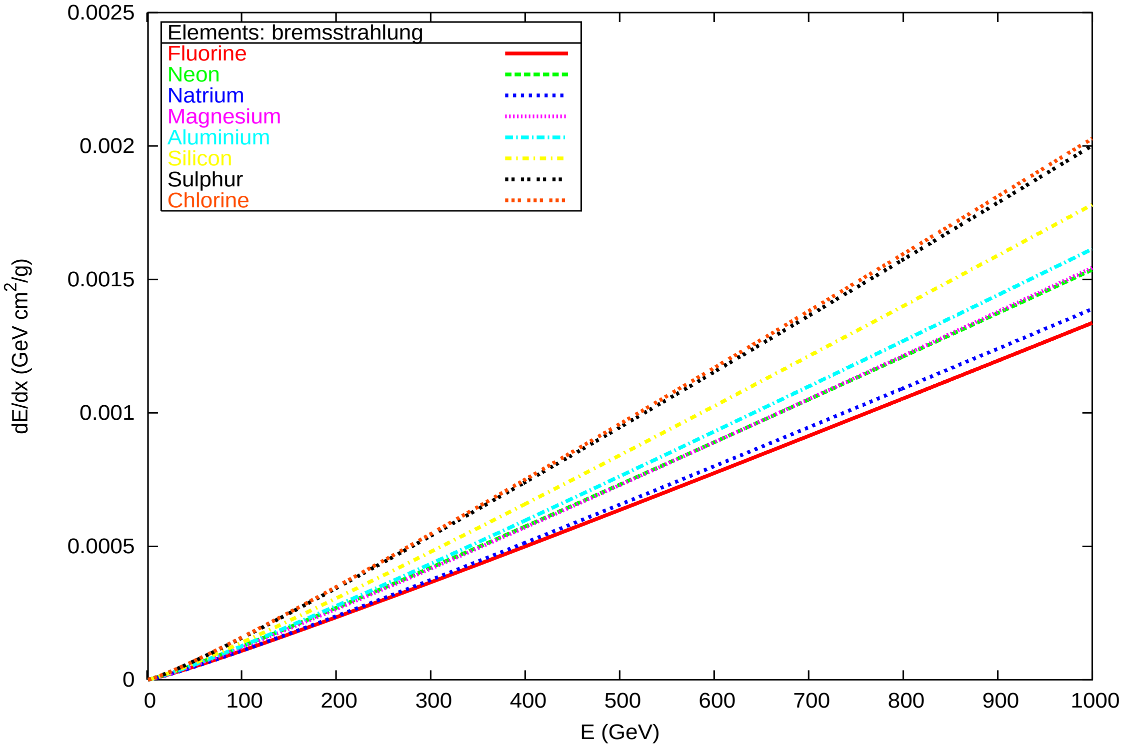

Figure 9.5: Muon bremsstrahlung energy losses in elements II

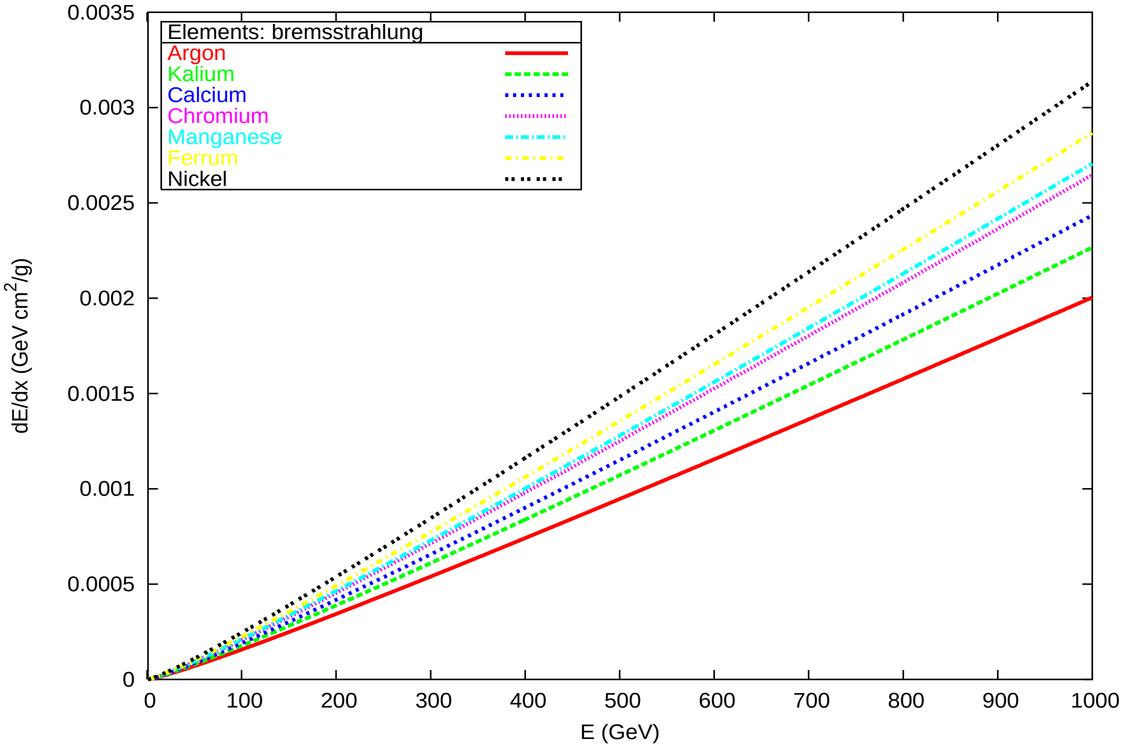

Figure 9.6: Muon bremsstrahlung energy losses in elements III

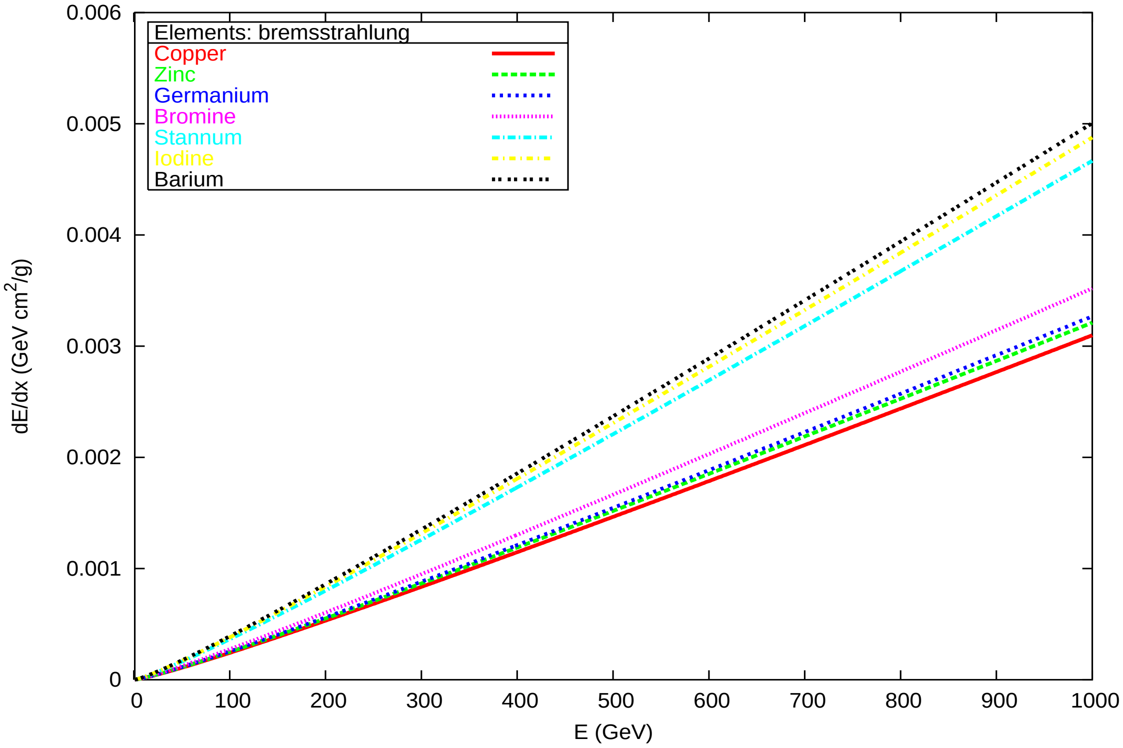

Figure 9.7: Muon bremsstrahlung energy losses in elements IV

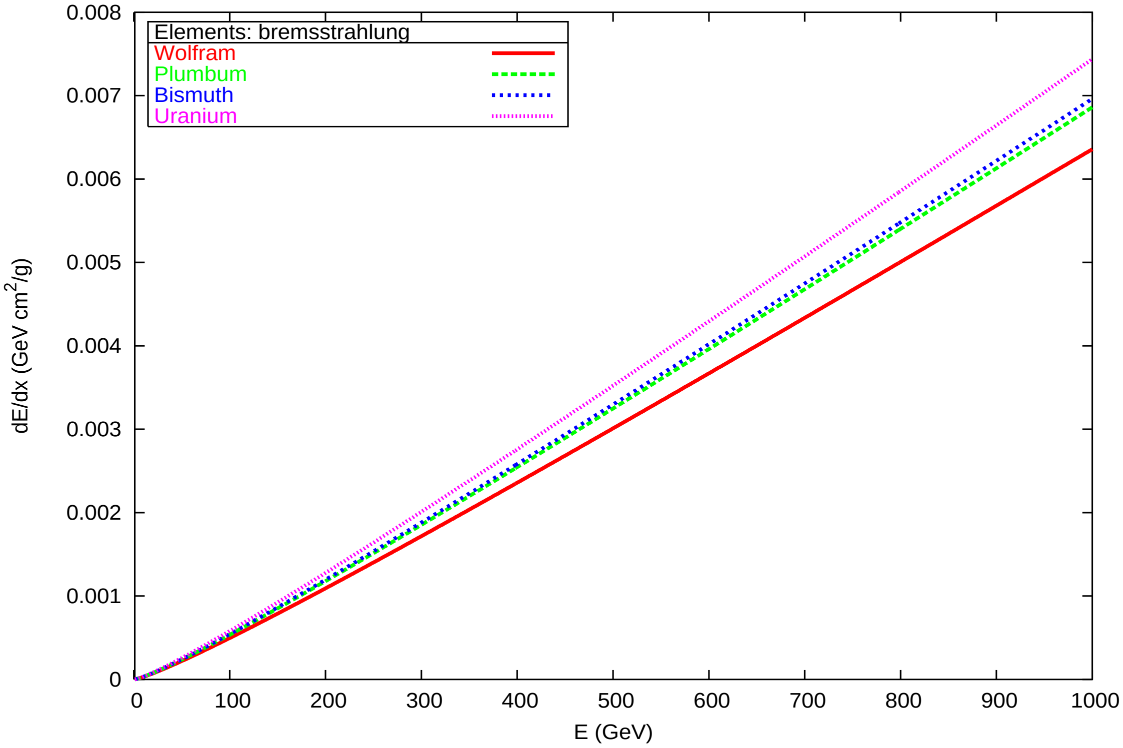

Figure 9.8: Muon bremsstrahlung energy losses in elements V

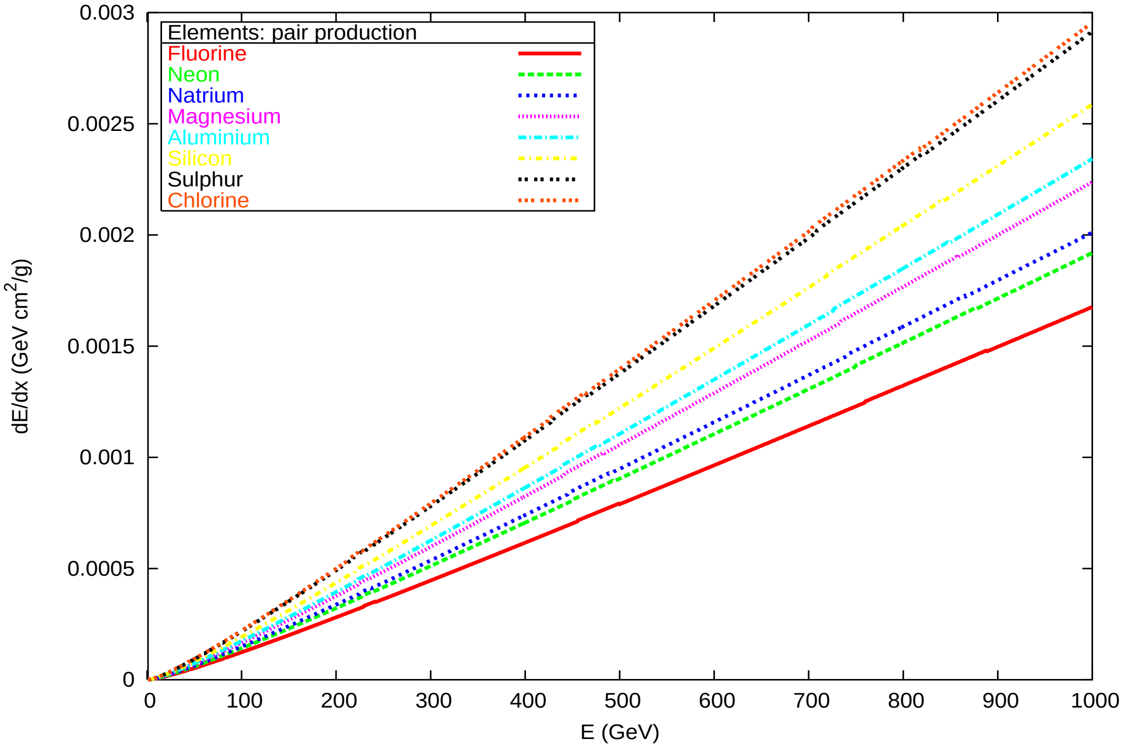

Figure 9.9: Muon energy losses via pair production in elements II.

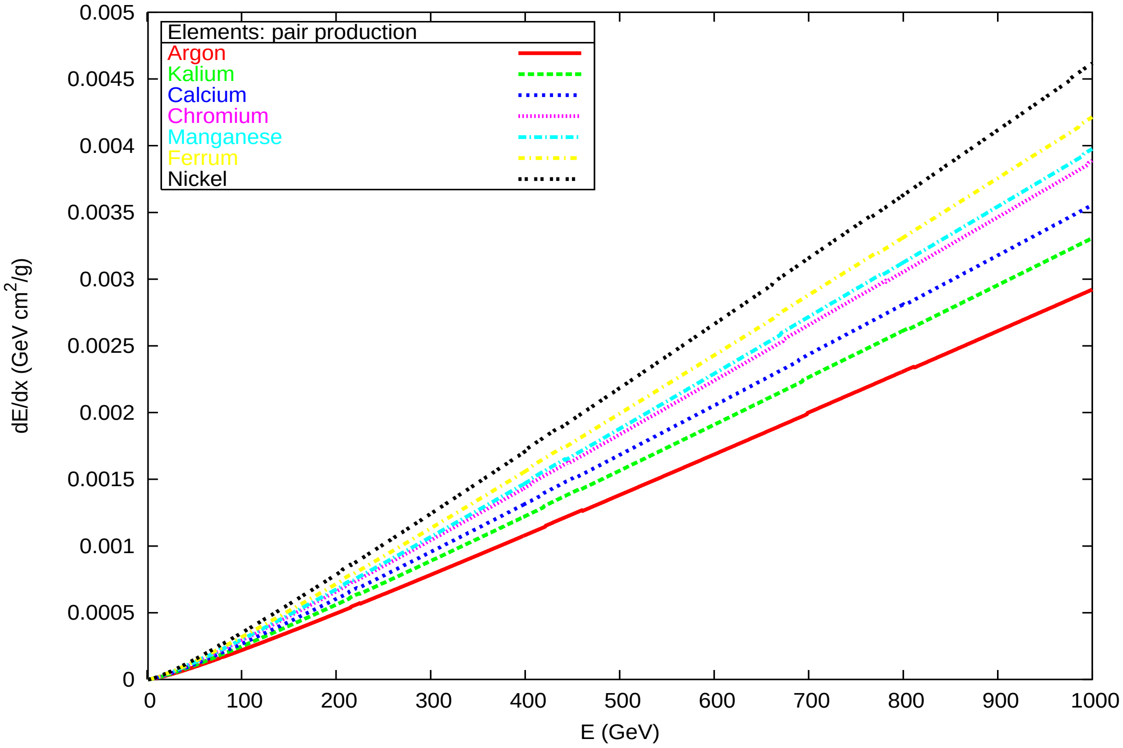

Figure 9.10: Muon energy losses via pair production in elements III.

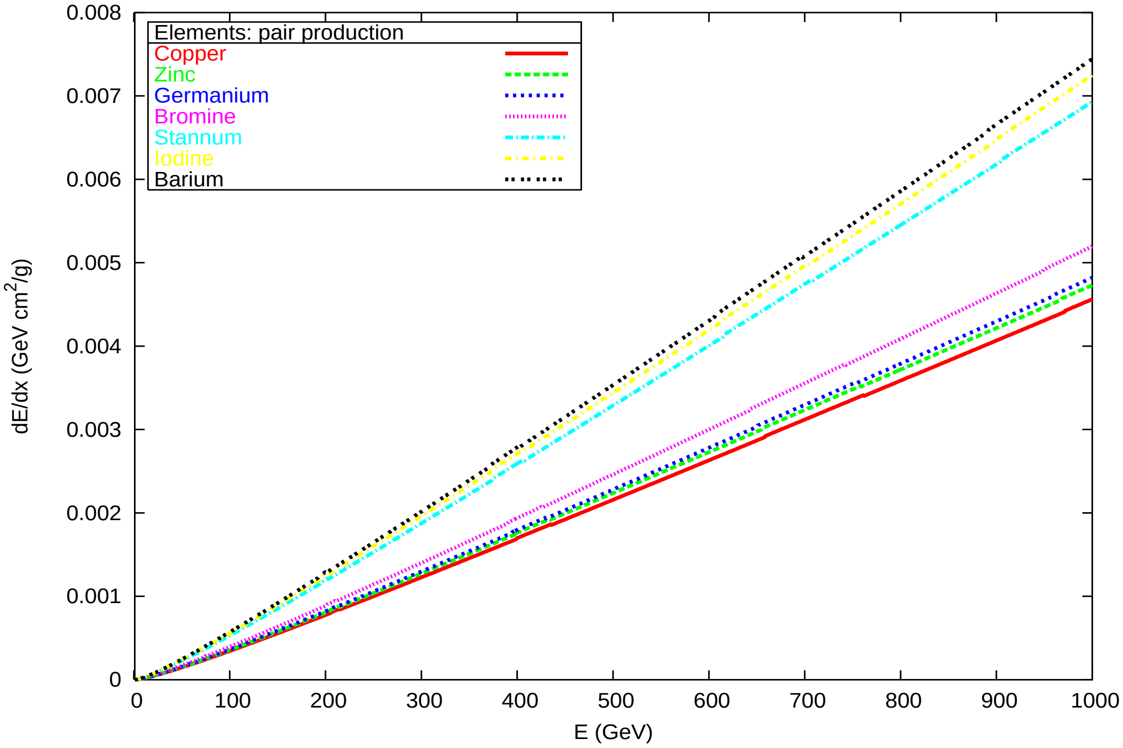

Figure 9.11: Muon energy losses via pair production in elements IV.

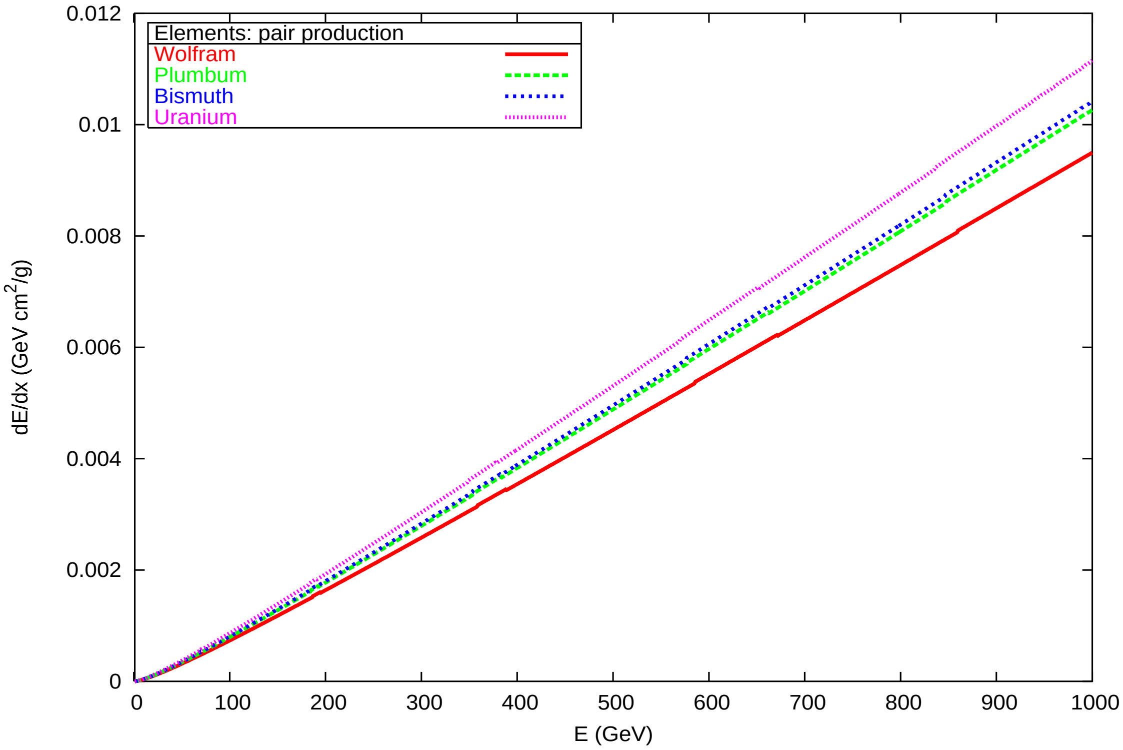

Figure 9.12: Muon energy losses via pair production in elements V.

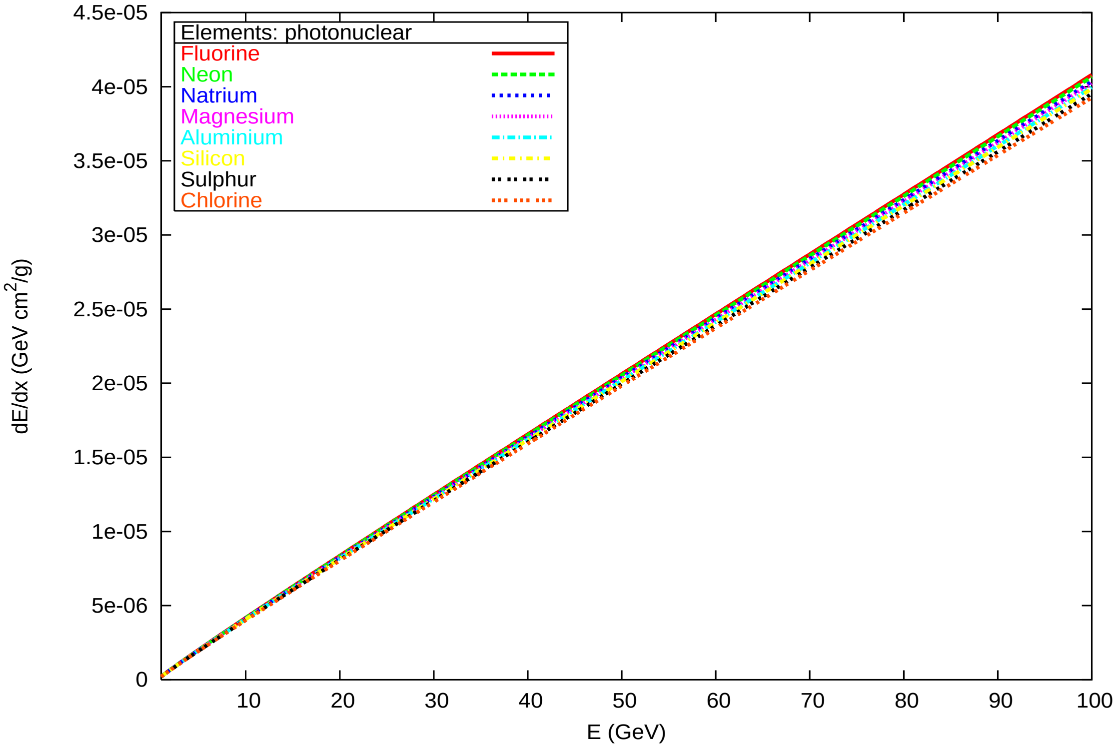

Figure 9.13: Muon energy losses via photonuclear interaction in elements II.

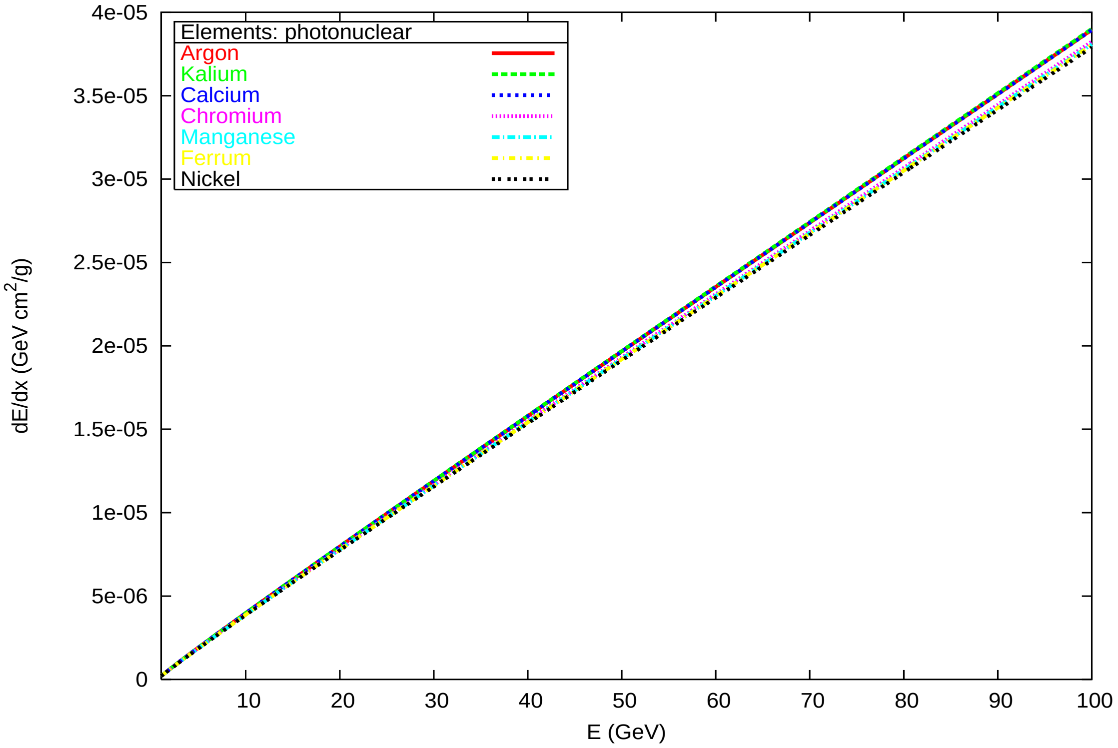

Figure 9.14: Muon energy losses via photonuclear interaction in elements III.

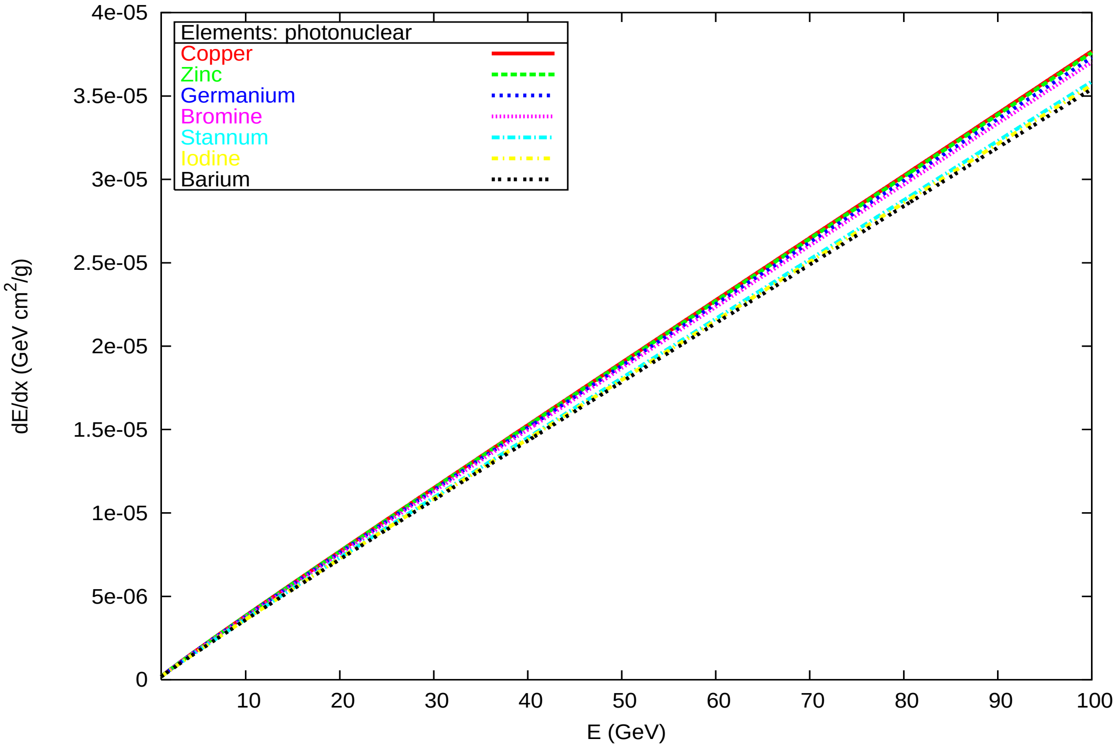

Figure 9.15: Muon energy losses via photonuclear interaction in elements IV.

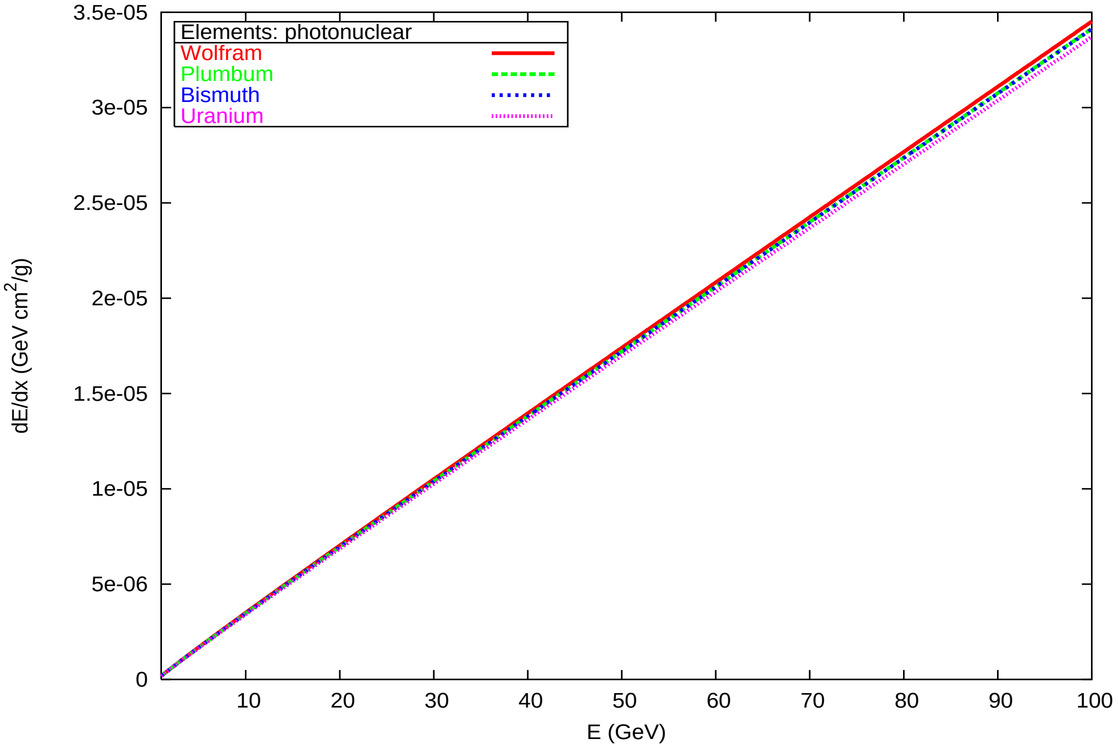

Figure 9.16: Muon energy losses via photonuclear interaction in elements V.

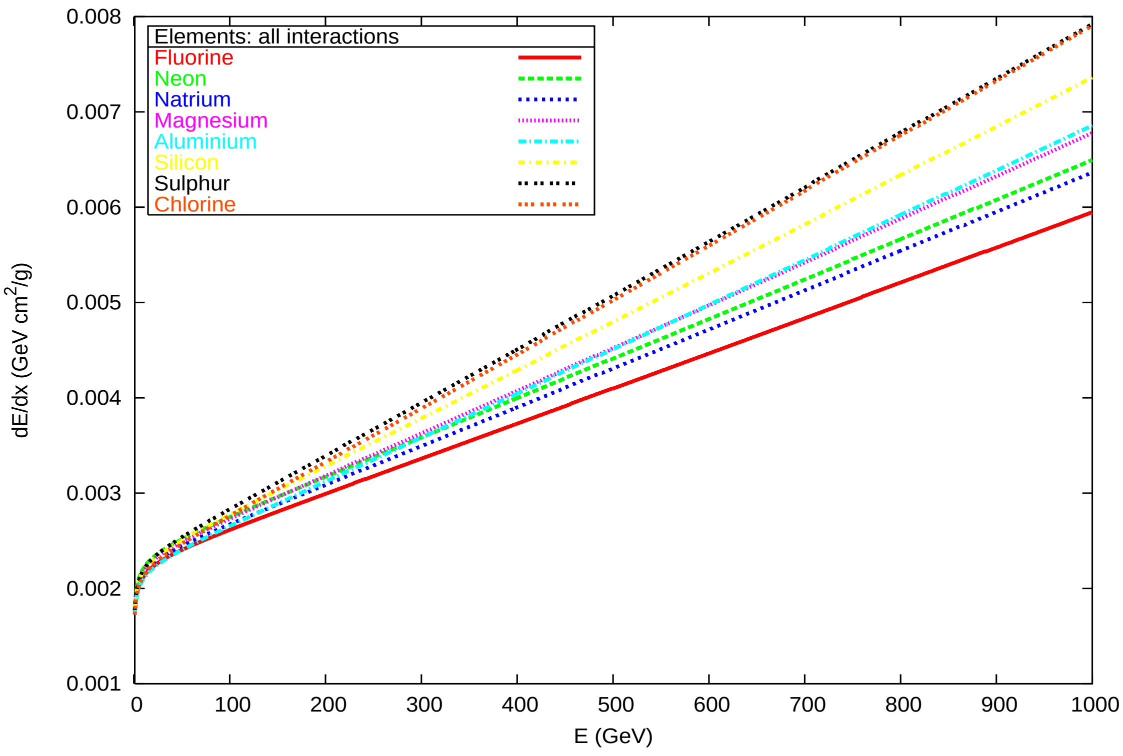

Figure 9.17: Muon energy loss in elements II.

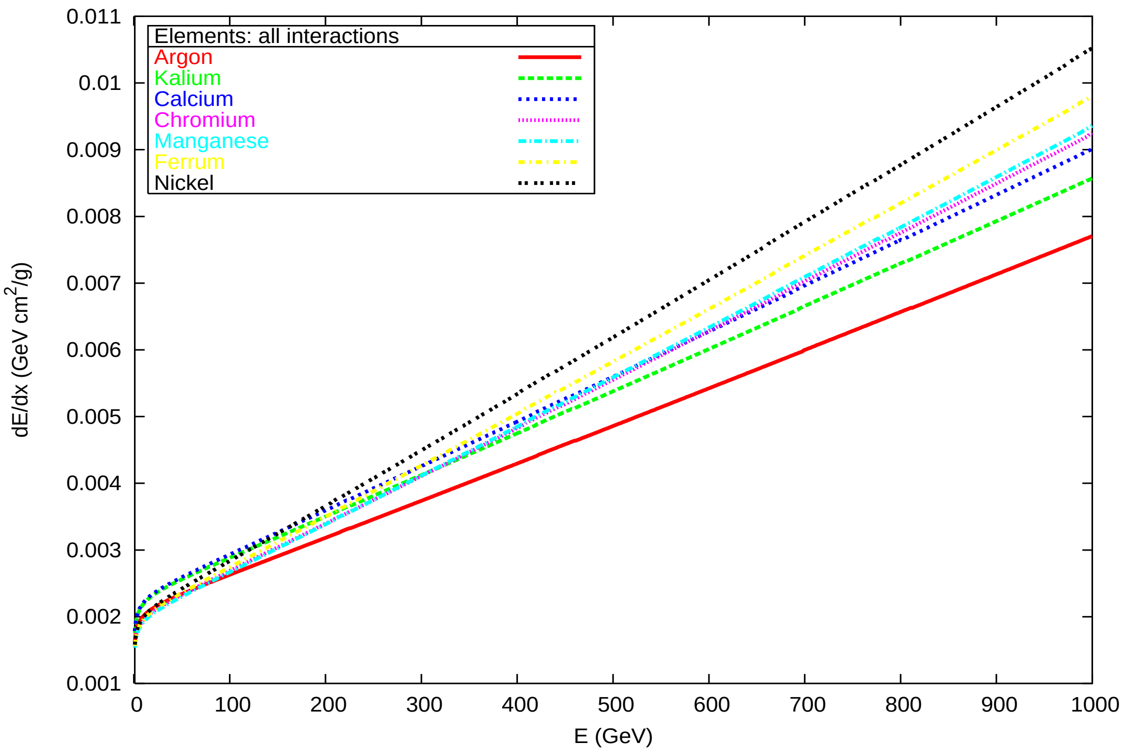

Figure 9.18: Muon energy loss in elements III.

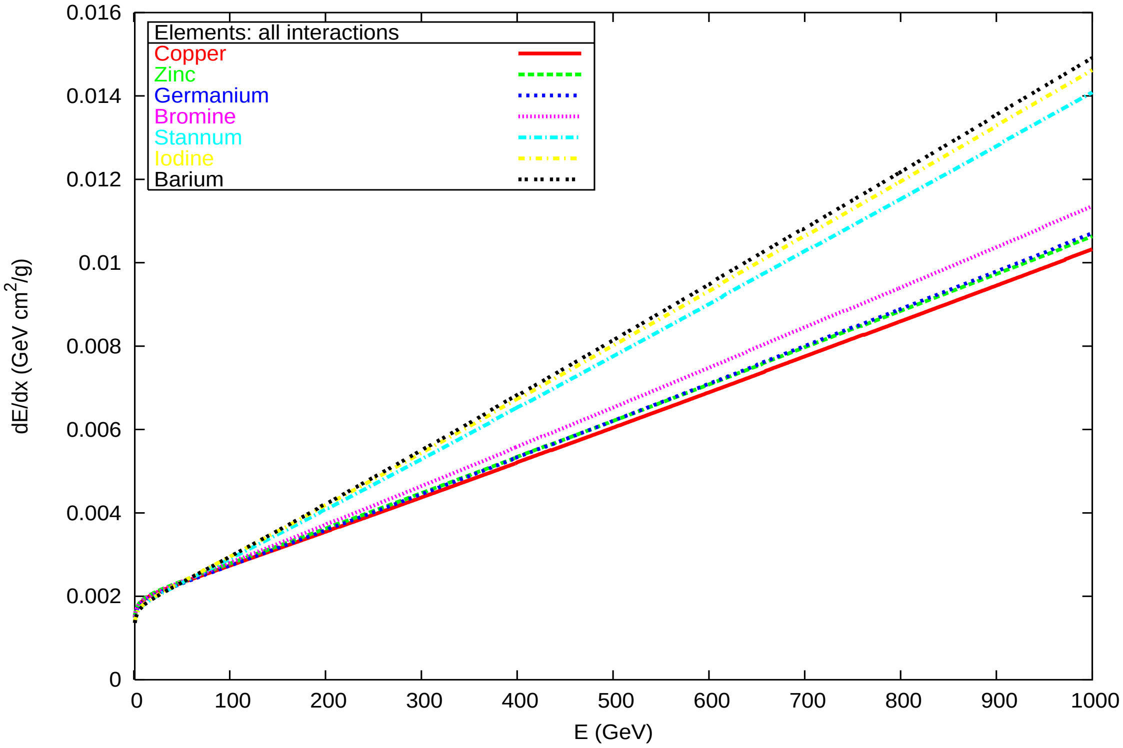

Figure 9.19: Muon energy loss in elements IV.

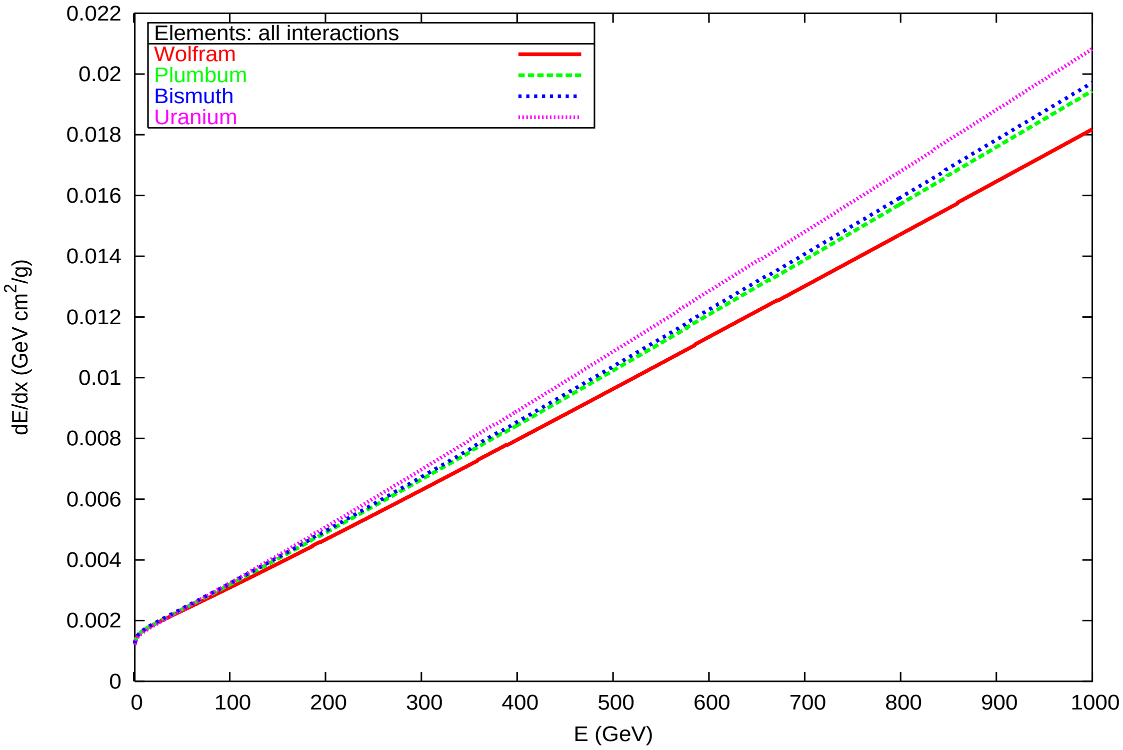

Figure 9.20: Muon energy loss in elements V.

9.2 Hadron Showers in TPC, background to muon trident interaction

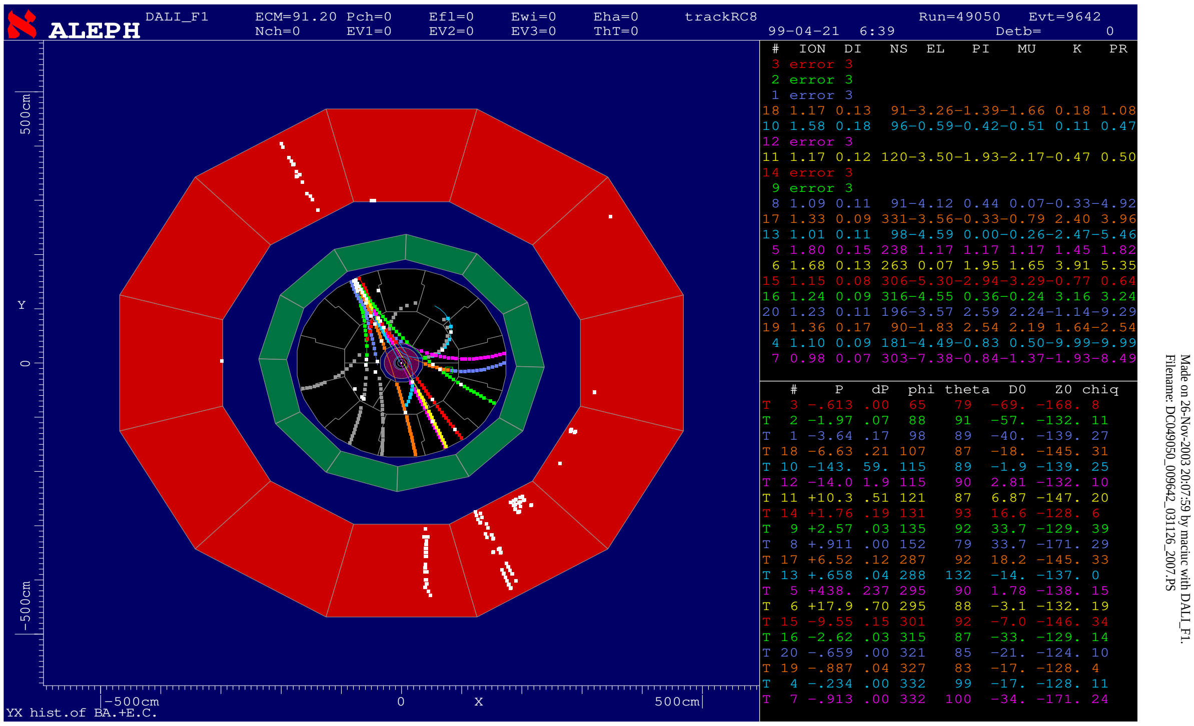

Figure 9.21: Hadron shower event I.

End of tracks

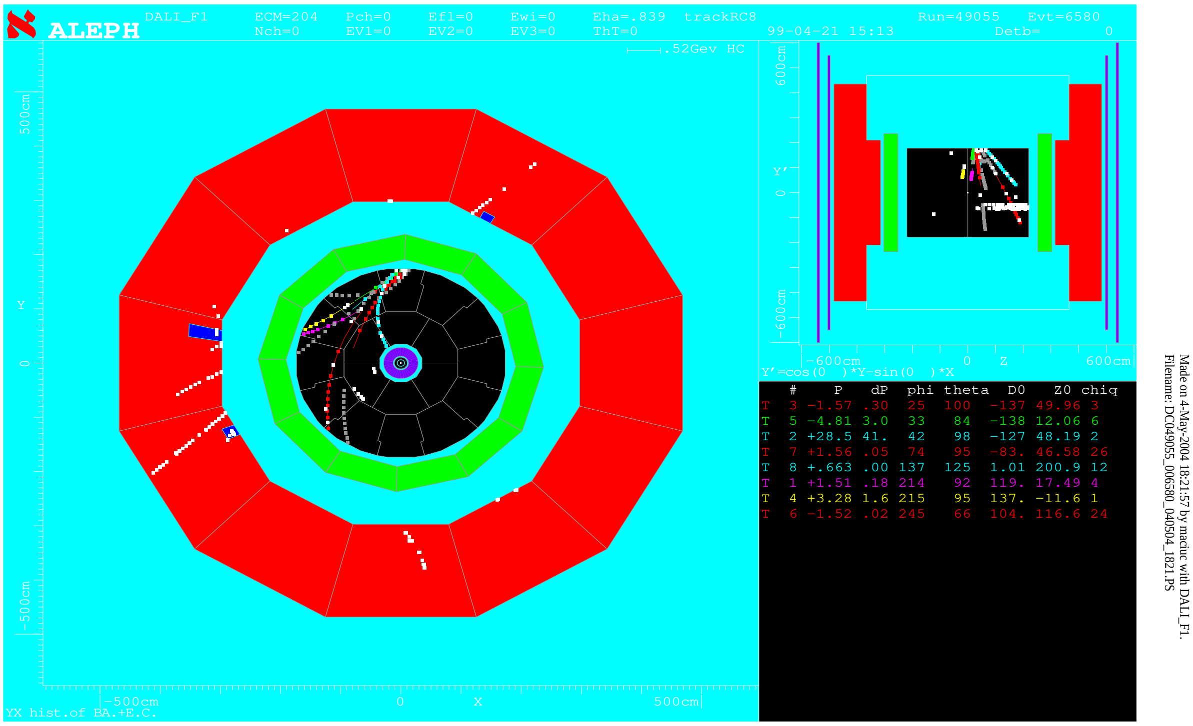

Figure 9.22: Hadron shower event II.

End of tracks

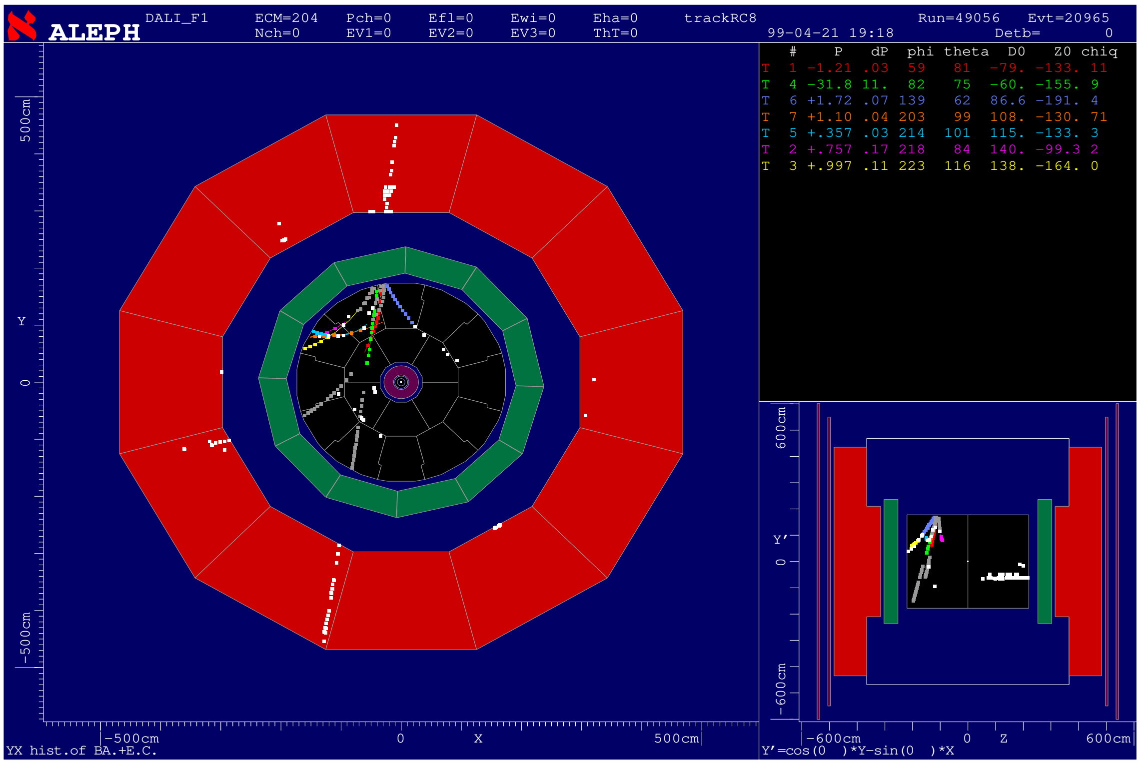

Made on 4-May-2004 19:08:03 by maciuc with DALI_F1.
Filename: DC049056_020965_040504_1908.PS

Figure 9.23: Hadron shower event III.

End of tracks

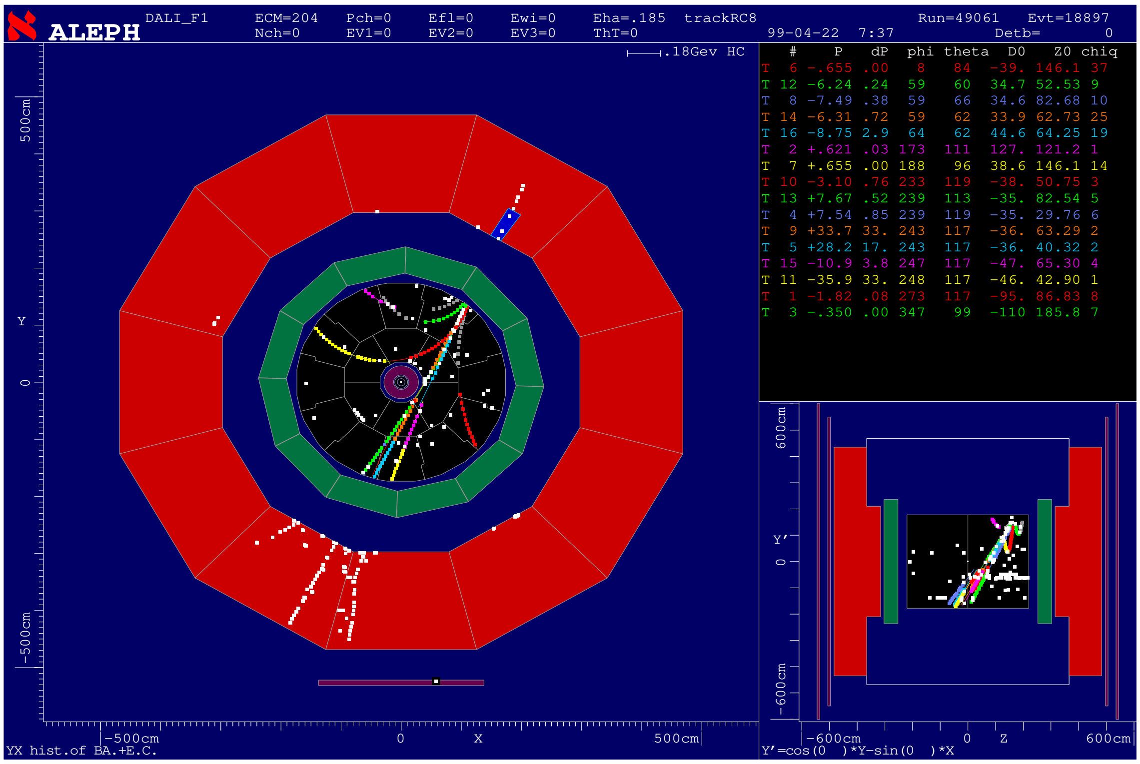

Made on 4-May-2004 19:35:58 by maciuc with DALI_F1.
Filename: DC049061_018897_040504_1935.PS

Figure 9.24: Hadron shower event IV.

End of tracks

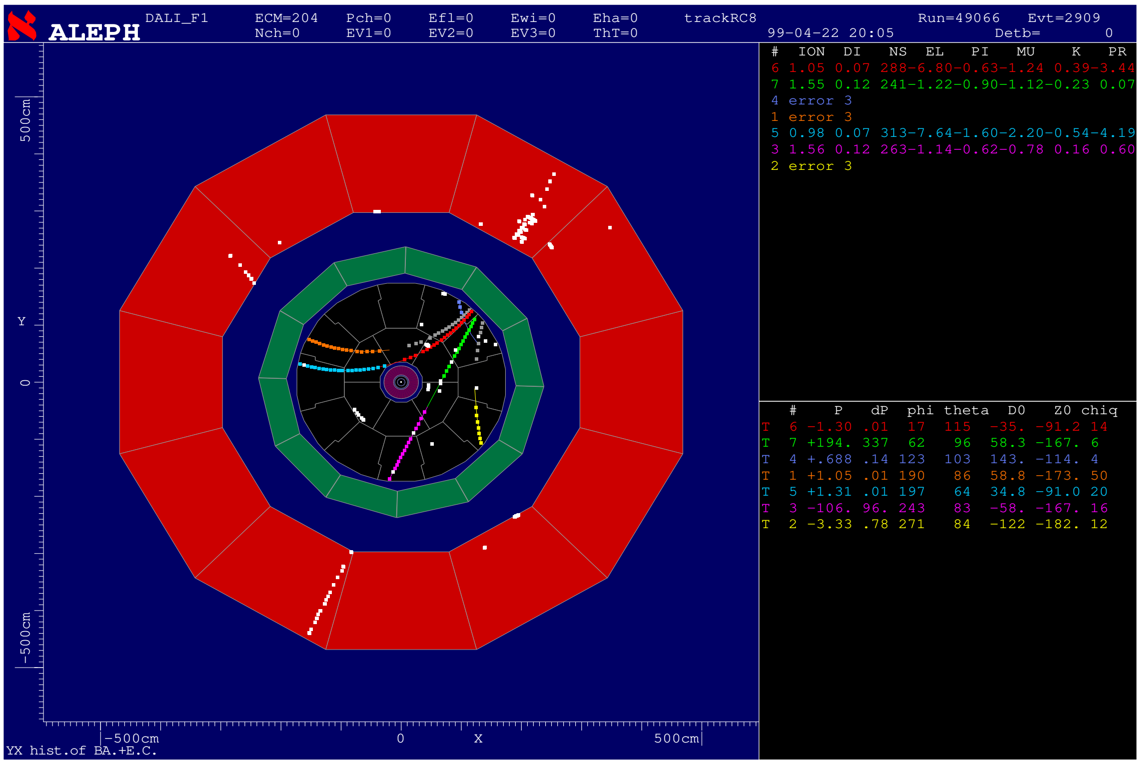

Made on 19-Oct-2003 22:28:26 by maciuc with DALI_F1.
Filename: DC049066_002909_031019_2228.PS

Figure 9.25: Hadron shower event V.

End of tracks

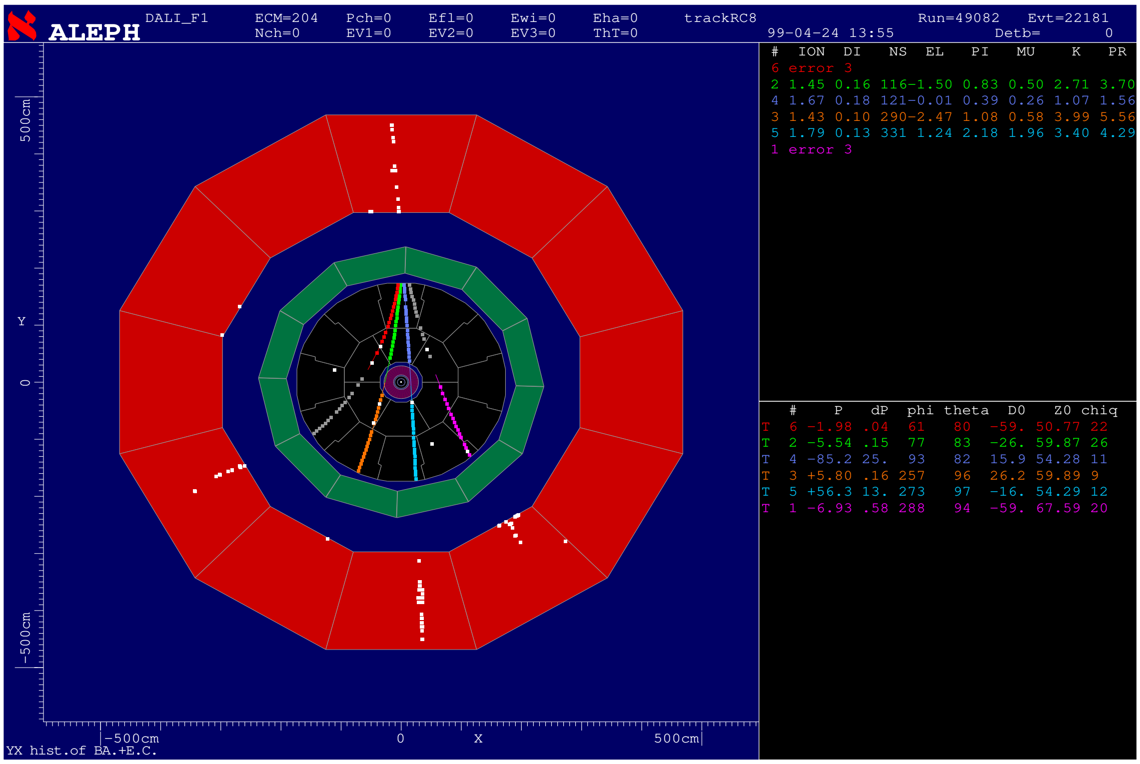

Made on 28-Nov-2003 02:28:35 by maciuc with DALI_F1.
Filename: DC049082_022181_031128_0228.PS

Figure 9.26: Hadron shower event VI.

End of tracks

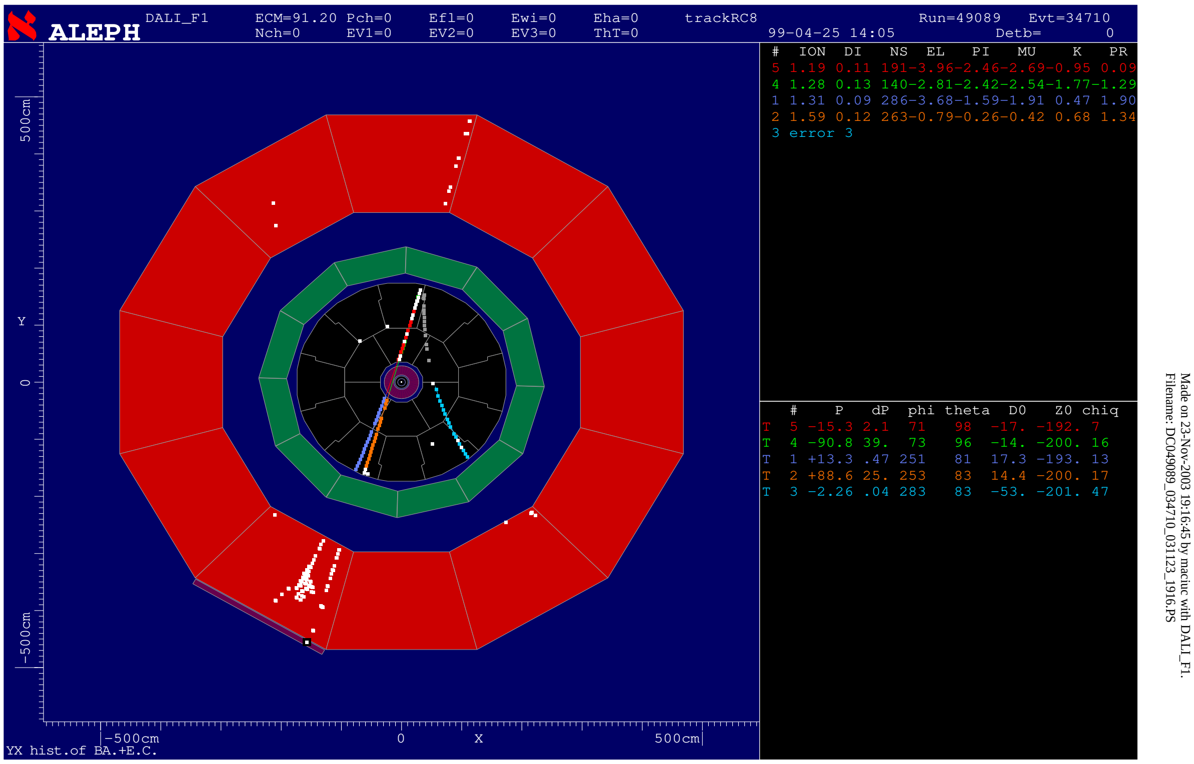

Figure 9.27: Hadron shower event VII.

End of tracks

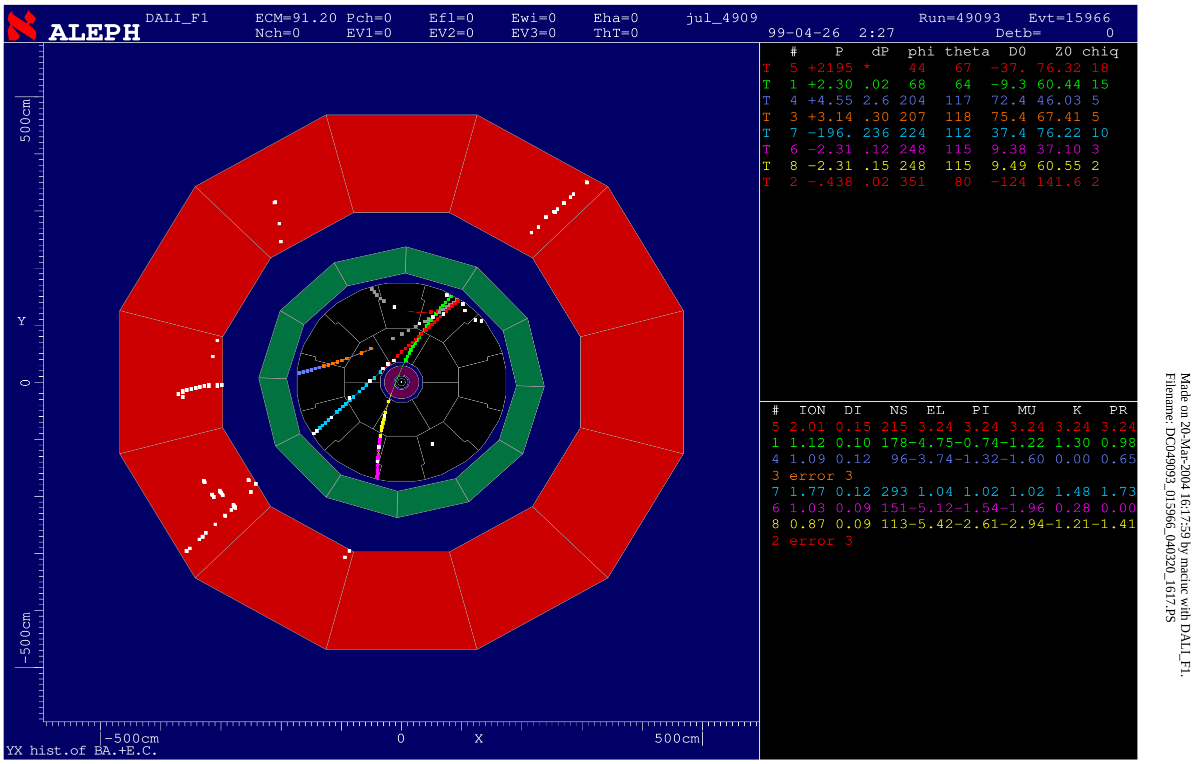

Figure 9.28: Hadron shower event VIII.

End of tracks

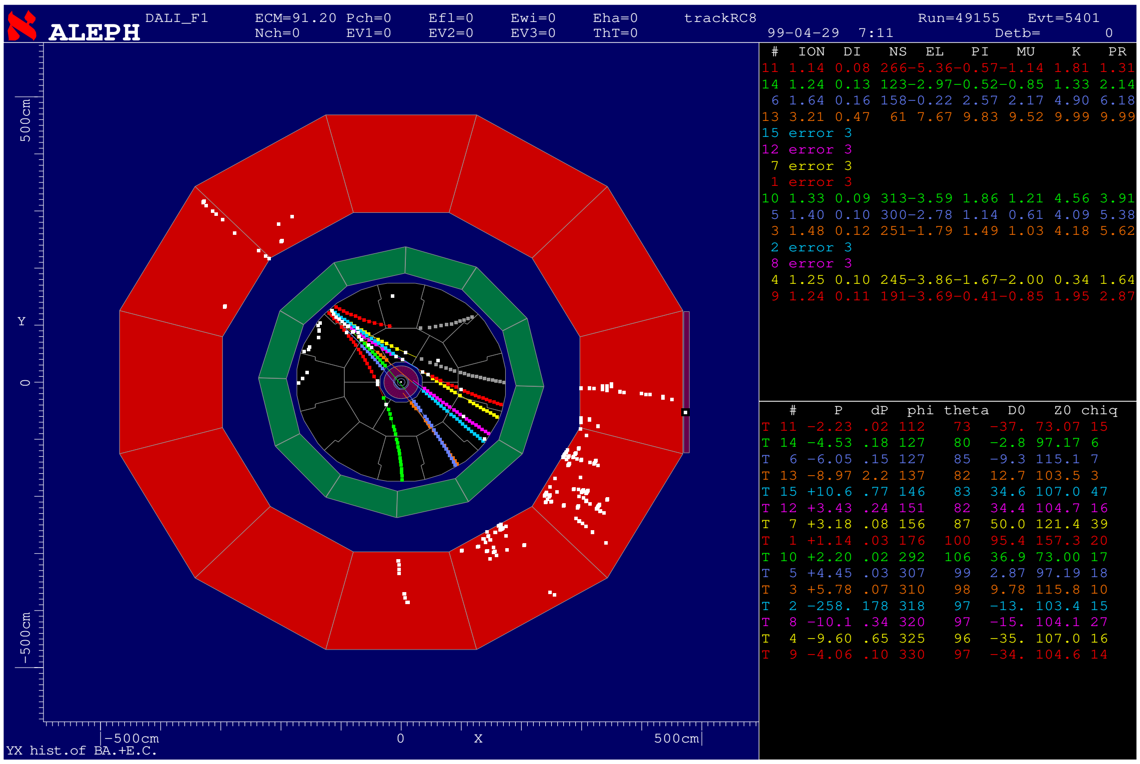

Made on 28-Nov-2003 21:55:51 by maciuc with DALI_F1.
Filename: DC049155_005401_031128_2155.PS

Figure 9.29: Hadron shower event IX.

End of tracks

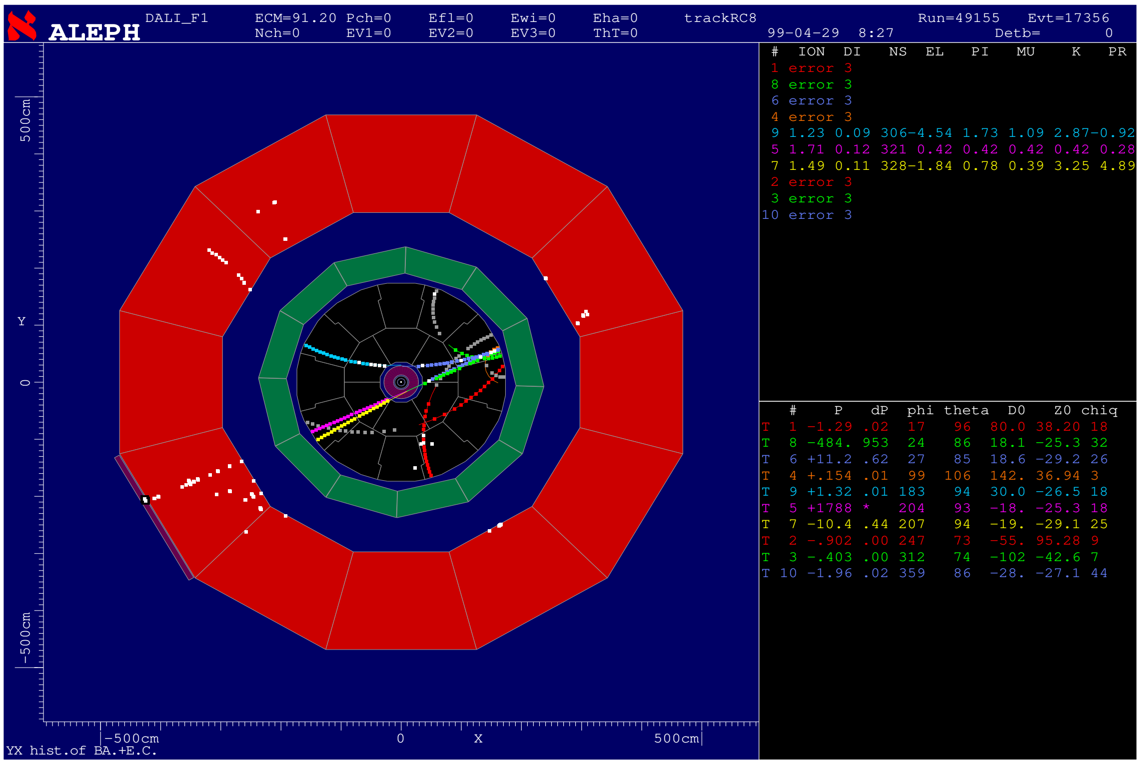

Made on 28-Nov-2003 19:53:32 by maciuc with DALI_F1.
Filename: DC049155_017356_031128_1953.PS

Figure 9.30: Hadron shower event X.

End of tracks

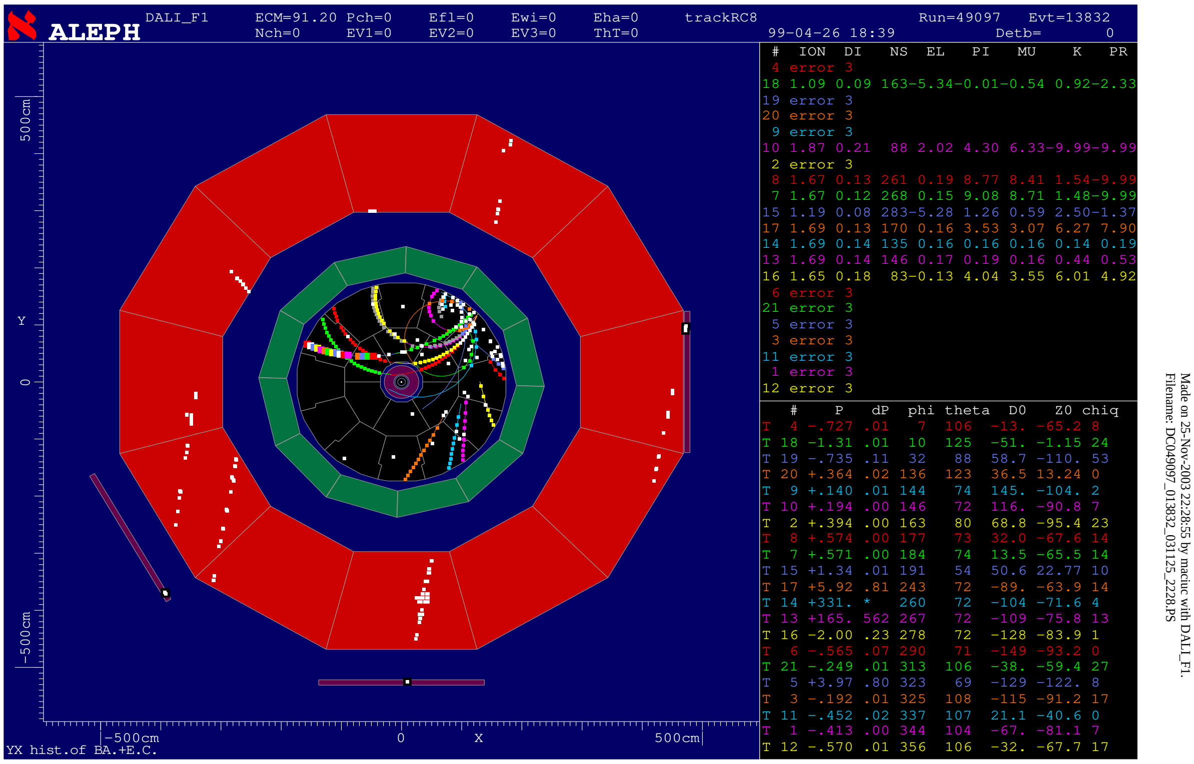

Figure 9.31: Possible Electromagnetic shower or electromagnetic remnant from hadronic event in ECAL, a muon or a pion is observed as secondary

End of tracks

9.3 High muon multiplicity sample

3-fold multiplicity events

run	event	run	event	run	event
49048	4109	49062	255	49071	25184
49048	10667	49062	2337	49072	1210
49048	18278	49062	3196	49072	9870
49049	4930	49062	11122	49072	14383
49049	15178	49062	17148	49073	41
49049	15771	49062	18871	49073	4605
49049	19914	49063	7861	49073	17352
49049	23282	49063	15484	49078	3724
49050	9399	49064	6478	49078	8676
49050	9626	49064	7184	49078	14336
49050	10893	49064	9449	49078	20918
49054	3846	49064	10821	49078	24280
49054	7821	49065	8918	49078	25503
49054	8575	49065	18410	49078	29667
49054	16352	49065	24510	49079	6018
49054	17300	49066	3351	49079	7501
49054	17581	49066	8164	49079	8242
49055	19465	49066	18830	49079	10209
49056	3434	49066	20367	49079	22792
49056	4123	49067	4663	49079	24993
49056	11616	49067	7933	49079	30636
49056	17136	49067	16346	49079	40098
49056	21928	49067	19171	49080	1562
49057	3454	49067	21171	49080	14693
49057	15390	49067	24235	49080	19764
49057	18922	49068	6250	49080	20285
49058	5265	49068	7095	49080	20499
49058	10703	49068	8951	49080	25068
49058	14119	49068	13323	49080	26023
49059	14814	49069	5320	49080	32959
49059	15069	49069	5475	49080	35608
49059	15697	49069	7188	49081	6822
49060	9125	49069	10325	49081	20689
49060	10738	49069	13631	49081	23053
49060	12554	49069	14090	49081	28624
49060	13257	49069	21101	49081	35837
49061	197	49070	108	49082	6185
49061	9145	49070	13029	49082	16816
49061	14655	49071	300	49082	22512
49061	18897	49071	2827	49082	24262
49061	19888	49071	3784	49082	29205
49061	21424	49071	14045	49082	30862

3-fold multiplicity muon events

run	event	run	event	run	event
49082	38099	49092	11540	49098	7525
49082	38691	49092	20033	49098	9742
49083	4935	49092	23317	49098	23120
49083	12737	49092	35492	49098	32234
49083	29526	49093	3326	49098	34506
49083	31913	49093	5858	49098	34710
49083	32676	49093	6185	49099	4182
49083	36354	49093	22277	49099	11412
49084	2772	49093	34949	49099	15429
49084	14613	49093	35214	49099	20633
49086	6380	49093	36725	49099	21646
49086	7906	49093	37632	49099	25511
49086	21051	49094	4254	49099	32220
49087	1896	49094	6986	49099	38997
49087	3212	49094	8311	49100	1063
49087	10886	49094	11361	49100	1867
49087	13844	49094	12400	49100	3667
49087	14516	49094	20224	49100	10575
49087	17395	49094	23480	49100	11688
49087	17671	49094	23518	49100	13244
49087	18417	49094	23603	49153	3346
49087	23023	49095	25113	49153	15058
49087	25583	49095	26216	49153	21442
49087	31674	49095	31238	49153	24866
49088	3350	49095	31699	49154	5110
49088	5303	49095	36030	49154	34080
49088	5900	49096	4456	49154	34845
49088	7441	49096	4574	49154	36086
49088	7680	49096	6166	49154	38686
49088	9800	49096	16874	49154	40456
49088	11717	49096	28218	49155	9625
49088	14583	49096	35387	49155	16325
49088	24755	49096	35507	49155	21583
49089	1878	49096	35837	49155	22698
49089	19941	49096	35982		
49089	30048	49097	684		
49089	34710	49097	2971		
49089	35715	49097	7265		
49089	36502	49097	13832		
49091	15535	49097	18104		
49091	22946	49097	21834		
49091	33868	49097	26092		
49091	36938	49098	3344		

2-fold multiplicity events

run	event
49155	22454
49155	22940
49155	23701

9-fold multiplicity tagged events

run	event
49064	6234
49099	8611

4-fold multiplicity tag

run	event
49048	4457
49050	1622
49050	9642
49054	1209
49054	14359
49055	3906
49055	18887
49056	7622
49056	13322
49064	187
49066	13428
49067	6619
49067	20660
49068	8931
49068	14416
49068	20637
49069	4151
49070	953
49070	3620
49071	6015
49071	6728
49071	18617
49079	136
49080	13351
49080	26445
49080	27937
49080	29881
49081	25725
49082	10691
49082	14101
49082	22181
49083	938
49083	5667
49083	27493
49086	8275
49086	29244
49086	33907
49087	8909
49088	5069
49088	9113
49089	17361
49089	25821
49092	36235
49093	480
49093	15890
49093	20883
49095	983
49095	23265
49097	8305

4-fold multiplicity tagged events

run	event
49098	1053
49098	3700
49098	5610
49099	8556
49099	16252
49153	15272
49153	16320
49154	3328
49154	20356
49154	21697
49154	36009
49155	15709
49155	17356

5-fold multiplicity tagged events

run	event
49056	1822
49068	13087
49068	14055
49068	23699
49071	2653
49082	31254
49084	10202
49086	28765
49087	34660
49095	3305
49099	17765
49153	10037
49155	5401

6-fold multiplicity tagged events

run	event
49048	18199
49063	4786
49065	10433
49080	6753
49083	29675
49089	22356
49096	16631
49098	19362
49099	8889
49154	40212
49155	15124

7-fold multiplicity tagged events

run	event
49062	711
49078	17737
49086	26436
49095	17780

2-fold multiplicity tagged events

run	event	run	event	run	event	run	event	run	event
49048	58	49048	13062	49049	7530	49050	6061	49054	13535
49048	264	49048	13218	49049	8167	49050	6360	49054	14159
49048	427	49048	13368	49049	9128	49050	6424	49054	14240
49048	558	49048	14442	49049	9919	49050	6881	49054	14286
49048	559	49048	14514	49049	10516	49050	6990	49054	14562
49048	709	49048	14640	49049	11040	49050	7096	49054	15039
49048	928	49048	15532	49049	11713	49050	7201	49054	15279
49048	1518	49048	15748	49049	11784	49050	7282	49054	15401
49048	2147	49048	15792	49049	13169	49050	7349	49054	15518
49048	2190	49048	16207	49049	13326	49050	7814	49054	15674
49048	2321	49048	17714	49049	13579	49050	9118	49054	15863
49048	2408	49048	17824	49049	13958	49050	10709	49054	17086
49048	2445	49048	18306	49049	14133	49050	10937	49054	17533
49048	3160	49048	18760	49049	14141	49050	11135	49054	17600
49048	3319	49048	19107	49049	14350	49050	11345	49054	18083
49048	3450	49048	19396	49049	14444	49050	11361	49054	20031
49048	3825	49048	19462	49049	14537	49050	12061	49054	20281
49048	4248	49048	19481	49049	15011	49050	12297	49054	20425
49048	4302	49048	19667	49049	15323	49054	210	49054	20692
49048	4554	49048	20590	49049	15902	49054	323	49054	21107
49048	4712	49048	20909	49049	16404	49054	1484	49054	21570
49048	4800	49048	20917	49049	17120	49054	1737	49054	21649
49048	5265	49048	20997	49049	17974	49054	2001	49054	22134
49048	5430	49048	22159	49049	18019	49054	2068	49054	23177
49048	5437	49048	22531	49049	18568	49054	2108	49054	23369
49048	5838	49048	22992	49049	19306	49054	2741	49055	426
49048	6613	49048	23261	49049	20153	49054	2780	49055	1178
49048	6864	49049	700	49049	20259	49054	3176	49055	2475
49048	7224	49049	1295	49049	20520	49054	3347	49055	2515
49048	7395	49049	1878	49049	21061	49054	4371	49055	2555
49048	7708	49049	2055	49049	21352	49054	4471	49055	2838
49048	7757	49049	2577	49049	21478	49054	4736	49055	4036
49048	7991	49049	2624	49049	21820	49054	5112	49055	4072
49048	8689	49049	2865	49049	22231	49054	5851	49055	4838
49048	8836	49049	3213	49049	22249	49054	6848	49055	5484
49048	8959	49049	3603	49049	23009	49054	6984	49055	5554
49048	9257	49049	3647	49049	23147	49054	7711	49055	6082
49048	9781	49049	3853	49049	23306	49054	7971	49055	6580
49048	10536	49049	3933	49049	23513	49054	8132	49055	6840
49048	10860	49049	4635	49050	203	49054	8214	49055	6996
49048	10963	49049	4666	49050	1473	49054	8326	49055	7484
49048	11173	49049	5139	49050	1689	49054	8382	49055	7667
49048	11331	49049	5266	49050	1814	49054	9002	49055	7954
49048	11396	49049	6214	49050	2725	49054	9017	49055	8148
49048	11579	49049	6234	49050	4279	49054	11496	49055	8471
49048	11595	49049	6412	49050	4796	49054	12174	49055	8569
49048	11801	49049	6496	49050	4942	49054	12398	49055	8619
49048	11905	49049	6569	49050	5568	49054	12510	49055	9558
49048	11971	49049	6710	49050	5672	49054	12753	49055	10974
49048	12148	49049	7057	49050	5814	49054	13090	49055	11746

2-fold multiplicity tagged events

run	event	run	event	run	event	run	event	run	event
49055	12201	49056	7894	49057	967	49057	19077	49058	14013
49055	12853	49056	7938	49057	1097	49057	19154	49058	14368
49055	13079	49056	8599	49057	1722	49057	19436	49058	14419
49055	13292	49056	9016	49057	1864	49057	20232	49058	14641
49055	13386	49056	9076	49057	2308	49057	20461	49058	15110
49055	13846	49056	9238	49057	2715	49057	20598	49058	16064
49055	14070	49056	10237	49057	2847	49057	21088	49058	16499
49055	14228	49056	10256	49057	4179	49057	21321	49058	16662
49055	15839	49056	10306	49057	4858	49057	21413	49058	16678
49055	15959	49056	10544	49057	5141	49057	21730	49058	17620
49055	16064	49056	10981	49057	5172	49057	22491	49058	17799
49055	16383	49056	11141	49057	5301	49057	23033	49058	17807
49055	16517	49056	11365	49057	5355	49057	23771	49058	17859
49055	16727	49056	11369	49057	5420	49057	23922	49058	17883
49055	17430	49056	11572	49057	5515	49058	104	49058	18266
49055	17450	49056	11987	49057	6357	49058	542	49058	18301
49055	17465	49056	12056	49057	6570	49058	622	49058	18303
49055	19342	49056	12168	49057	6718	49058	1011	49058	18442
49055	19363	49056	13949	49057	6752	49058	1238	49058	18656
49055	19444	49056	14281	49057	7050	49058	1305	49058	19698
49055	20485	49056	14405	49057	7177	49058	1785	49058	20524
49055	20507	49056	14900	49057	7306	49058	2097	49058	20795
49055	20661	49056	15178	49057	7342	49058	2616	49058	21206
49055	20670	49056	15358	49057	7413	49058	3068	49058	21384
49055	20783	49056	15517	49057	7499	49058	3077	49058	21425
49055	21074	49056	15548	49057	8754	49058	3185	49058	21622
49055	22142	49056	17042	49057	9178	49058	3893	49058	21871
49055	22515	49056	17160	49057	9809	49058	4645	49058	21886
49055	23268	49056	18315	49057	10474	49058	6240	49058	22241
49055	23476	49056	18479	49057	10863	49058	6955	49058	22375
49055	23734	49056	18544	49057	11042	49058	7384	49058	22717
49056	23	49056	18576	49057	11436	49058	7516	49058	23307
49056	235	49056	19117	49057	11768	49058	7925	49058	23596
49056	356	49056	19197	49057	12105	49058	7946	49058	23654
49056	1272	49056	19210	49057	12726	49058	8123	49058	23768
49056	1552	49056	19319	49057	12764	49058	8396	49059	778
49056	1833	49056	19879	49057	12824	49058	8478	49059	1646
49056	2120	49056	20055	49057	13139	49058	9558	49059	1735
49056	2587	49056	20571	49057	13212	49058	9673	49059	2332
49056	4507	49056	20965	49057	13729	49058	9971	49059	2364
49056	4578	49056	21065	49057	13874	49058	10153	49059	3661
49056	4693	49056	21895	49057	13971	49058	10214	49059	3671
49056	4823	49056	22625	49057	14373	49058	10460	49059	3714
49056	5463	49056	22690	49057	15930	49058	10952	49059	4538
49056	5647	49056	22770	49057	16009	49058	11576	49059	4603
49056	5706	49056	22803	49057	16106	49058	11643	49059	5355
49056	6021	49056	22908	49057	16256	49058	12248	49059	5521
49056	6503	49056	23313	49057	16445	49058	12684	49059	5697
49056	6724	49056	23343	49057	17047	49058	13238	49059	5890
49056	7092	49056	23893	49057	18156	49058	13984	49059	5976

2-fold multiplicity tagged events

run	event	run	event	run	event	run	event	run	event
49059	6413	49059	23800	49060	16557	49061	18316	49062	12225
49059	6603	49060	26	49060	16872	49061	18504	49062	12917
49059	7072	49060	826	49060	17054	49061	19067	49062	13260
49059	7668	49060	1203	49060	17469	49061	19139	49062	13455
49059	8235	49060	2051	49060	17585	49061	19976	49062	13933
49059	9298	49060	2520	49060	17685	49061	20064	49062	13972
49059	9313	49060	2654	49060	17686	49061	20136	49062	14585
49059	9344	49060	3023	49060	17711	49061	20168	49062	14681
49059	9421	49060	3517	49060	17760	49061	20362	49062	15008
49059	9613	49060	3536	49060	18010	49061	20735	49062	15024
49059	9781	49060	4003	49061	754	49061	21154	49062	15536
49059	10049	49060	5861	49061	1665	49061	22697	49062	17019
49059	10234	49060	5909	49061	1841	49061	23380	49062	17662
49059	10587	49060	5988	49061	1864	49061	23397	49062	17972
49059	11349	49060	6099	49061	2034	49061	23629	49062	18239
49059	11562	49060	6142	49061	2188	49061	23761	49062	19069
49059	12017	49060	6657	49061	2596	49061	23870	49062	19660
49059	12087	49060	6953	49061	2836	49061	24274	49062	20368
49059	12551	49060	7109	49061	3633	49062	445	49062	20896
49059	12729	49060	7268	49061	3706	49062	627	49062	21002
49059	13673	49060	7414	49061	4167	49062	654	49062	21011
49059	14481	49060	7707	49061	4859	49062	717	49062	21094
49059	15059	49060	8571	49061	5088	49062	2574	49062	21123
49059	15213	49060	8871	49061	5262	49062	2955	49062	22759
49059	15295	49060	8887	49061	6674	49062	3558	49062	22874
49059	15340	49060	9395	49061	6864	49062	3744	49062	22886
49059	15558	49060	9419	49061	7531	49062	3828	49062	23753
49059	16517	49060	9436	49061	8403	49062	4111	49062	23855
49059	16670	49060	9868	49061	8708	49062	4597	49062	24003
49059	16820	49060	9875	49061	9032	49062	4725	49063	262
49059	17678	49060	9932	49061	9746	49062	4955	49063	1066
49059	18557	49060	10109	49061	10086	49062	5153	49063	1637
49059	19271	49060	10306	49061	10739	49062	5588	49063	2017
49059	19361	49060	10385	49061	10904	49062	5783	49063	2370
49059	19367	49060	10425	49061	10981	49062	6084	49063	2498
49059	19700	49060	10623	49061	13191	49062	7438	49063	2803
49059	20037	49060	11711	49061	13271	49062	7858	49063	2827
49059	20275	49060	11741	49061	13515	49062	8399	49063	3256
49059	20852	49060	11907	49061	13569	49062	8532	49063	3719
49059	21194	49060	13323	49061	13665	49062	8830	49063	3752
49059	21916	49060	13344	49061	14940	49062	9115	49063	4669
49059	22216	49060	13359	49061	15176	49062	9237	49063	5051
49059	22548	49060	13711	49061	15598	49062	9332	49063	5720
49059	22995	49060	13826	49061	15606	49062	9490	49063	5849
49059	23019	49060	15087	49061	15690	49062	9961	49063	6360
49059	23021	49060	15325	49061	15858	49062	9988	49063	6454
49059	23226	49060	15382	49061	16129	49062	10365	49063	6840
49059	23252	49060	15456	49061	16674	49062	10391	49063	7457
49059	23268	49060	15753	49061	17062	49062	10810	49063	8264
49059	23436	49060	16459	49061	17763	49062	10841	49063	8317

2-fold multiplicity tagged events

run	event	run	event	run	event	run	event	run	event
49063	8778	49064	1540	49065	7919	49065	24924	49066	17036
49063	9042	49064	1660	49065	8417	49065	25197	49066	17233
49063	9798	49064	1683	49065	8624	49065	25236	49066	17477
49063	10297	49064	1935	49065	9033	49066	95	49066	17699
49063	11154	49064	2355	49065	9596	49066	464	49066	17839
49063	11633	49064	2958	49065	9880	49066	727	49066	18699
49063	11988	49064	3808	49065	9889	49066	855	49066	19022
49063	12074	49064	4155	49065	10875	49066	1748	49066	19033
49063	12244	49064	4207	49065	11206	49066	2044	49066	19156
49063	12444	49064	4262	49065	11446	49066	2246	49066	19394
49063	12657	49064	4565	49065	11466	49066	2644	49066	19903
49063	12781	49064	4587	49065	11853	49066	2702	49066	20595
49063	13717	49064	4972	49065	13633	49066	2899	49066	20818
49063	13902	49064	5360	49065	13670	49066	2909	49066	21247
49063	13956	49064	6053	49065	13715	49066	2961	49066	21754
49063	14293	49064	6080	49065	14579	49066	3410	49066	21796
49063	14569	49064	6171	49065	14990	49066	3596	49066	22003
49063	14984	49064	7604	49065	16018	49066	5611	49066	22603
49063	15430	49064	7640	49065	16211	49066	5678	49066	22960
49063	15498	49064	8133	49065	16526	49066	6048	49066	23599
49063	15634	49064	8785	49065	16773	49066	7036	49066	23660
49063	15734	49064	9055	49065	17010	49066	7510	49066	24168
49063	16008	49064	9319	49065	17190	49066	7740	49066	24581
49063	17179	49064	9421	49065	17452	49066	7928	49066	24691
49063	17205	49064	9594	49065	17540	49066	8165	49066	24883
49063	17258	49064	9787	49065	17615	49066	9785	49066	25230
49063	17429	49064	10021	49065	17652	49066	10362	49066	25301
49063	17825	49064	10211	49065	17842	49066	10592	49067	184
49063	17869	49064	11145	49065	17986	49066	10685	49067	218
49063	17912	49064	12187	49065	18653	49066	10956	49067	321
49063	17970	49064	12567	49065	18786	49066	11244	49067	459
49063	18034	49065	177	49065	19230	49066	11475	49067	643
49063	18137	49065	929	49065	19520	49066	11552	49067	980
49063	18568	49065	972	49065	19667	49066	12091	49067	1516
49063	18736	49065	1265	49065	19840	49066	12309	49067	1536
49063	19039	49065	1295	49065	19865	49066	12327	49067	1681
49063	19167	49065	2252	49065	20527	49066	12479	49067	2106
49063	20773	49065	2576	49065	20639	49066	13599	49067	2703
49063	21308	49065	2670	49065	20868	49066	14036	49067	3471
49063	21323	49065	3002	49065	21343	49066	14791	49067	4846
49063	22228	49065	3761	49065	21371	49066	14892	49067	5286
49063	22319	49065	4239	49065	21785	49066	15008	49067	5353
49063	22779	49065	4479	49065	21942	49066	15408	49067	5376
49063	23507	49065	4858	49065	22509	49066	15429	49067	5499
49063	24099	49065	4908	49065	22575	49066	15586	49067	6157
49064	529	49065	5058	49065	22620	49066	15614	49067	6339
49064	594	49065	5522	49065	23496	49066	15652	49067	6585
49064	753	49065	5926	49065	23902	49066	15840	49067	7239
49064	912	49065	7062	49065	24314	49066	16484	49067	7266
49064	1329	49065	7289	49065	24786	49066	16674	49067	7504

2-fold multiplicity tagged events

run	event	run	event	run	event	run	event	run	event
49067	7904	49068	4126	49068	20767	49069	12409	49070	7397
49067	7959	49068	4525	49068	21015	49069	12439	49070	7740
49067	8724	49068	5181	49068	21138	49069	13316	49070	7843
49067	10001	49068	5529	49068	21821	49069	14319	49070	7962
49067	10264	49068	5729	49068	21947	49069	14668	49070	8052
49067	11016	49068	5817	49068	22837	49069	15773	49070	8561
49067	11201	49068	6247	49068	23840	49069	15950	49070	9961
49067	11522	49068	6374	49068	23892	49069	16206	49070	11079
49067	11951	49068	6978	49068	24378	49069	16228	49070	11138
49067	12169	49068	7189	49068	24641	49069	17198	49070	11233
49067	12674	49068	7199	49068	25123	49069	17822	49070	11513
49067	12807	49068	8015	49069	6	49069	18204	49070	11645
49067	13248	49068	8593	49069	228	49069	18295	49070	11760
49067	13374	49068	8793	49069	381	49069	18421	49070	12124
49067	13466	49068	9054	49069	618	49069	18700	49070	12216
49067	13683	49068	9173	49069	701	49069	18795	49070	12470
49067	13944	49068	9237	49069	1127	49069	18990	49070	13394
49067	14088	49068	10419	49069	1284	49069	19383	49070	13573
49067	14372	49068	10546	49069	2142	49069	20257	49070	14056
49067	14473	49068	11226	49069	2637	49069	20412	49070	14672
49067	14827	49068	11300	49069	3097	49069	20997	49070	14933
49067	15127	49068	11442	49069	3138	49069	21174	49070	15067
49067	15553	49068	12000	49069	3420	49069	21238	49070	15565
49067	16080	49068	12170	49069	3507	49069	21790	49070	15638
49067	16209	49068	12719	49069	3720	49069	22415	49070	15690
49067	16356	49068	13829	49069	3940	49069	22680	49071	238
49067	16505	49068	14096	49069	4076	49069	23106	49071	952
49067	16710	49068	14567	49069	4140	49069	23759	49071	1102
49067	16858	49068	14714	49069	4678	49069	24473	49071	1215
49067	17338	49068	14722	49069	4923	49069	24532	49071	1789
49067	17784	49068	15267	49069	4963	49069	24548	49071	2414
49067	18157	49068	15295	49069	5229	49069	24894	49071	2640
49067	18621	49068	15415	49069	5778	49069	25209	49071	2678
49067	18641	49068	15813	49069	5893	49070	156	49071	2838
49067	18657	49068	16425	49069	6316	49070	995	49071	4052
49067	20681	49068	16621	49069	6347	49070	1002	49071	4061
49067	23550	49068	16680	49069	6419	49070	1102	49071	4151
49067	25047	49068	16719	49069	6457	49070	1312	49071	4306
49067	25086	49068	17347	49069	7422	49070	2725	49071	4401
49068	169	49068	17589	49069	8356	49070	3467	49071	4569
49068	171	49068	18473	49069	8681	49070	3878	49071	4614
49068	175	49068	18565	49069	9472	49070	4046	49071	5221
49068	1053	49068	18622	49069	9475	49070	4151	49071	5735
49068	1674	49068	18750	49069	9818	49070	4451	49071	6103
49068	2829	49068	18764	49069	10071	49070	4643	49071	6119
49068	3059	49068	19622	49069	10274	49070	4928	49071	6153
49068	3240	49068	20060	49069	10542	49070	5253	49071	6246
49068	3502	49068	20191	49069	10691	49070	5771	49071	6311
49068	3625	49068	20294	49069	11137	49070	6092	49071	6361
49068	3665	49068	20514	49069	12367	49070	7065	49071	6392

2-fold multiplicity tagged events

run	event	run	event	run	event	run	event	run	event
49071	6956	49071	24776	49072	18879	49078	2499	49078	25405
49071	7638	49071	25034	49073	81	49078	3396	49078	25790
49071	7705	49071	25163	49073	674	49078	3902	49078	26305
49071	8153	49072	841	49073	1238	49078	4852	49078	27819
49071	8568	49072	1128	49073	1900	49078	4925	49078	28075
49071	8749	49072	1921	49073	2210	49078	5274	49078	28140
49071	9810	49072	2073	49073	2901	49078	5455	49078	28869
49071	9982	49072	2531	49073	3142	49078	5655	49078	29868
49071	10302	49072	2868	49073	3462	49078	5890	49078	30376
49071	10492	49072	3014	49073	4040	49078	6704	49078	30626
49071	10524	49072	3651	49073	5502	49078	7148	49078	31569
49071	10693	49072	3998	49073	5566	49078	8009	49078	32096
49071	10980	49072	4742	49073	5787	49078	8548	49078	32644
49071	11520	49072	6973	49073	5888	49078	8935	49078	32882
49071	11856	49072	7102	49073	6025	49078	9222	49078	33932
49071	11973	49072	7340	49073	6659	49078	9485	49078	34970
49071	12214	49072	7433	49073	6914	49078	9631	49078	34971
49071	12800	49072	7632	49073	7614	49078	9821	49078	35108
49071	12881	49072	8294	49073	7712	49078	9918	49078	35424
49071	12961	49072	8339	49073	8348	49078	10747	49078	35532
49071	13148	49072	8552	49073	8805	49078	10916	49078	35552
49071	13258	49072	9345	49073	9126	49078	12251	49078	35817
49071	13594	49072	9812	49073	9254	49078	12505	49078	36637
49071	13688	49072	10320	49073	9270	49078	14558	49078	37656
49071	13725	49072	11133	49073	9629	49078	14829	49078	37803
49071	14140	49072	11134	49073	10184	49078	14963	49078	37828
49071	14177	49072	11416	49073	10260	49078	15783	49078	37894
49071	14346	49072	11596	49073	10434	49078	16042	49078	38088
49071	14753	49072	11886	49073	10589	49078	16186	49078	38569
49071	14939	49072	12028	49073	10926	49078	16823	49078	38630
49071	15478	49072	12396	49073	11429	49078	16923	49078	38644
49071	15745	49072	12669	49073	11850	49078	17774	49078	38730
49071	16214	49072	12714	49073	12384	49078	17895	49078	38878
49071	16980	49072	13567	49073	12433	49078	18139	49078	39288
49071	17063	49072	13618	49073	12444	49078	18517	49078	39423
49071	17510	49072	14204	49073	12857	49078	18563	49078	39615
49071	18743	49072	14213	49073	13228	49078	19607	49078	39627
49071	19142	49072	14249	49073	13244	49078	20017	49078	40065
49071	19570	49072	14772	49073	13791	49078	21196	49078	40181
49071	20037	49072	14845	49073	14154	49078	21646	49078	40409
49071	20704	49072	15684	49073	14448	49078	21865	49079	49
49071	21644	49072	15908	49073	14930	49078	21879	49079	133
49071	21932	49072	16205	49073	16326	49078	22190	49079	1931
49071	22275	49072	16697	49073	17244	49078	22449	49079	2312
49071	22767	49072	17073	49073	17866	49078	22451	49079	2925
49071	22930	49072	17491	49073	17902	49078	22648	49079	3013
49071	23030	49072	17635	49078	3	49078	23084	49079	3731
49071	24133	49072	17842	49078	105	49078	23985	49079	3969
49071	24610	49072	18455	49078	1005	49078	24047	49079	4613
49071	24675	49072	18604	49078	2315	49078	25194	49079	5430

2-fold multiplicity tagged events

run	event	run	event	run	event	run	event	run	event
49079	6238	49079	25890	49080	3628	49080	18461	49080	37268
49079	6300	49079	26375	49080	3663	49080	19677	49080	38080
49079	6569	49079	26401	49080	4544	49080	19909	49080	38118
49079	7083	49079	26500	49080	4896	49080	20855	49080	38561
49079	8278	49079	26593	49080	5275	49080	21719	49080	38885
49079	8700	49079	26664	49080	5426	49080	21923	49080	39536
49079	8724	49079	27149	49080	6089	49080	22021	49080	39700
49079	9091	49079	28073	49080	6161	49080	22527	49080	39703
49079	9209	49079	28187	49080	6216	49080	23480	49080	39765
49079	10124	49079	28321	49080	6358	49080	23762	49080	39865
49079	10370	49079	28674	49080	7114	49080	24015	49080	40427
49079	10903	49079	28927	49080	7424	49080	24108	49081	562
49079	11355	49079	29148	49080	7440	49080	24152	49081	1385
49079	11404	49079	29773	49080	7728	49080	24200	49081	1554
49079	12104	49079	30742	49080	7747	49080	24302	49081	2118
49079	12300	49079	31121	49080	8132	49080	24665	49081	2363
49079	12996	49079	31749	49080	8372	49080	24712	49081	2693
49079	13272	49079	31986	49080	8964	49080	24760	49081	2753
49079	13515	49079	32003	49080	9001	49080	24837	49081	2781
49079	13966	49079	32067	49080	9286	49080	24994	49081	3351
49079	14251	49079	32114	49080	9762	49080	25908	49081	3469
49079	15296	49079	32490	49080	9794	49080	26091	49081	3902
49079	15502	49079	32783	49080	10003	49080	26288	49081	3915
49079	15562	49079	32827	49080	10032	49080	26494	49081	3971
49079	15593	49079	32842	49080	10172	49080	26866	49081	3997
49079	16032	49079	33118	49080	10696	49080	27468	49081	4160
49079	16841	49079	33190	49080	10775	49080	27796	49081	4631
49079	17157	49079	33573	49080	11173	49080	28013	49081	4813
49079	17632	49079	33924	49080	11241	49080	28693	49081	5078
49079	17751	49079	34853	49080	12012	49080	28850	49081	5791
49079	17983	49079	35076	49080	12655	49080	29545	49081	6330
49079	18242	49079	35367	49080	12704	49080	29976	49081	7236
49079	18267	49079	35458	49080	13001	49080	30138	49081	7615
49079	18421	49079	35778	49080	13541	49080	30271	49081	7713
49079	18553	49079	36649	49080	13741	49080	30752	49081	8038
49079	18849	49079	37294	49080	14742	49080	31027	49081	8096
49079	19352	49079	37518	49080	14939	49080	31057	49081	8443
49079	19879	49079	38232	49080	14955	49080	31367	49081	8574
49079	20326	49079	38236	49080	15218	49080	31669	49081	8584
49079	21546	49079	40748	49080	15222	49080	32497	49081	9054
49079	22539	49079	41180	49080	15408	49080	32736	49081	9080
49079	22737	49080	16	49080	15674	49080	33889	49081	9310
49079	22754	49080	120	49080	16493	49080	34191	49081	9662
49079	22907	49080	913	49080	16700	49080	34409	49081	9891
49079	23532	49080	1254	49080	17138	49080	34642	49081	10134
49079	23619	49080	1272	49080	17350	49080	35016	49081	10210
49079	24279	49080	1769	49080	17499	49080	36822	49081	10495
49079	24744	49080	2067	49080	17539	49080	36981	49081	10816
49079	25404	49080	2766	49080	17595	49080	37010	49081	11337
49079	25834	49080	2929	49080	17624	49080	37248	49081	11502

2-fold multiplicity tagged events

run	event	run	event	run	event	run	event	run	event
49081	11879	49081	33991	49082	12075	49082	27913	49083	6594
49081	11910	49081	34053	49082	12377	49082	28124	49083	6923
49081	12778	49081	34349	49082	13118	49082	28189	49083	7001
49081	12806	49081	34560	49082	14248	49082	28261	49083	7108
49081	13013	49081	34584	49082	14702	49082	28453	49083	7362
49081	13899	49081	34618	49082	15167	49082	29761	49083	7595
49081	14131	49081	34658	49082	15365	49082	29780	49083	8094
49081	14643	49081	35156	49082	15645	49082	30173	49083	8397
49081	15115	49081	35432	49082	16025	49082	30465	49083	8399
49081	15218	49081	35433	49082	16034	49082	30981	49083	8730
49081	15369	49081	35790	49082	16957	49082	31593	49083	9403
49081	15928	49081	36646	49082	17102	49082	31813	49083	9929
49081	16417	49081	36995	49082	17211	49082	32093	49083	9963
49081	16473	49081	37233	49082	17302	49082	32384	49083	10194
49081	16656	49081	37357	49082	17374	49082	32681	49083	10307
49081	16720	49081	37806	49082	17575	49082	33407	49083	10414
49081	17289	49081	38199	49082	17615	49082	33757	49083	10556
49081	17977	49081	38240	49082	17681	49082	34639	49083	10569
49081	18191	49081	38652	49082	18001	49082	34789	49083	10614
49081	18222	49081	39060	49082	18034	49082	35159	49083	11008
49081	18481	49081	39193	49082	18578	49082	35412	49083	11045
49081	19474	49081	39271	49082	18827	49082	35765	49083	11145
49081	20364	49081	39488	49082	18957	49082	36117	49083	11481
49081	20462	49081	39821	49082	19377	49082	36424	49083	11482
49081	20953	49081	40196	49082	20093	49082	37802	49083	11568
49081	21794	49082	410	49082	21001	49082	38303	49083	11634
49081	21809	49082	899	49082	21147	49082	40138	49083	11966
49081	21945	49082	1019	49082	21546	49082	40146	49083	12425
49081	22251	49082	1907	49082	21600	49082	40205	49083	12445
49081	22501	49082	3600	49082	22014	49082	40223	49083	13649
49081	23525	49082	3841	49082	22052	49082	40273	49083	13670
49081	24250	49082	4352	49082	22259	49082	40366	49083	14186
49081	24403	49082	4480	49082	22375	49083	465	49083	14389
49081	25329	49082	4802	49082	22814	49083	548	49083	14724
49081	25832	49082	5373	49082	22912	49083	953	49083	15444
49081	26069	49082	5917	49082	22939	49083	1545	49083	15574
49081	26625	49082	6956	49082	22979	49083	2585	49083	15769
49081	27507	49082	7188	49082	23751	49083	2644	49083	15843
49081	27791	49082	8463	49082	23841	49083	2695	49083	15949
49081	28826	49082	8634	49082	24550	49083	3235	49083	16156
49081	28879	49082	8745	49082	24717	49083	3244	49083	16379
49081	29260	49082	8773	49082	24862	49083	3387	49083	16410
49081	29946	49082	9113	49082	24919	49083	3593	49083	16912
49081	30565	49082	9525	49082	25067	49083	3786	49083	17607
49081	30619	49082	10118	49082	25394	49083	4605	49083	18170
49081	31451	49082	11284	49082	25449	49083	5229	49083	18394
49081	31576	49082	11325	49082	26002	49083	5481	49083	18476
49081	32049	49082	11878	49082	26011	49083	6298	49083	18712
49081	32253	49082	11909	49082	26321	49083	6429	49083	19320
49081	33463	49082	11973	49082	26955	49083	6489	49083	19546

2-fold multiplicity tagged events

run	event	run	event	run	event	run	event	run	event
49083	19949	49083	34218	49084	15799	49086	16102	49086	32817
49083	20533	49083	34851	49084	16197	49086	16251	49086	32864
49083	20914	49083	35006	49084	16365	49086	16328	49086	33149
49083	21945	49083	35233	49084	16714	49086	16470	49086	33259
49083	22520	49083	36303	49084	16744	49086	16494	49086	34899
49083	22625	49084	579	49084	16919	49086	16548	49086	35219
49083	23040	49084	1370	49084	17241	49086	16850	49086	35250
49083	23176	49084	1898	49086	31	49086	16966	49086	35328
49083	23238	49084	2765	49086	323	49086	17243	49086	36859
49083	23447	49084	2951	49086	731	49086	17810	49086	37458
49083	23549	49084	3196	49086	935	49086	18428	49086	37468
49083	23613	49084	3285	49086	1390	49086	19052	49087	272
49083	23870	49084	3547	49086	1736	49086	19848	49087	479
49083	24240	49084	3692	49086	1898	49086	19866	49087	2749
49083	24621	49084	4984	49086	1977	49086	20061	49087	3256
49083	25125	49084	5108	49086	2146	49086	20470	49087	3279
49083	25485	49084	5537	49086	2258	49086	20791	49087	3501
49083	26161	49084	5769	49086	2587	49086	20905	49087	3886
49083	26304	49084	5829	49086	3301	49086	21298	49087	4216
49083	26333	49084	6163	49086	3835	49086	21352	49087	4422
49083	26372	49084	6409	49086	4801	49086	21505	49087	5852
49083	26472	49084	6854	49086	5037	49086	21604	49087	6404
49083	26756	49084	7089	49086	5068	49086	22061	49087	6468
49083	27095	49084	7301	49086	5072	49086	22338	49087	6956
49083	27128	49084	7489	49086	5082	49086	23026	49087	7376
49083	27129	49084	7510	49086	5187	49086	23105	49087	7380
49083	27321	49084	7511	49086	5243	49086	24147	49087	8095
49083	27504	49084	7577	49086	5343	49086	24305	49087	8119
49083	28164	49084	8060	49086	5389	49086	24851	49087	8259
49083	28269	49084	8344	49086	7025	49086	26823	49087	9583
49083	28583	49084	8437	49086	8190	49086	27743	49087	9944
49083	28889	49084	9171	49086	8595	49086	27825	49087	9962
49083	29370	49084	9597	49086	9099	49086	27888	49087	10042
49083	29592	49084	9621	49086	10833	49086	28066	49087	10678
49083	29697	49084	10367	49086	10986	49086	28424	49087	11467
49083	30178	49084	11167	49086	11474	49086	28770	49087	11819
49083	30426	49084	11249	49086	12233	49086	28850	49087	11926
49083	30440	49084	11797	49086	12454	49086	29004	49087	12473
49083	30476	49084	11870	49086	12552	49086	29357	49087	12917
49083	30680	49084	12045	49086	12605	49086	29455	49087	13141
49083	30779	49084	12079	49086	12839	49086	29499	49087	13401
49083	30998	49084	12284	49086	13677	49086	30436	49087	13550
49083	32069	49084	12307	49086	13787	49086	30757	49087	13699
49083	32162	49084	12433	49086	14324	49086	30794	49087	13873
49083	32306	49084	12565	49086	14581	49086	31200	49087	14418
49083	32332	49084	12787	49086	14670	49086	31243	49087	14726
49083	32618	49084	13701	49086	15068	49086	31281	49087	15390
49083	32808	49084	14052	49086	15150	49086	32267	49087	15541
49083	33180	49084	14300	49086	15243	49086	32482	49087	15785
49083	33451	49084	15213	49086	16062	49086	32747	49087	15901

2-fold multiplicity tagged events

run	event	run	event	run	event	run	event	run	event
49087	16294	49087	31735	49088	16770	49089	226	49089	18538
49087	17293	49087	32213	49088	16809	49089	510	49089	18924
49087	17593	49087	32751	49088	16854	49089	1229	49089	19315
49087	17800	49087	33062	49088	16856	49089	1247	49089	19435
49087	18439	49087	33827	49088	18027	49089	2068	49089	19550
49087	18712	49087	34051	49088	18415	49089	2212	49089	19780
49087	18781	49087	34414	49088	18622	49089	2646	49089	19805
49087	18827	49087	34544	49088	18783	49089	2696	49089	19838
49087	19038	49087	35566	49088	18841	49089	2952	49089	20149
49087	19072	49087	35725	49088	19762	49089	3044	49089	20716
49087	20567	49087	35740	49088	19967	49089	3485	49089	20976
49087	20864	49087	35807	49088	20037	49089	3680	49089	21483
49087	21250	49088	255	49088	20197	49089	3991	49089	21788
49087	21344	49088	1036	49088	20198	49089	4623	49089	21853
49087	21347	49088	1418	49088	21851	49089	4912	49089	22034
49087	21673	49088	2086	49088	22100	49089	5044	49089	22110
49087	21933	49088	2321	49088	22251	49089	5094	49089	22162
49087	22072	49088	2505	49088	22875	49089	5763	49089	22429
49087	22090	49088	4654	49088	23085	49089	5870	49089	22435
49087	22452	49088	5007	49088	23371	49089	6561	49089	22736
49087	22548	49088	5223	49088	23407	49089	6728	49089	22887
49087	22935	49088	5697	49088	23467	49089	8054	49089	23193
49087	23027	49088	6211	49088	23647	49089	8243	49089	23277
49087	23664	49088	8431	49088	24007	49089	8567	49089	23807
49087	24636	49088	8794	49088	24130	49089	8994	49089	24489
49087	24731	49088	9266	49088	24134	49089	9493	49089	25133
49087	25476	49088	9343	49088	24153	49089	9796	49089	26639
49087	25650	49088	9934	49088	24609	49089	10531	49089	26674
49087	25699	49088	10058	49088	24886	49089	10691	49089	26695
49087	25780	49088	10189	49088	24957	49089	11423	49089	26901
49087	25929	49088	10503	49088	25417	49089	11676	49089	27176
49087	26666	49088	10611	49088	26046	49089	12106	49089	27271
49087	27239	49088	11096	49088	26120	49089	12262	49089	28415
49087	27265	49088	11225	49088	27800	49089	12504	49089	28790
49087	27969	49088	11277	49088	28009	49089	12508	49089	28981
49087	28486	49088	11516	49088	28596	49089	13681	49089	29101
49087	28488	49088	11532	49088	28836	49089	13741	49089	29314
49087	29319	49088	12299	49088	29020	49089	13805	49089	29779
49087	29459	49088	13479	49088	29144	49089	14967	49089	31379
49087	29504	49088	14736	49088	29152	49089	15201	49089	31798
49087	30013	49088	14774	49088	29439	49089	15347	49089	31896
49087	30144	49088	14940	49088	29888	49089	15411	49089	32246
49087	30295	49088	15045	49088	30218	49089	15874	49089	32813
49087	30564	49088	15684	49088	30527	49089	16073	49089	33380
49087	30818	49088	15809	49088	30662	49089	17107	49089	33643
49087	30931	49088	15915	49088	30913	49089	17458	49089	34064
49087	31047	49088	15934	49088	32567	49089	17645	49089	34193
49087	31317	49088	16101	49088	33479	49089	17763	49089	34283
49087	31724	49088	16280	49088	34302	49089	18150	49089	34783
49087	31732	49088	16639	49088	34580	49089	18166	49089	34850

2-fold multiplicity tagged events

run	event	run	event	run	event	run	event	run	event
49089	34854	49091	13866	49091	28048	49092	7863	49092	25871
49089	35323	49091	14334	49091	28127	49092	8146	49092	25894
49089	35327	49091	14444	49091	28638	49092	8278	49092	26336
49089	35531	49091	14457	49091	30189	49092	8369	49092	26980
49089	35716	49091	14616	49091	30440	49092	8672	49092	27073
49089	35878	49091	15027	49091	30724	49092	9056	49092	27427
49089	36085	49091	15241	49091	31127	49092	9315	49092	28359
49089	36099	49091	15731	49091	31618	49092	9542	49092	28493
49089	36890	49091	15775	49091	32176	49092	10174	49092	28785
49089	37546	49091	16224	49091	32198	49092	10773	49092	29130
49089	38398	49091	16315	49091	32375	49092	11631	49092	29352
49089	38497	49091	16691	49091	32556	49092	11828	49092	30178
49089	38592	49091	16882	49091	32645	49092	12360	49092	30942
49091	412	49091	17164	49091	32672	49092	13076	49092	31303
49091	1110	49091	17424	49091	32958	49092	14471	49092	31308
49091	1600	49091	18423	49091	33476	49092	14507	49092	31532
49091	1897	49091	19950	49091	33623	49092	14699	49092	31620
49091	2341	49091	20640	49091	33691	49092	14736	49092	31706
49091	2648	49091	21036	49091	34243	49092	15013	49092	32025
49091	3230	49091	21186	49091	34315	49092	15133	49092	32115
49091	3718	49091	21648	49091	34582	49092	15233	49092	32175
49091	4080	49091	21962	49091	35237	49092	16136	49092	32883
49091	4383	49091	21996	49091	35892	49092	16975	49092	33363
49091	4400	49091	22173	49091	35926	49092	17414	49092	34156
49091	5676	49091	22227	49091	36175	49092	17689	49092	34303
49091	5893	49091	22603	49091	36215	49092	18225	49092	34748
49091	5901	49091	22697	49091	36828	49092	18381	49092	35096
49091	6414	49091	22794	49091	37662	49092	18443	49092	35450
49091	7489	49091	22935	49091	37709	49092	19088	49092	35998
49091	7965	49091	23024	49091	37748	49092	19163	49092	37208
49091	8037	49091	23065	49091	37766	49092	19265	49092	37307
49091	8145	49091	23546	49091	38263	49092	19650	49092	37352
49091	9059	49091	23570	49091	39558	49092	19673	49092	37562
49091	9399	49091	23990	49091	40622	49092	19685	49092	37570
49091	9683	49091	24031	49092	753	49092	20077	49092	37829
49091	9920	49091	24426	49092	1194	49092	20361	49092	37917
49091	10040	49091	24642	49092	1309	49092	20919	49092	39010
49091	10136	49091	24693	49092	2606	49092	20930	49092	39520
49091	10242	49091	25435	49092	2800	49092	20938	49092	40035
49091	10578	49091	25607	49092	3016	49092	21494	49093	485
49091	11049	49091	25722	49092	4244	49092	21875	49093	706
49091	11310	49091	25865	49092	4275	49092	21968	49093	798
49091	11716	49091	26335	49092	4573	49092	22460	49093	1102
49091	11740	49091	26601	49092	4625	49092	22475	49093	1209
49091	11834	49091	26720	49092	4941	49092	22686	49093	1744
49091	12123	49091	27496	49092	5086	49092	22935	49093	2413
49091	12537	49091	27535	49092	6366	49092	23017	49093	2638
49091	12604	49091	27595	49092	6841	49092	23338	49093	3089
49091	12779	49091	27760	49092	6909	49092	25137	49093	3266
49091	13700	49091	27961	49092	7431	49092	25820	49093	3547

2-fold multiplicity tagged events

run	event	run	event	run	event	run	event	run	event
49093	4048	49093	19943	49094	976	49094	24365	49095	1012
49093	4240	49093	20005	49094	1620	49094	24580	49095	1335
49093	4428	49093	21354	49094	1623	49094	24972	49095	1882
49093	4822	49093	21983	49094	1653	49094	26157	49095	2797
49093	4926	49093	22012	49094	2315	49094	26727	49095	3469
49093	5166	49093	22045	49094	2319	49094	26821	49095	3674
49093	6709	49093	22177	49094	3310	49094	27023	49095	4063
49093	6762	49093	22707	49094	4055	49094	27293	49095	4492
49093	7102	49093	22946	49094	5164	49094	27315	49095	4787
49093	7252	49093	24765	49094	5200	49094	27441	49095	5085
49093	7903	49093	26295	49094	6489	49094	27739	49095	5405
49093	7944	49093	26513	49094	9536	49094	27803	49095	5608
49093	8513	49093	26663	49094	9585	49094	28118	49095	6244
49093	8545	49093	26986	49094	12152	49094	28123	49095	6342
49093	8749	49093	27371	49094	12960	49094	28457	49095	6593
49093	8902	49093	27656	49094	12962	49094	28684	49095	6961
49093	8994	49093	28023	49094	13059	49094	29502	49095	7083
49093	9188	49093	28054	49094	13285	49094	29738	49095	7102
49093	9498	49093	28591	49094	13526	49094	29903	49095	7209
49093	9565	49093	28606	49094	13878	49094	29904	49095	8191
49093	9691	49093	28916	49094	14031	49094	30103	49095	8211
49093	9836	49093	28957	49094	14344	49094	30144	49095	8430
49093	10195	49093	29586	49094	14942	49094	30167	49095	8594
49093	10310	49093	29627	49094	15706	49094	30273	49095	8761
49093	10985	49093	29843	49094	16192	49094	30378	49095	9818
49093	11175	49093	30098	49094	16718	49094	30549	49095	9891
49093	11178	49093	30324	49094	17660	49094	30778	49095	9996
49093	11216	49093	31034	49094	18140	49094	30899	49095	10089
49093	11895	49093	31297	49094	18256	49094	31108	49095	10093
49093	12153	49093	31393	49094	18587	49094	31291	49095	10474
49093	12578	49093	32813	49094	18773	49094	31477	49095	10475
49093	13669	49093	34424	49094	18889	49094	31826	49095	11116
49093	13862	49093	34680	49094	19523	49094	32079	49095	11371
49093	14165	49093	34788	49094	19539	49094	32108	49095	11540
49093	14390	49093	34934	49094	19622	49094	32331	49095	11771
49093	14437	49093	36440	49094	20393	49094	33300	49095	11919
49093	14936	49093	36617	49094	20505	49094	33365	49095	12065
49093	15393	49093	36731	49094	20573	49094	33370	49095	12290
49093	15734	49093	37014	49094	20668	49094	34132	49095	12762
49093	15862	49093	37945	49094	21157	49094	34221	49095	12803
49093	16053	49093	38109	49094	21544	49094	34312	49095	12928
49093	16335	49093	38746	49094	21799	49094	35011	49095	14591
49093	16998	49093	39143	49094	22375	49094	35085	49095	14808
49093	17145	49093	39234	49094	22607	49094	36047	49095	15350
49093	17533	49093	39395	49094	22749	49094	36089	49095	15388
49093	17605	49093	39442	49094	22881	49094	36518	49095	15434
49093	17621	49094	99	49094	22996	49094	37419	49095	15773
49093	17759	49094	130	49094	23143	49094	38303	49095	16488
49093	18179	49094	238	49094	23167	49095	431	49095	16506
49093	19295	49094	526	49094	24070	49095	539	49095	16671

2-fold multiplicity tagged events

run	event	run	event	run	event	run	event	run	event
49095	16723	49096	2540	49096	17800	49096	37079	49097	17446
49095	18588	49096	3695	49096	17886	49096	37595	49097	17742
49095	19056	49096	4551	49096	19043	49096	38071	49097	17751
49095	19214	49096	4655	49096	19271	49097	38	49097	17869
49095	19630	49096	4783	49096	19555	49097	109	49097	17908
49095	19681	49096	5060	49096	19793	49097	266	49097	18086
49095	20142	49096	5658	49096	20332	49097	309	49097	18508
49095	20478	49096	5784	49096	20671	49097	374	49097	18720
49095	21669	49096	6209	49096	21666	49097	1645	49097	18724
49095	21769	49096	6256	49096	22051	49097	2150	49097	19113
49095	21943	49096	6268	49096	22248	49097	2218	49097	19430
49095	22318	49096	6284	49096	22406	49097	2683	49097	20021
49095	22448	49096	6419	49096	22514	49097	3010	49097	22923
49095	22820	49096	6544	49096	22643	49097	3514	49097	23379
49095	22832	49096	6689	49096	22663	49097	4007	49097	23527
49095	23639	49096	6827	49096	22878	49097	4265	49097	23698
49095	24924	49096	6871	49096	23127	49097	4269	49097	24054
49095	25150	49096	7031	49096	25253	49097	4514	49097	24108
49095	25578	49096	7671	49096	25325	49097	4837	49097	24437
49095	25581	49096	8052	49096	25383	49097	4875	49097	25051
49095	26365	49096	8310	49096	25539	49097	4945	49097	25337
49095	26622	49096	8313	49096	25549	49097	5240	49097	25393
49095	27481	49096	8372	49096	25555	49097	5252	49097	25400
49095	27547	49096	8675	49096	25955	49097	5479	49097	25701
49095	27677	49096	8720	49096	26278	49097	5879	49097	26441
49095	28102	49096	8943	49096	26623	49097	6080	49097	27494
49095	28935	49096	9054	49096	26667	49097	6412	49097	27647
49095	29147	49096	9137	49096	27494	49097	8142	49097	28106
49095	29685	49096	9160	49096	27829	49097	8207	49097	29098
49095	29891	49096	9489	49096	28073	49097	8733	49097	29837
49095	30019	49096	9848	49096	28716	49097	8891	49097	29952
49095	30183	49096	11407	49096	28980	49097	8918	49097	30150
49095	30196	49096	11498	49096	29332	49097	9092	49097	30280
49095	31059	49096	11793	49096	31019	49097	9385	49097	30323
49095	33678	49096	12257	49096	31222	49097	9608	49097	30549
49095	34238	49096	12446	49096	33231	49097	9612	49097	30883
49095	34359	49096	12674	49096	33233	49097	10183	49097	31182
49095	34363	49096	12891	49096	33255	49097	10840	49097	31507
49095	34754	49096	13497	49096	33363	49097	11105	49097	31528
49095	34821	49096	13803	49096	33738	49097	11349	49097	32213
49095	35461	49096	14189	49096	33939	49097	11440	49097	32314
49095	36168	49096	14686	49096	34050	49097	12985	49097	32492
49096	15	49096	14751	49096	34456	49097	13630	49097	33506
49096	410	49096	15455	49096	34988	49097	13873	49097	34316
49096	442	49096	16313	49096	35361	49097	14165	49097	34420
49096	483	49096	16400	49096	35771	49097	14473	49097	34709
49096	814	49096	16884	49096	35803	49097	14912	49097	35164
49096	964	49096	16953	49096	36154	49097	15391	49097	35228
49096	1006	49096	16961	49096	36635	49097	15679	49097	35251
49096	2413	49096	17171	49096	37039	49097	17267	49097	35927

2-fold multiplicity tagged events

run	event	run	event	run	event	run	event	run	event
49097	36306	49098	18851	49098	38468	49099	22526	49100	921
49097	36418	49098	19459	49098	38748	49099	22595	49100	1014
49097	36462	49098	19946	49099	619	49099	23101	49100	1846
49098	616	49098	20372	49099	845	49099	23559	49100	2412
49098	654	49098	20379	49099	1238	49099	23666	49100	2515
49098	680	49098	20382	49099	1285	49099	23762	49100	2778
49098	1135	49098	21377	49099	1496	49099	23957	49100	3034
49098	2480	49098	22017	49099	1798	49099	24017	49100	3187
49098	2887	49098	22151	49099	2033	49099	24074	49100	3257
49098	3159	49098	22590	49099	2661	49099	24271	49100	3369
49098	3669	49098	24566	49099	2918	49099	24284	49100	3504
49098	3803	49098	24894	49099	4135	49099	24400	49100	3731
49098	4151	49098	25741	49099	5018	49099	24767	49100	3739
49098	5004	49098	26055	49099	5939	49099	25463	49100	5675
49098	5767	49098	26346	49099	6221	49099	26568	49100	5868
49098	6086	49098	27140	49099	6823	49099	27884	49100	6379
49098	6147	49098	27387	49099	7081	49099	28342	49100	6389
49098	6271	49098	27509	49099	7278	49099	28452	49100	6956
49098	6308	49098	27655	49099	7842	49099	28766	49100	6971
49098	6686	49098	27687	49099	8263	49099	29149	49100	7100
49098	7903	49098	27699	49099	8358	49099	29726	49100	7240
49098	8970	49098	27925	49099	8623	49099	29886	49100	7716
49098	9304	49098	28110	49099	8921	49099	31197	49100	7981
49098	9446	49098	28173	49099	8938	49099	31414	49100	8141
49098	9447	49098	28342	49099	9589	49099	31757	49100	8503
49098	10633	49098	28847	49099	10168	49099	31805	49100	8853
49098	11195	49098	29265	49099	10309	49099	32215	49100	8882
49098	11711	49098	29515	49099	12370	49099	32390	49100	9938
49098	12099	49098	30005	49099	12440	49099	32669	49100	10441
49098	12185	49098	30251	49099	13434	49099	32796	49100	10492
49098	12215	49098	30337	49099	13983	49099	33003	49100	10798
49098	12261	49098	30475	49099	14555	49099	33106	49100	10825
49098	12289	49098	31543	49099	15066	49099	33215	49100	11044
49098	12654	49098	31547	49099	15420	49099	33558	49100	11521
49098	13180	49098	32121	49099	15606	49099	34293	49100	12022
49098	13458	49098	32780	49099	16020	49099	34347	49100	12718
49098	14371	49098	32993	49099	16094	49099	35367	49100	12734
49098	14680	49098	33290	49099	16198	49099	36036	49100	13376
49098	14692	49098	33619	49099	17081	49099	36245	49100	13629
49098	15161	49098	33800	49099	17087	49099	37529	49100	13672
49098	15817	49098	34581	49099	18383	49099	38215	49100	15603
49098	16359	49098	34815	49099	19523	49099	38669	49100	15874
49098	17043	49098	35249	49099	19672	49099	38719	49100	15971
49098	17383	49098	35675	49099	19771	49099	39474	49100	16274
49098	17484	49098	35933	49099	19943	49100	14	49100	16694
49098	17658	49098	36800	49099	20063	49100	34	49100	16903
49098	17889	49098	37426	49099	20483	49100	255	49100	17084
49098	18160	49098	37623	49099	20567	49100	297	49100	17330
49098	18427	49098	37872	49099	21755	49100	705	49153	464
49098	18677	49098	38020	49099	22123	49100	735	49153	1394

2-fold multiplicity tagged events

run	event	run	event	run	event	run	event	run	event
49153	1849	49153	19818	49154	9582	49154	30609	49155	5757
49153	2055	49153	19910	49154	10897	49154	30851	49155	5809
49153	2456	49153	20057	49154	11211	49154	30864	49155	6274
49153	2688	49153	20832	49154	11783	49154	31239	49155	6888
49153	2776	49153	20940	49154	12141	49154	31248	49155	7245
49153	3221	49153	21694	49154	12670	49154	31401	49155	8237
49153	3595	49153	21878	49154	14329	49154	31441	49155	8585
49153	3622	49153	22229	49154	14411	49154	32096	49155	8728
49153	3858	49153	22368	49154	14886	49154	32621	49155	9792
49153	4252	49153	22442	49154	15109	49154	32901	49155	9945
49153	4334	49153	23726	49154	15852	49154	32920	49155	10081
49153	4515	49153	24307	49154	16291	49154	33089	49155	10332
49153	5570	49153	24855	49154	16330	49154	33199	49155	10762
49153	5673	49153	25164	49154	17464	49154	33903	49155	12136
49153	6551	49153	25708	49154	18484	49154	34197	49155	12397
49153	6986	49153	25748	49154	19411	49154	34877	49155	13075
49153	8453	49153	25929	49154	19817	49154	35093	49155	13230
49153	8500	49153	26660	49154	19900	49154	35900	49155	13292
49153	8545	49153	26823	49154	20697	49154	36247	49155	13324
49153	9744	49153	27297	49154	20729	49154	36622	49155	14128
49153	9829	49153	27472	49154	20743	49154	37104	49155	14521
49153	9935	49154	1000	49154	20909	49154	37140	49155	14554
49153	10506	49154	1827	49154	20984	49154	37329	49155	14694
49153	10838	49154	2288	49154	21310	49154	37355	49155	15504
49153	10892	49154	2558	49154	22275	49154	37415	49155	15996
49153	11757	49154	2644	49154	22330	49154	37580	49155	16344
49153	12073	49154	3229	49154	22486	49154	37608	49155	16692
49153	12708	49154	3301	49154	22627	49154	38075	49155	16776
49153	12861	49154	3336	49154	23299	49154	38148	49155	16906
49153	13076	49154	3499	49154	23660	49154	38443	49155	17048
49153	13585	49154	3551	49154	23747	49154	38730	49155	17345
49153	13619	49154	3651	49154	24120	49154	38868	49155	17366
49153	14018	49154	3940	49154	24203	49154	38923	49155	17510
49153	14055	49154	5053	49154	24625	49154	39062	49155	17616
49153	14128	49154	5552	49154	24801	49154	40243	49155	17733
49153	14439	49154	6566	49154	24934	49154	40261	49155	17786
49153	14490	49154	6640	49154	25131	49154	40674	49155	18246
49153	15088	49154	6739	49154	25391	49155	24	49155	18338
49153	15587	49154	6950	49154	25424	49155	1565	49155	18371
49153	16278	49154	7617	49154	25950	49155	2669	49155	18833
49153	16658	49154	7730	49154	26446	49155	2860	49155	18914
49153	16828	49154	7784	49154	26672	49155	2973	49155	19344
49153	16868	49154	7903	49154	26952	49155	3266	49155	19621
49153	17348	49154	7944	49154	27118	49155	3468	49155	20221
49153	18136	49154	8031	49154	27239	49155	4231	49155	20586
49153	18164	49154	8041	49154	28290	49155	5018	49155	20659
49153	18546	49154	8044	49154	28410	49155	5124	49155	21538
49153	18892	49154	8240	49154	28609	49155	5293	49155	21554
49153	19573	49154	8699	49154	30356	49155	5347	49155	21652
49153	19742	49154	9282	49154	30530	49155	5635	49155	21945

First sample (preliminary selection, prior to several patches of reconstruction algorithm), selection is based on 3-fold multiplicity tagging.

run	event	run	event	run	event
49048	4109	49072	7433	49093	30098
49048	14479	49072	11133	49093	34503
49048	15080	49072	17252	49093	35214
49049	1295	49073	41	49093	36725
49049	1878	49073	2210	49093	37632
49050	5568	49073	4605	49094	8511
49054	2001	49073	10926	49094	23518
49054	20197	49073	14448	49094	28457
49055	15839	49078	7608	49094	30103
49056	2116	49078	21879	49095	983
49056	2971	49079	2887	49095	21788
49056	19949	49079	23532	49095	25113
49057	3574	49080	20499	49096	9489
49057	11285	49080	32959	49096	12891
49057	15390	49080	35016	49096	13497
49057	23097	49081	6822	49096	16631
49060	3536	49081	28770	49096	16874
49061	19888	49082	31254	49096	28218
49062	445	49083	10556	49097	21834
49062	717	49083	12737	49097	29837
49062	7279	49083	23447	49097	30267
49062	8399	49083	32162	49098	7525
49062	18871	49083	32676	49098	22896
49064	1683	49084	5108	49098	23361
49064	2820	49086	662	49098	29265
49064	4207	49086	4801	49098	34710
49064	4807	49086	21051	49099	16252
49064	12567	49086	32747	49099	31496
49065	8290	49087	16609	49100	7716
49066	23660	49087	18781	49100	9231
49067	10001	49087	21344	49100	17084
49067	15553	49088	5303	49153	10037
49067	24235	49089	1878	49153	18668
49068	6593	49089	2068	49153	26660
49068	10546	49089	28415	49153	27472
49068	13087	49091	1110	49154	6950
49069	5797	49091	10170	49154	16330
49069	12665	49091	26182	49154	24625
49069	14090	49091	36938	49154	34877
49069	17822	49092	25137	49155	2849
49069	24548	49092	26336	49155	5466
49070	14978	49092	28401	49155	21583
49071	300	49092	37352	49155	23215
49071	9982	49093	15966		